**Fakultät für Medizin**

**Institut für Klinische Chemie und Pathobiochemie**

# Analysis of Card9 signaling in innate immunity

**Susanne Ilona Roth**

Vollständiger Abdruck der von der Fakultät für Medizin der Technischen Universität München zur Erlangung des akademischen Grades eines

**Doctor of Philosophy (Ph.D.)**

genehmigten Dissertation.

**Vorsitzende:** Prof. Dr. Agnes Görlach

**Betreuer:** Prof. Dr. Jürgen Ruland

**Prüfer der Dissertation:**

1. Prof. Dr. Thomas Korn

2. Prof. Dr. Mathias Heikenwälder

3. Prof. Dr. Anne Krug

Die Dissertation wurde am 17.06.2017 bei der Fakultät für Medizin der Technischen Universität München eingereicht und durch die Fakultät für Medizin am 21.09.2017 angenommen.

**Table of content**

## List of Abbreviations

| | |
|---|---|
| AIM2 | Absent in melanoma 2 |
| APC | Antigen presenting cell |
| ASC | Apoptosis-associated speck-like protein containing a CARD |
| ATM | Ataxia-teleangiectasia mutated |
| ATR | ATM- and Rad3-related |
| Bcl10 | B cell lymphoma 10 |
| BMDC | Bone marrow-derived dendritic cell |
| BRET | Bioluminescence resonance energy transfer |
| Card9 | Caspase recruitment domain-containing protein 9 |
| Carma | CARD-containing MAGUK protein |
| CBM | Card9-Bcl10-Malt1 |
| CD | Crohn's disease |
| cGAMP | cyclic-GMP-AMP |
| cGAS | cGAMP synthase |
| CLR | C-type lectin receptor |
| CTLD | C-type lectin-like domain |
| DAMP | Damage-associated molecular pattern |
| DDR | DNA damage response |
| dsDNA | double-stranded DNA |
| FcRγ | Fc receptor γ |
| GEF | Guanine-nucleotide exchange factor |
| IBD | Inflammatory bowl disease |
| IFN | Interferon |
| IFN-I | Type I interferon |
| IKK | IκB kinase |
| IL | Interleukin |
| IRF3 | Interferon regulatory factor 3 |
| ITAM | Immunoreceptor tyrosine-based activation motif |
| IκB | Inhibitor of kappa B |
| MAGUK | Membrane-associated guanylate kinase |
| Malt1 | Mucosa-associated lymphoid tissue lymphoma translocation protein 1 |
| MAPK | Mitogen activated protein kinase |
| MAVS | Mitochondrial antiviral-signaling protein |

| | |
|---|---|
| Mda5 | Melanoma differentiation-associated gene 5 |
| Mincle | Macrophage inducible C-type lectin |
| MRN | Mre11-Rad50-Nbs1 |
| NALP3 | NACHT, LRR and PYD domains-containing protein 3 |
| NF-κB | Nuclear factor kappa-light-chain-enhancer of activated B-cells |
| NIK | NF-κB-inducing kinase |
| NLR | NOD-like receptor |
| PAMP | Pathogen-associated molecular pattern |
| PRR | Pattern recognition receptor |
| RIG-I | Retinoic acid-inducible gene I |
| RIP2 | Receptor-interacting serine-threonine kinase 2 |
| RLR | RIG-I-like receptors |
| ROS | Reactive oxygen species |
| SFK | Src family kinase |
| SH | Src homology |
| STING | Stimulator of interferon genes |
| Syk | Spleen tyrosine kinase |
| TBK1 | TANK-binding kinase 1 |
| TDB | Trehalose-6,6-dibehenate |
| TDM | Trehalose-6,6-dimycolate |
| TLR | Toll-like receptor |
| UC | Ulcerative colitis |
| VSV | Vesicular stomatitis virus |
| WTCCC | Wellcome Trust Case Control Consortium |

# 1. Introduction

## 1.1 Pattern recognition receptors

A conceptual framework how innate and adaptive immunity might integrate was formulated more than 20 years ago by Charles A. Janeway, Jr.[1]. Besides antigen binding to specific antigen receptors, activation of adaptive immune responses requires a costimulatory signal that is provided by antigen presenting cells (APCs) of the innate immune system. Janeway suggested that this costimulatory signal would not be constantly, but inducibly supplied by APCs. Conserved microbial products, known as pathogen-associated molecular patterns (PAMPs), would be recognized by a limited number of germline-encoded innate immune receptors and would thereby lead to the induction of the costimulatory signal. The detection of infection, identifying the microbial origin of antigens, would be mediated via these pattern recognition receptors (PRRs) by the innate immune system[1, 2]. It is astonishing how research over the last two decades has proven that Janeway's fundamental concepts from 1989 hold true[2]. Since Janeway's hypothesis a multitude of PRRs has been identified. Shared characteristics of PRRs include that they are germline-encoded and therefore expressed by all cells of a given type, evolutionary conserved, and recognize PAMPs. Yet, recent evidence indicates that PRRs not only recognize structures derived from pathogens, but can also detect endogenous ligands released upon tissue damage or cellular injury, so-called damage-associated molecular patterns (DAMPs). Distinct PRRs monitor different cellular compartments for the presence of PAMPs or DAMPs. To this end, they are located at the cell surface, in endosomes, or in the cytosol. Based on their phylogeny and structure different families of PRRs have been indentified, including Toll-like receptors (TLRs), C-type lectin receptors (CLRs), Retinoic acid-inducible gene (RIG)-I-like receptors (RLRs) and NOD-like receptors (NLRs)[3]. Besides these well established PRRs families several cytosolic DNA sensing proteins have recently been discovered. Upon ligand binding PRRs trigger intracellular signaling cascades via a limited number of evolutionary conserved signaling modules, which integrate information and link recognition to appropriate immune effector responses[3, 4]. The cytosolic adaptor caspase recruitment domain-containing protein (Card)9 is one central signaling molecule, which assembles Card9-B cell lymphoma (Bcl)10-mucosa-associated lymphoid tissue lymphoma translocation protein (Malt)1 (CBM) signalosomes and thereby relays signals from multiple PRRs to inflammatory responses[4]. Following ligand binding, several PRRs modify gene transcription via different signaling pathways, inducing proinflammatory cytokines, interferons (IFNs), chemokines and other immune mediators,

which mediate acute inflammatory responses and initiate adaptive immunity[3]. Central to the expression of proinflammatory cytokines in response to PRR activation is the transcription factor nuclear factor kappa-light-chain-enhancer of activated B-cells (NF-κB). Because aberrant production of proinflammatory mediators can cause severe tissue damage or inflammatory diseases, some highly potent cytokines such as interleukin (IL)-1β are tightly controlled by additional mechanisms. Besides the transcriptional upregulation of pro-IL-1β mRNA, proteolytic processing of the inactive pro-IL-1β precursor is needed to generate the mature IL-1β protein. Pro-IL-1β is typically cleaved by caspase-1 within inflammasomes, which are multiprotein complexes that oligomerize in the cytosol and engage distinct PRRs for different ligands[5]. The cytosolic DNA sensor absent in melanoma (AIM)2 forms specific inflammasomes after binding to cytosolic DNA by engaging the common inflammasome adaptor apoptosis-associated speck-like protein containing a CARD (ASC)[6], whereas NACHT, LRR and PYD domains-containing protein 3 (NALP3)-containing inflammasomes are activated in response to a large array of PAMPs and DAMPs, while a specific NALP3 ligand is still unknown[7].

## 1.2 Cytosolic DNA recognition receptors

The ability of DNA to induce inflammatory and antiviral responses has been known for more than 50 years[8]. Yet, only within the past decade the molecular mechanisms involved have been unraveled. In 2000, TLR9 was the first PRR being identified to induce cytokine and type I interferon (IFN-I) production upon DNA recognition. TLR9 specifically detects unmethylated DNA, so-called CpG DNA motifs, which are more abundant in microbial than in mammalian genomes[9]. However, the ligand binding domain of TLR9 faces the endosomal lumen and is thereby unable to detect DNA that has entered into the cytosol[6]. Prior to the identification of individual cytosolic DNA recognizing PRRs, TANK-binding kinase (TBK)1 has been shown to be crucial for type I interferon production in response to cytosolic DNA, as well as DNA virus infections. TBK1 mediates phosphorylation and activation of the transcription factor interferon regulatory factor (IRF)3 leading to IFN-β expression[10]. In 2008, the endoplasmic reticulum-associated adapter protein stimulator of interferon genes (STING) was identified as being absolutely essential for IFN-I induction in response to cytosolic DNA and DNA viruses[11]. In addition, in vivo studies highlighted a central role for STING in host defense against DNA viruses[12]. Mechanistically, STING directly engages TBK1 for IRF3 activation[13]. Multiple putative cytosolic DNA sensing PRRs, including DAI, IFI16, DDX41, DNA-PK and Mre11,

5

have been shown to converge on STING for triggering interferon responses[10]. Recently, the identification of cyclic-GMP-AMP (cGAMP) synthase (cGAS), a cytosolic enzyme generating the second messenger cGAMP, has significantly advanced our understanding of cytosolic DNA recognition. Following direct DNA binding cGAS generates cGAMP, which directly engages STING for IRF3 activation[14, 15]. The functional importance of cGAS has also been confirmed in vivo[16]. However, the mechanisms by which NF-κB is activated upon cytosolic DNA recognition are still not well understood. Moreover, STING seems to be largely dispensable for DNA-induced IL-1β production[12, 17]. While AIM2 upon cytosolic DNA recognition engages the common inflammasome adaptor ASC to activate caspase-1 for pro-IL-1β processing[6], the signals that trigger pro-IL-1β expression remain unclear.
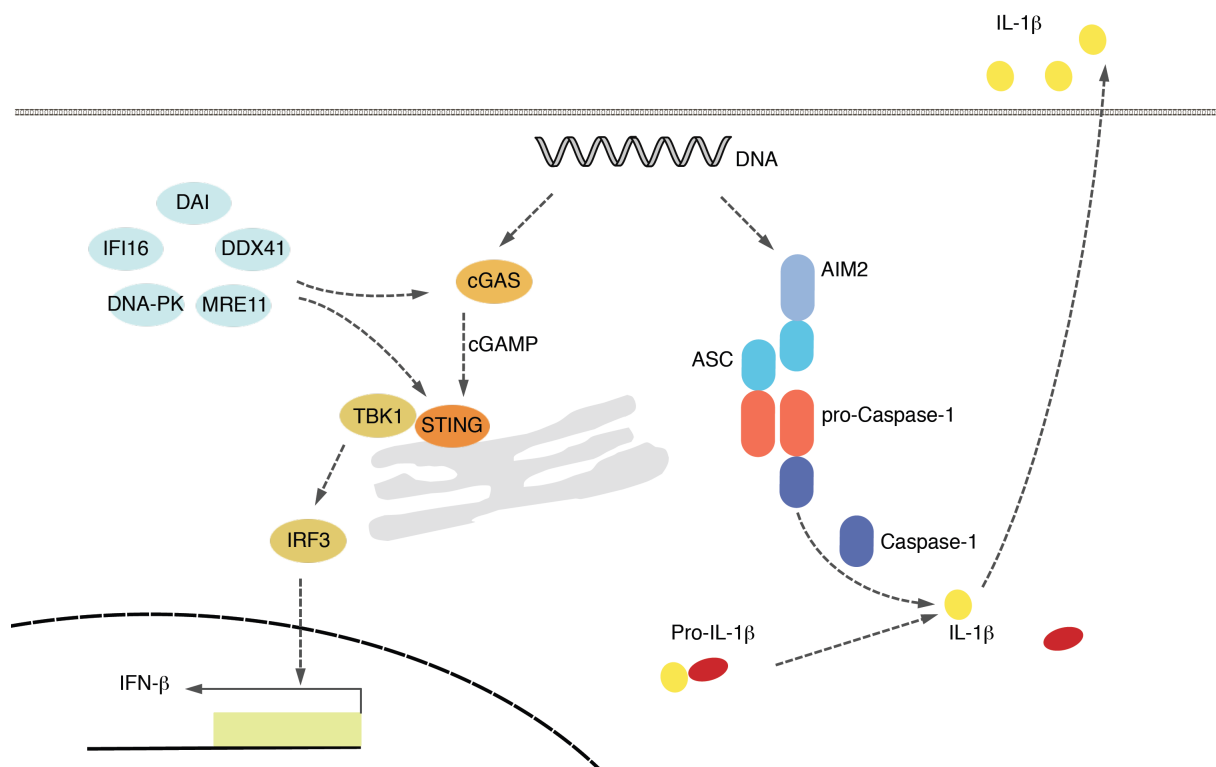


**Figure 1. Schematic representation of cytosolic DNA recognition.** Multiple cytosolic DNA receptors, including cGAS, DAI, IFI16, DDX41, DNA-PK and Mre11 have been implicated in interferon responses via the endoplasmic reticulum-associated adaptor protein STING. After direct DNA binding cGAS produces the second messenger cGAMP that directly associates with STING and thereby triggers type I interferon responses. In parallel, cytosolic DNA recognition by AIM2 leads to the activation of caspase-1 via the formation of AIM2 inflammasomes. Activated caspase-1 then proteolytically cleaves pro-IL-1β generating mature, active IL-1β.

**1.3 Syk-coupled C-type lectin receptors**

C-type lectins were originally defined as proteins containing a conserved calcium-dependent („C-type") carbohydrate-binding („lectin") domain. Later however, sequence homology analysis revealed that this domain was also present in proteins that do not bind to carbohydrates or calcium. Therefore, the term C-type lectin-like domain (CTLD) was introduced[18, 19]. CLRs are soluble or transmembrane proteins containing a CTLD that mostly, but not only recognize carbohydrate structures. A group of transmembrane CLRs, which are able to initiate signaling pathways for reprogramming gene expression in response to ligand binding independent of other PRRs, uses spleen tyrosine kinase (Syk) as a signaling adaptor[18, 19]. These so-called Syk-coupled CLRs comprise Dectin-1, Dectin-2, and macrophage inducible C-type lectin (Mincle)[19, 20]. All three Syk-coupled CLRs recognize carbohydrate structures present in fungal cell walls and have been found to be important in anti-fungal host defense. Dectin-1 specifically detects β-1,3 and β-1,6-linked β-glucans, while Dectin-2 and Mincle recognize α-mannans[19, 21]. Besides fungi, CLRs have been shown to detect mycobacteria[22, 23, 24], viruses[25], helminths[26] and endogenous ligands released from apoptotic or necrotic cells[19, 27, 28].

Dectin-1 is the best studied Syk-coupled CLR, which activates several cellular effector responses upon ligand binding. Within its cytoplasmic tail Dectin-1 contains an immunoreceptor tyrosine-based activation motif (ITAM)-like sequence, which is similar in structure and function to the classical ITAM module in T and B cell antigen receptors[18, 19, 29]. Yet, while the ITAM consensus sequence ($YxxI/L\text{-}x_{6\text{-}12}\text{-}YxxI/L$) contains tandem tyrosines, the ITAM-like motif in Dectin-1 includes only a single YxxL sequence and thus has also been named hemITAM[18, 19, 29]. Recognition of particulate ligands by Dectin-1 leads to its clustering into „synapse-like structures"[30] and phosphorylation of the tyrosine residue within its ITAM-like motif by Src family kinases (SFKs). Analogous to antigen receptor signaling, in which tandem Src homology (SH)2-domain containing kinases such as Syk are recruited to the phosphorylated ITAM motifs, Syk binds to the clustered, phosphorylated hemITAMs of Dectin-1[18, 19, 29]. Activated Syk then mediates phagocytosis and reactive oxygen species (ROS) production, which triggers NALP3 inflammasome activation[31, 32]. In addition, Syk relays signals to downstream signaling pathways, including mitogen activated protein kinase (MAPK) and NF-κB signaling that reprogram gene transcription to produce inflammatory cytokines and chemokines[18, 19, 29, 32]. Central to CLR-induced NF-κB activation is the adaptor protein Card9[4, 33]. Dectin-1 ligation and Syk-activation mediate phosphorylation of Card9 at

Thr231 via PKCδ, which leads to the formation of Card9-Bcl10-Malt1 (CBM) signalosomes, essential for inhibitor of kappa B (IκB) kinase (IKK) activation that controls canonical NF-κB[4, 34]. Yet in contrast to Card9 and Bcl10, Malt1 paracaspase seems to selectively regulate c-Rel[35]. Remarkable for a PRR, Dectin-1 signaling also leads to the induction of the non-canonical NF-κB pathway, via Syk and NF-κB-inducing kinase (NIK), mediating RelB activation[35, 36]. In parallel, ligand recognition by Dectin-1 triggers activation of the serine-threonine kinase Raf-1 in a Syk-independent manner. Activated Raf-1 phosphorylates the NF-κB subunit p65 at Ser276, which modulates p65 and RelB activity[36].
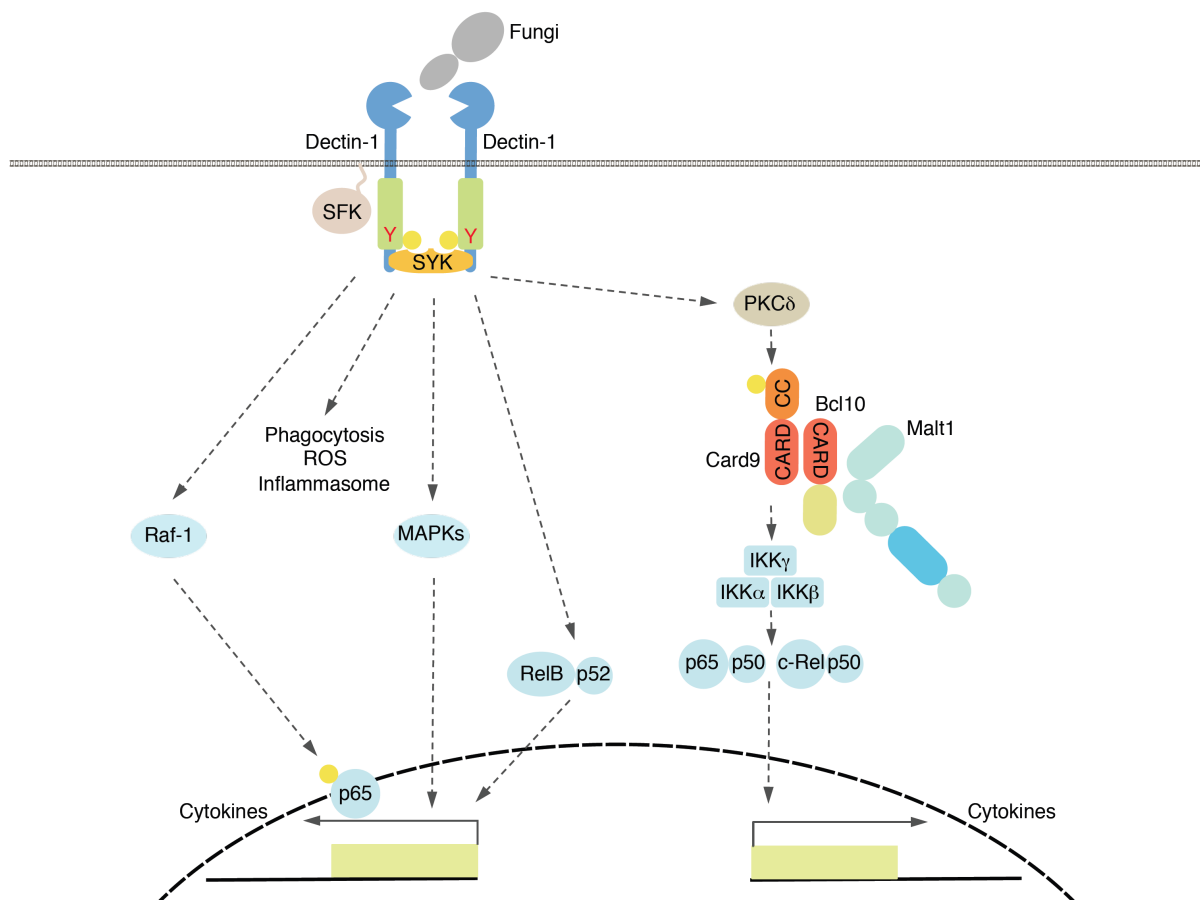


**Figure 2. Dectin-1 signaling pathways.** Following ligand recognition, Dectin-1 is tyrosine phosphorylated by SFKs within its cytoplasmic ITAM-like motif, which leads to the recruitment of Syk. Activated Syk then mediates phagocytosis, ROS production and inflammasome activation, and regulates gene transcription via MAPKs and NF-κB signaling. Crucial for Dectin-1-induced canonical NF-κB activation is the Card9-Bcl10-Malt1 complex. The serine-threonine kinase PKCδ regulates Card9 function via Thr231 phosphorylation. Independent of Syk, Dectin-1 activates Raf-1, leading to p65 phosphorylation, which

modulates NF-κB-dependent gene transcription. CARD, caspase-recruitment domain; CC, coiled coil domain; IκB kinase (IKK); adapted from Roth and Ruland[4].

In contrast to Dectin-1, Dectin-2 and Mincle do not carry an internal ITAM-like motif, but instead associate with the ITAM-containing adaptor protein Fc receptor γ (FcRγ) chain to initiate downstream signaling[19, 29]. Upon ligand recognition FcRγ chain-associated Dectin-2 and Mincle also engage the common Syk-PKCδ-Card9 signaling axis for NF-κB activation and cytokine production[4, 34].



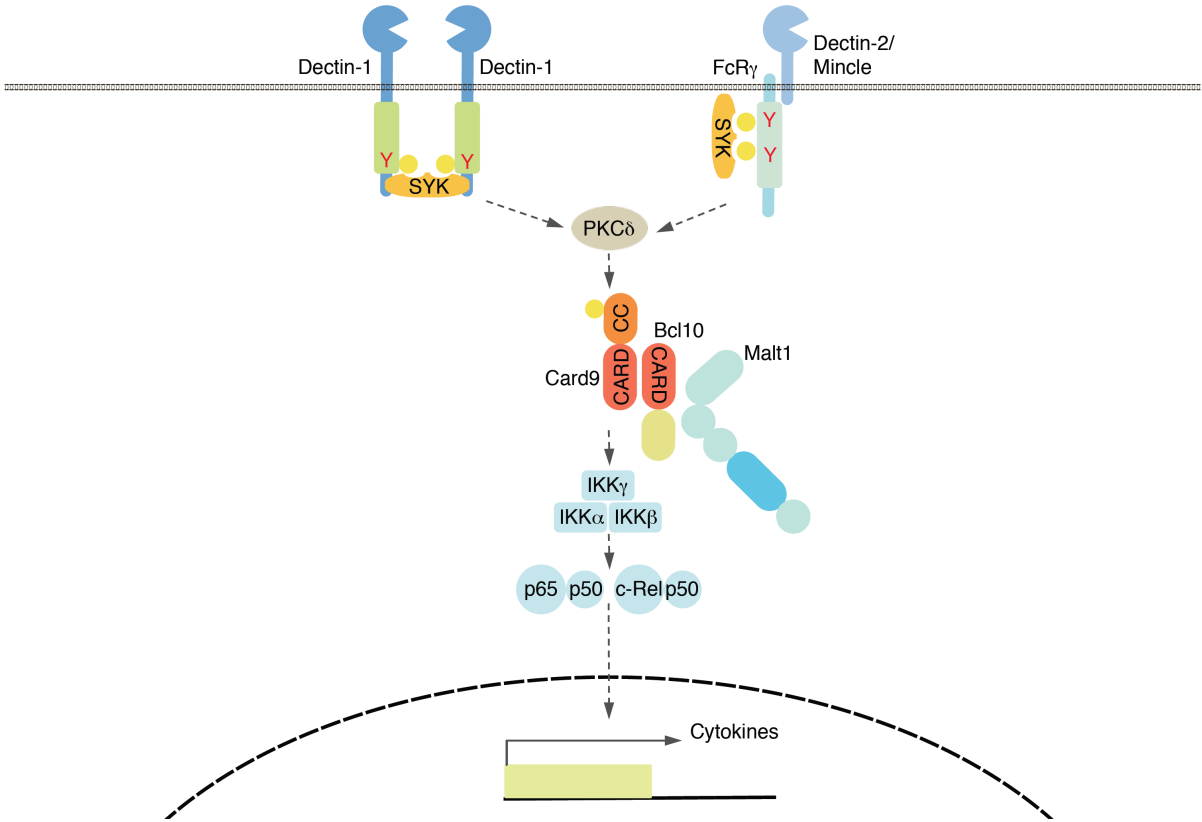**Figure 3. Syk-coupled CLR signaling.** Ligand binding leads to tyrosine phosphorylation of ITAM-like motifs within Dectin-1, or Dectin-2/Mincle-associated ITAM-containing FcRγ chains. Syk is thereby recruited and mediates NF-κB activation via the central PKCδ-Card9-Bcl10-Malt1 signaling cascade. CARD, caspase-recruitment domain; CC coiled coil domain; IκB kinase (IKK); adapted from Roth and Ruland[4].

## 1.4 Card9 structure, expression and biochemistry

Card9 was originally identified in a mammalian two-hybrid screen for CARD-containing proteins, which directly interact with the signaling adaptor protein Bcl10 that has been known already for its essential role in NF-κB signaling pathways. Card9 and Bcl10 were shown to selectively associate via CARD-CARD interactions, and overexpression of Card9 in HEK293T cells induced NF-κB activity[4, 37]. Besides its N-terminal CARD, at its C-terminus Card9 contains a coiled-coil domain, which functions as an oligomerization domain in a variety of proteins[37]. The domain composition of Card9 is similar to the CARD-containing membrane-associated guanylate kinase (MAGUK) (Carma) family of proteins, including Carma1 (also known as Card11), Carma2 and Carma3. Yet, in contrast to the Carma family, Card9 lacks the MAGUK domain, which has been shown to mediate membrane association[4]. Card9 has been shown to be expressed in a variety of tissues, including peripheral blood, bone marrow, thymus, spleen, liver, lung, placenta and brain. At a cellular level, highest expression levels of Card9 were detected in myeloid cells, especially in APCs, such as macrophages and dendritic cells[4]. As mentioned above, the first functional insight into Card9 derived from its direct association with Bcl10. In lymphoid cells, Bcl10 together with Card11 and Malt1 forms signaling complexes, which are crucial for antigen receptor-induced NF-κB activation. Subsequently it has been shown, that in myeloid cells Card9 takes over the role of Card11 in forming CBM signalosomes that regulate NF-κB activity in response to ITAM-receptor stimulation[4, 38]. Therefore, depending on the cell-type distinct CBM complexes function as central signaling platforms downstream of ITAM receptors for NF-κB activation.

## 1.5 Card9-mediated PRR signaling

Card9 is a multifunctional signaling adaptor, on which signals from distinct PRRs converge[4]. Pathogens mostly comprise complex compositions of PAMPs that engage multiple PRRs. The signals initiated by diverse PRRs are integrated by a limited number of signaling molecules, which orchestrate context-specific innate and adaptive immune responses[39]. Card9 has been shown to link a variety of PRRs to downstream effector pathways[4]. Card9 is absolutely essential for Syk-coupled CLR-induced inflammatory responses. Card9-deficient dendritic cells are defective in NF-κB activation and cytokine production after stimulation with *Candida albicans (C. albicans)* or the fungal cell wall preparation zymosan, which contains β-glucans that bind to Dectin-1[33]. Consistently, the selective Dectin-1 agonist curdlan, a

particulate β-glucan, induced Card9-dependent inflammatory responses in dendritic cells[40]. Moreover, cross-linking of Dectin-2, or stimulation with α-mannans has been demonstrated to trigger Syk-Card9-dependent NF-κB activation and cytokine production in myeloid cells[41, 42]. Remarkably, in response to *C. albicans* inflammatory responses were almost completely abolished in Card9^{-/-} cells, whereas they were only partially impaired in Dectin-2-deficient cells, indicating redundancy at the receptor level and that Card9 is the common adaptor downstream of additional fungal PRRs[4]. The Syk-coupled CLR Mincle also recognizes fungi and mycobacteria[20, 22, 23, 43]. Mincle detects mycobacteria via their abundant cell wall glycolipid trehalose-6,6-dimycolate (TDM)[22, 23]. TDM and its synthetic analogue trehalose-6,6-dibehenate (TDB) activate myeloid cells via Mincle-FcRγ and the common Syk-CBM-NF-κB signaling axis[23, 24]. Consistently, Card9^{-/-} cells are impaired in cytokine production following infection with *Mycobacterium tuberculosis*[4, 44]. Besides its major role in CLR signaling, Card9 has been shown to be also involved in mediating inflammatory responses downstream of intracellular PRRs, including NOD2 and RLRs[4]. NOD2 is an NLR family member that recognizes structures derived from bacterial cell wall peptidoglycans and has a crucial role in intestinal homeostasis. Via its N-terminal CARD NOD2 recruits the CARD-containing adaptor receptor-interacting serine-threonine kinase (RIP)2 to activate NF-κB[3, 45]. Card9 has been shown to be involved in a parallel pathway that mediates NOD2-induced MAPK activation and cytokine responses[4, 46].

RLRs, such as RIG-I and melanoma differentiation-associated gene (Mda)5, recognize viral RNA in the cytosol and initiate signaling pathways for IRF and NF-κB activation via the mitochondrial antiviral-signaling protein (MAVS)[47]. Recently we have discovered that RIG-I and Mda5 engage Card9 and Bcl10 specifically for NF-κB-dependent proinflammatory cytokine responses. Recognition of 5´pppRNA or vesicular stomatitis virus (VSV) by RIG-I triggered IL-6 and IL-1β generation in wild type dendritic cells, which was impaired by the lack of Card9 or Bcl10[48]. A previous study has shown that Card9^{-/-} macrophages are defective in MAPK activation in response to VSV infection[46]. In addition to reprogramming gene transcription RIG-I signaling also induces caspase-1 dependent inflammasome activation and thereby leads to mature IL-1β production[48]. Besides viral RNA, RLRs also detect bacterial nucleic acids. *Listeria monocytogenes*, a gram-positive intracellular bacterium, secretes nucleic acids into the cytosol, which induce type I interferon responses in a RIG-I-, Mda5- and STING-dependent manner[49]. In addition, cytosolic Listeria derived nucleic acids trigger inflammasome activation and IL-1β production via RIG-I. In contrast,

Card9 selectively regulates Listeria-induced IL-1β production without affecting inflammasome activation or IFN responses[49].

**1.6 CLR-Card9 signaling in anti-fungal host defense**

The importance of CLR-Card9-mediated inflammatory responses in anti-fungal host defense has been shown in numerous studies in mice and humans. Card9-deficient mice were impaired in fungal clearance and rapidly succumbed after systemic *C. albicans* infection[33]. Excitingly, recent genetic analyses have revealed an association of Card9 and susceptibility to fungal infections in humans[50]. A loss-of-function mutation of *CARD9* leads to an autosomal recessive form of chronic mucocutaneous candidiasis. Patients with the homozygous point mutation Q295X in *CARD9*, resulting in a premature stop codon, completely lacked wild-type Card9 protein. In vitro reconstitution experiments of bone marrow cells from Card9-deficient mice demonstrated that in contrast to human full-length *CARD9*, the *CARD9* Q295X mutant could not restore the Dectin-1 signaling defect of Card9$^{-/-}$ cells[51]. Subsequently, several mutations in the *CARD9* gene have been associated with invasive candidiasis, and infections with other fungal species[50]. In addition, Dectin-1, Dectin-2, or Mincle deficient mice are impaired in host defense against *C. albicans, Aspergillus fumigatus,* or *Pneumocystis carinii*[4]. Yet, the significance of individual receptors varies for different fungal species and strains. Interestingly, Dectin-1 polymorphisms have been associated with increased susceptibilities to infection with *C. albicans* and invasive aspergillosis in immunosuppressive settings[52, 53, 54].

**1.7 Card9 in inflammatory diseases**

While innate immune responses are crucial for host defense against pathogens, uncontrolled activation of immune effector pathways can lead to tissue damage and inflammatory diseases. Inflammatory bowl diseases (IBDs), including Crohn's disease (CD) and ulcerative colitis (UC) are common, chronic, relapsing and remitting gastrointestinal inflammatory disorders, which are supposed to be caused by aberrant immune responses against an altered intestinal microbiome in a genetically susceptible host [55]. After years IBDs greatly increase the risk of colorectal cancer development[56]. Despite large efforts the mechanisms involved in IBD and inflammation-associated carcinogenesis remain incompletely understood. The *NOD2* gene was the first identified susceptibility gene for CD[4, 55]. Since then

the role of innate immunity in IBD has been studied extensively. A candidate-gene analysis of innate immune pathways in IBD identified an association of the *CARD9* gene (rs10870077) with CD and UC[57]. The association of Card9 with IBD was confirmed by the Crohn's disease Wellcome Trust Case Control Consortium (WTCCC) dataset[57] and replicated in genome-wide association studies (rs4077515)[4, 58, 59]. Several subsequent analyses further corroborated a potential role of Card9 in IBDs[4, 60, 61, 62, 63]. In addition, Dectin-1^{-/-} mice are more susceptible to colitis, and a polymorphism in the human *Dectin-1* gene (*CLEC7A*) has been associated with a severe form of UC[64], indicating that CLR-Card9 signaling might be involved in the etiology of IBDs. Other chronic inflammatory diseases that often co-occur with IBDs have also been associated with the *CARD9* gene, including primary sclerosing cholangitis[65], and ankylosing spondylitis[66, 67, 68].

## 2. Aim of the present study and scientific approach

Card9 is a central signaling adaptor of the innate immune system that is engaged by different transmembrane and cytosolic PRRs to mediate inflammatory responses[4]. To get insight into the mechanisms how Card9 signaling is regulated and whether Card9 mediates additional PRRs signaling pathways we performed a yeast two-hybrid screen with full-length Card9. Newly identified Card9-interacting proteins were validated for their association with Card9 using a variety of biochemical techniques and were functionally characterized[69].

In order to further elucidate the molecular mechanisms of CLR signaling, especially to identify receptor proximal events that link the tyrosine kinase Syk to Card9 we determined inducibly tyrosine phosphorylated proteins in response to CLR activation via mass spectrometry[34]. In parallel, we used a targeted genetic approach to investigate proteins, which were already known to be involved in other ITAM receptor pathways, for their potential role in CLR signaling. In particular, we analyzed inflammatory responses in myeloid cells derived from mice with targeted deficiencies in those signaling proteins, including the Vav family[70].

Besides inducing proinflammatory cytokines, recently fungal infections have been shown to lead to type I IFN production[71, 72]. Yet, the involved receptors and signaling mechanisms remain unclear. To explore the mechanisms how fungal infections induce IFN responses we

mapped the signaling pathway using mice lacking specific PRRs and signaling adaptor proteins, respectively[73].

The results of these studies might contribute to our understanding of protective anti-fungal immune responses and inflammatory diseases, and potentially help to develop novel therapeutic strategies.

## 3. Results and discussion

### 3.1 Role of Card9 in cytosolic DNA-induced inflammatory responses

Whereas diverse DNA sensing pathways important for type I interferon production have been discovered[6, 47], the understanding of DNA-induced inflammatory signaling and IL-1β production is still very limited but of prime importance. In fact, evolution has selected a specific inflammasome that mediates DNA-induced pro-IL-1β processing, the AIM2 inflammasome[6, 47]. We have now identified a key upstream mechanism for DNA-induced pro-IL-1β generation[69].

In a yeast two-hybrid screen with Card9 as bait we identified Rad50 as a potential Card9-interacting candidate. We confirmed the association of Rad50 with Card9 via bioluminescence resonance energy transfer (BRET) and co-immunoprecipitation experiments of endogenously expressed proteins[69]. So far Rad50 has been most intensively studied as a component of the Mre11-Rad50-Nbs1 (MRN) complex that plays a prominent role in the DNA damage response (DDR)[74]. Two Rad50 nucleotide-binding motifs at its N- and C-terminus together with two Mre11 nucleases form a globular DNA-binding structure. The interjacent amino acids of the Rad50 molecule constitute a long (~500 Å) flexible anti-parallel coiled-coil with an apical zinc-hook motif. Nbs1 associates with the globular core complex. This evolutionarily highly conserved protein complex can detect DNA double-strand breaks[74, 75] and initiate signaling cascades to DNA repair and DDR by activating the transducing kinases ataxia-teleangiectasia mutated (ATM) or ATM- and Rad3-related (ATR). Since it has been previously shown that the $Mre11_2Rad50_2$ core complex binds DNA[74], we investigated whether Rad50 links DNA recognition to Card9 engagement. DNA pull-down experiments combined with immunodepletion of Rad50 revealed that Card9 associated with double-stranded DNA (dsDNA) selectively in the presence of Rad50, indicating that Rad50 is essential to bridge DNA binding to Card9. Mapping experiments demonstrated that Rad50-

14

Card9 interactions involved the Rad50 zinc-hook region that is separated from its DNA-binding domains. In addition, immunofluorescence microscopy showed that Rad50 indeed associates with Card9 under physiological conditions. Cytosolic dsDNA initiated the interaction of Rad50 and Card9 in the cytoplasm[69]. In the steady state Mre11 and Rad50 are mainly localized in the nucleus[76]. Yet, previous studies have shown that viral proteins can mediate relocalization of the MRN complex into cytoplasmic aggreates[77] and that Mre11 and Rad50 localize to dsDNA in the cytosol[78]. This is consistent with our results, showing that intracytoplasmic delivery of dsDNA or DNA virus infection induces rapid redistribution of Rad50 from the nucleus to the cytosol. Within two hours, nuclear levels of Rad50 are dramatically reduced and Rad50 mainly localizes to cytoplasmic dsDNA foci, which also contain Mre11 and Nbs1. To these foci the innate immune signaling adaptor proteins Card9 and Bcl10 are recruited[69].

Next we were interested whether this dsDNA-Rad50-Card9-Bcl10 complex formation might have a potential physiological role. Experiments with primary cells from a series of knockout mouse lines, uncovered the pathway how dsDNA triggers pro-IL-1β synthesis. Dendritic cells of Rad50-depleted, Card9$^{-/-}$ and Bcl10$^{-/-}$ mice were defective in cytosolic DNA-induced IL-1β production, whereas ATM$^{-/-}$ cells showed normal IL-1β responses[69]. These studies indicate that the DNA-sensing protein Rad50 couples to Card9 and Bcl10 for IL-1β generation, but that the transducing kinase ATM, which is essential for the DDR initiated by the MRN complex in the nucleus[74], is dispensable for this immune response.

Mechanistically, our data show that dsDNA-Rad50-Card9 complexes recruit Bcl10 for NF-κB activation. While NF-κB activation and pro-IL-1β production were defective in Card9- and Bcl10-deficient cells, interferon responses were normal. Cytosolic DNA-induced IRF3 phosphorylation and nuclear translocation, as well as IFN production were completely independent of Card9 and Bcl10[69]. Since these events are critically controlled by STING it seems that the Rad50-Card9-Bcl10 pathway does not affect the cGAS-STING signaling cascade. This notion is further supported by the fact that cGAMP-induced type I IFN production was independent of Card9. Moreover, Card9- or Bcl10-deficient cells were not impaired in caspase-1 activation upon DNA transfection, indicating that the Card9-Bcl10 signaling axis is not involved in DNA-triggered inflammasome activation[69]. Thus, our genetic results unequivocally demonstrate that the Rad50-Card9-Bcl10 pathway defines a specific signaling cascade for DNA-induced pro-IL-1β generation.

In this context it is also important to note that previous independent reports demonstrated that STING^{-/-} cells produce normal amounts of IL-1β upon DNA virus infection, although the IFN response was found to be completely defective[12]. Moreover, siRNA against STING did not affect DNA-induced IL-1β generation, whereas it dramatically diminished type I IFN, IL-6 and TNF production[17]. We confirmed that STING^{-/-} cells produce substantial amounts of IL-1β in response to cytosolic DNA, while they were defective in IFN generation[69]. Consistent with previously published data[12, 17], our results thus indicate that STING, is largely dispensable for IL-1β responses. It is interesting to note, that DNA-induced IL-6 and TNF production are profoundly affected by the lack of STING, whereas these responses are only partially diminished in Card9- or Bcl10-deficient cells[69]. Therefore, it seems that STING-dependent signaling pathways might regulate certain NF-κB-controlled responses distinct from IL-1β.

While this work was ongoing an independent study supposed that Mre11 and Rad50 association with transfected dsDNA in the cytoplasm might regulate STING trafficking[78]. Kondo et al. implicated that Rad50 mediates IFN responses using cell line transfection models and siRNA. We now demonstrate in primary gene deficient cells, that the Rad50-Card9-Bcl10 axis is specifically involved in NF-κB activation upon cytosolic DNA recognition, but dispensable for IRF activation or IFN production[69]. Still, it is conceivable, that Rad50 could couple to STING in a Card9-independent manner. However, multiple additional upstream regulators of the IFN response have also been proposed including DAI, IFI16 and DDX41, but recent genetic data demonstrated that cGAS is the sine qua non activator of the STING pathway[14, 15, 47].

Cytosolic DNA seems to trigger several parallel signaling pathways, including activation of STING for type I IFN production, induction of autophagy through p62 and NDP52, stimulation of apoptosis or necrosis via caspase-9 or RIP3, and AIM2 inflammasome formation for maturation of pro-IL-1β[6, 47]. Our data now indicate another potentially STING-independent signaling cascade upon dsDNA recognition in the cytoplasm. Thus, Card9 seems to be indeed multifunctionally engaged by several innate immune signaling pathways, including CLRs, Nod-2, RIG-I[4] and Rad50. Similar observations have been made for most intracellular signaling molecules (MyD88, TBK1 and many others), which are also involved in a variety of PRR pathways.

In vivo infection experiments further supported a physiologically relevant function of Card9 in DNA virus induced IL-1β generation and anti-viral CD8 T cell responses[69]. IL-1β responses provide security checkpoints for anti-viral immunity particularly under circumstances in which

viruses subvert the IFN system[79, 80]. In addition, IL-1β generation upon viral infection is important for optimal anti-viral CD8 T cell responses[81, 82]. Moreover, several viruses have evolved strategies to inhibit IL-1β production and IL-1β signaling[79, 80, 83], demonstrating that IL-1β provides an anti-viral selective pressure. In this respect it is interesting to note, that several DNA viruses, including adenoviruses, have developed strategies to inhibit Rad50 signaling, suggesting that the Rad50 pathway could be a target for viral subversion[84, 85].

IL-1β is a very potent cytokine, which is tightly controlled, but when deregulated can lead to autoinflammation. The pathological importance of IL-1β in autoinflammatory diseases is best supported by the efficacy of IL-1β blocking therapies[5]. Because endogenous, cytosolic DNA triggers pathological IL-1β responses in autoimmunity[86, 87, 88], it will be important to explore the contributions of Rad50-Card9 signaling under those conditions. Ultimately, such studies may lead to the development of novel rational therapies for infections or inflammatory diseases.
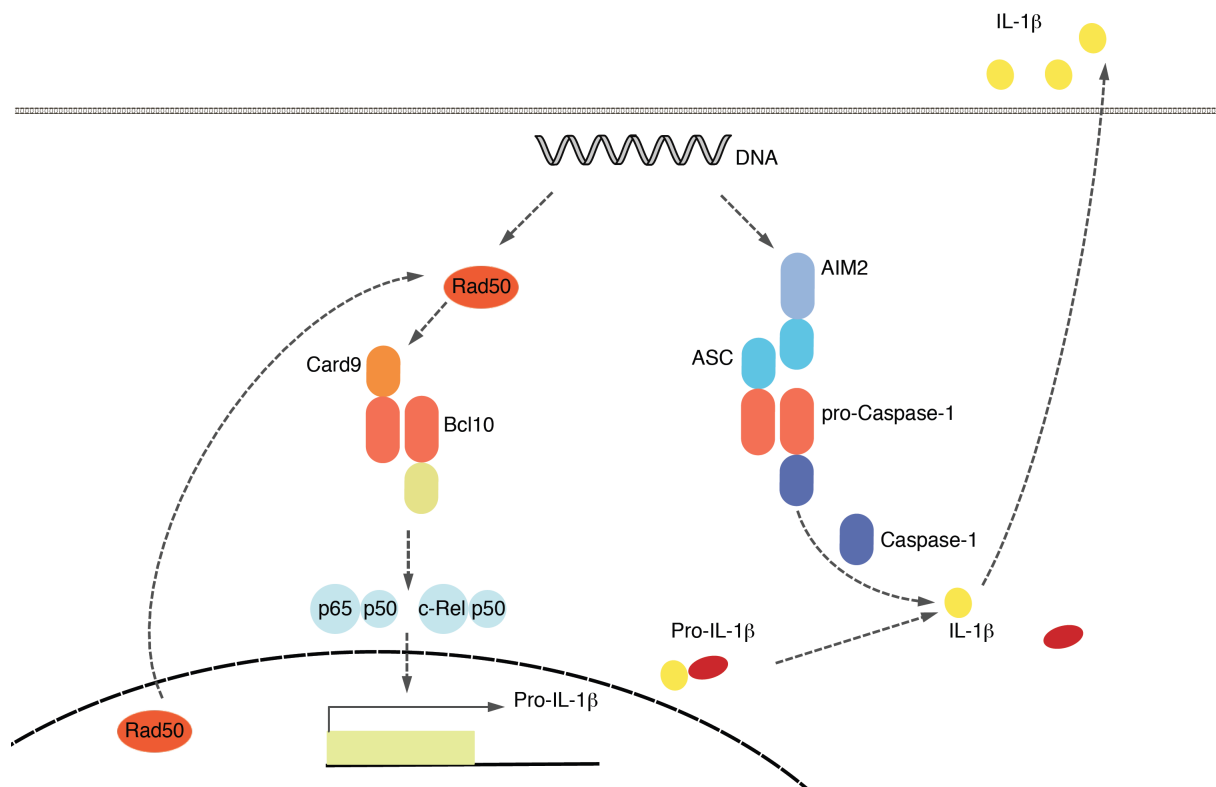


**Figure 4. Cytosolic DNA-induced IL-1β responses.** Rad50 recognizes cytosolic DNA, relocates from the nucleus to the cytoplasm, and associates with Card9, which further recruits Bcl10 for NF-κB activation and pro-IL-1β transcription. In parallel, DNA-triggered

AIM2 inflammasome formation activates caspase-1 for processing of pro-IL-1β to biologically active IL-1β.

## 3.2 Vav proteins control Syk-coupled C-type lectin receptor triggered inflammatory responses via Card9-Bcl10-Malt1 signalosomes

The incidence of fungal infections has dramatically increased, related to rising numbers of patients at risk, due to HIV infection, antineoplastic and immunosuppressive therapy, broad-spectrum antibiotics, implantation of alloplastic materials, or central venous access in medicine. Candida species are the most prevalent opportunistic fungi causing superficial and invasive disease. Since effective anti-fungal therapies for the treatment of systemic mycoses are lacking, the mortality rates are still very high[89, 90]. Elucidating the molecular mechanisms involved in anti-fungal immune defense will enable the development of novel therapeutic strategies. Recent evidence indicates that CLR-Card9 signaling is of central importance in host protection against fungi[4, 50]. Yet, the molecular mechanisms that connect Syk-coupled CLR activation to effector pathways are incompletely understood. Our data now demonstrate that signals from Syk-coupled CLRs converge on Vav proteins for NF-κB activation and inflammatory responses, essential for anti-fungal immunity in mice and humans[70].

To identify potential signaling intermediates that are regulated by the tyrosine kinase Syk in response to CLR activation, we used an unbiased proteomic approach determining inducibly tyrosine phosphorylated proteins after zymosan stimulation in bone marrow-derived dendritic cells (BMDCs)[34]. Interestingly, Vav1 and Vav3 were among the identified potential candidates[70]. Phosphorylation of Vav1 at Tyr174 has been previously shown to occur downstream of different ITAM receptors in a Src and Syk kinase dependent-manner, leading to a conformational change of Vav1 and activation of its guanine-nucleotide exchange factor (GEF) activity[91, 92, 93]. Consistently, *C. albicans* infection of dendritic cells triggered Vav Tyr174 phosphorylation via Src and Syk[70].

Functional analysis of Vav proteins in Candida infected dendritic cells revealed that the Vav family was absolutely essential for regulating inflammatory responses. We further determined the individual role of all three Vav isoforms in distinct Syk-coupled CLR signaling pathways. Our results demonstrated that Vav proteins specifically control cytokine production following Dectin-1, Dectin-2, or Mincle activation. Like within other ITAM receptor pathways, Vav

isoforms seem to be at least partially redundant in CLR-triggered inflammatory responses. Notably, Vav3 appears to have the strongest impact on CLR signaling[70]. We thus discovered a novel crucial role of Vav family proteins in innate immunity, which complements their well-known functions in phagocytosis and ROS production[91, 94, 95, 96].

Mechanistically, we identified that Vav regulates Candida-induced activity of the CBM complex, as determined by Malt1 paracaspase function, and controls NF-κB activation, essential for reprogramming gene expression. In contrast to the central role of the Vav family in regulating Candida-induced NF-κB signaling, MAPK and inflammasome activation are not affected by the loss of all three Vav isoforms[70], indicating that Vav controls only specific subsets of CLR-triggered innate immune responses.

The functional relevance of Vav proteins in inflammatory responses to CLR ligands was also confirmed in vivo. A previous study has shown that the mycobacterial cord factor TDM induces inflammation in mice via Mincle[22]. Interestingly, mice lacking all three Vav isoforms were almost completely defective in cytokine production following systemic administration of TDM. Moreover, inflammatory responses after *C. albicans* infections were largely impaired in Vav triple knockout animals[70]. These results together indicate that the Vav family, similar to components of the CBM complex, is absolutely essential for Syk-coupled CLR-mediated cytokine production in vitro and in vivo.

The central role of CLR-Card9 signaling and cytokine responses in anti-fungal host defense is well-established[4, 97]. Recently, it has been shown that Vav-deficient mice are highly susceptible to systemic Candida infections[95, 96]. Our results confirm and extend these previous reports by determining the individual role of all three Vav isoforms. Intriguingly, their relative functional importance in anti-fungal host defense mirrors their impact on CLR-induced inflammatory responses in vitro[70]. In this regard it is interesting to note that Vav3 potentially is the most important isoform for host protection. However, the specific mechanisms how Vav controls fungal infection in vivo remain unclear. Although defective inflammatory responses probably contribute to the impaired anti-fungal defense, diminished phagocytosis and ROS production might also be involved.

Excitingly, the importance of Vav proteins in anti-fungal immunity is validated by our identification of a SNP in the gene encoding *VAV3* that is significantly associated with susceptibility to candidemia in humans[70]. Since Syk-coupled CLRs detect structures derived

19

from a variety of pathogens as well as endogenous ligands[19, 29], our results might have implications beyond anti-fungal immunity.

## 3.3 Dectin-1-Syk-Card9-IRF5 signaling regulates Interferon-β responses in anti-fungal immunity

Type I interferons are best known for their essential role in immunity against viruses and intracellular bacteria by regulating cellular intrinsic antiviral effector mechanisms and orchestrating innate and adaptive immune responses[98, 99]. Several PRRs have been shown to initiate signaling cascades leading to the activation of IFN response factors, especially IRF3 and IRF7, which regulate IFN-I gene expression[98, 99]. Recent evidence indicates that not only viruses and bacteria, but also fungi induce IFN-I production[71, 72]. However, the mechanisms and physiological role of anti-fungal interferon responses remain unclear. Here we discovered a novel pathway that controls Candida-induced IFNβ production via Dectin-1 and Dectin-2, which requires Syk, Card9 and IRF5[73]. Thus our data expand the group of IFN-inducing PRR families by Syk-coupled CLRs.

To get insight into the receptors and molecular mechanisms involved in Candida-triggered type I IFN responses, we determined the role of potentially important PRRs and signaling molecules by genetic experiments using targeted knockout mice. *C. albicans* structures have been shown to be recognized by Syk-coupled CLRs and some TLRs[100]. In contrast to two previous reports, which proposed an important role of TLR7 and TLR9 for fungal-induced IFNβ production[71, 72], our data clearly demonstrate that Candida induces type I IFN mainly via Dectin-1 and Dectin-2, with a minor contribution of TLR2[73]. These apparently conflicting results might rely on differences in cell wall composition among distinct Candida species and strains. Previously it has been shown already that the relative functional importance of specific Syk-coupled CLRs in anti-fungal defense varies depending on the particular Candida strain[29, 101, 102]. In this regard it is interesting to note, that the specific Dectin-1 ligand curdlan induced considerable amounts of IFNβ, indicating that in principal selective Dectin-1 activation is able to trigger type I IFN responses. Further pathway analyses revealed that Syk was absolutely required for Dectin-1-induced IFN production[73]. Since NF-κB contributes to transcriptional activation of the *IFNβ* gene[103] and Card9 is the central signaling adaptor that regulates CLR-induced NF-κB activity[4, 33], we determined the role of Card9 in IFNβ production. Interestingly, curdlan or Candida-induced type I IFN responses were almost

completely inhibited by the lack of Card9 or Syk, while in Dectin-1-deficient cells residual amounts of IFNβ were generated[73], indicating functional redundancy at the receptor level and a potential involvement of other Syk-coupled CLRs. Similar redundancy of CLRs is known for inflammatory cytokine responses[4]. Besides Dectin-1, Dectin-2 seems to be equally important for Candida-induced IFNβ production, while Mincle is apparently not involved[73].

IRF3 and IRF7 are essential for type I IFN production upon recognition of viral or bacterial infection by TLRs or cytosolic PRRs[98, 99]. Surprisingly, Dectin-1 induced IFNβ production was independent of IRF3 and IRF7, while it required IRF5[73]. A role of IRF5 in pathogen-induced type I IFN responses has only recently been proposed[104, 105]. Interestingly, a recent study indicated that IRF5 is activated by IKKβ[106], which centrally controls NF-κB activity downstream of the CBM complex, indicating that the CBM signalosome might regulate via IKKβ inflammatory cytokine and type I IFN responses.

The physiological importance of type I IFNs in anti-fungal host defense is supported by our in vivo results demonstrating an increased susceptibility of IFNAR$^{-/-}$ mice to Candida infections[73], consistent with previous studies[71, 107]. However, IFN responses might also have detrimental effects in fungal infections[72, 108]. Beneficial versus harmful properties of type I IFNs have also been reported for viral or bacterial infections[98, 99]. Yet, a recent study indicates that type I IFNs contribute to anti-fungal host protection in humans. Defective expression of genes in the type I interferon pathways was associated with chronic mucocutaneous candidiasis[109].


## 4. Summary of each publication and individual contribution of the candidate

### 4.1 Rad50-Card9 interactions link cytosolic DNA sensing to IL-1β production

The appearance of dsDNA in the cytoplasm is highly immunogenic as it triggers potent inflammatory pathways that culminate in the production of IL-1β and type I interferons[6]. These responses are part of the regular defense against viruses but, under pathological conditions, can trigger inflammatory disease. Our understanding of the innate immune response to DNA is incomplete. Here we discovered a surprising direct interaction between the DNA-binding protein Rad50, which is also involved in the eukaryotic DNA double-strand break response, and the innate immune signaling adapter Card9[69]. Rad50 is recruited to cytosolic dsDNA upon DNA transfection or DNA virus infection and couples to Card9 binding,

resulting in the formation of distinct dsDNA/Rad50/Card9 signalosomes. These complexes further recruit the downstream effector Bcl10, leading to selective activation of the inflammatory NF-κB signaling cascade. This mechanism is crucial for DNA-induced pro-IL-1β synthesis and IL-1β production and is distinct from AIM2 inflammasome activation or cGAS-STING-mediated IFN control[69]. Experiments in primary Rad50-, Card9-, Bcl10-, STING- and ATM-deficient cells revealed the mechanism and the hierarchy of the Rad50/Card9/NF-κB signaling cascade. Rad50, Card9 or Bcl10-deficient dendritic cells were defective in IL-1β generation upon viral, bacterial, mammalian or synthetic DNA recognition and Card9^{-/-} mice presented severely impaired IL-1β responses upon DNA virus infection *in vivo*[69]. Thus, our results define a non-redundant DNA recognition pathway for inflammation and demonstrate a previously unrecognized connection between an evolutionary conserved DNA damage sensor and an innate immune signaling system.

Susanne Roth, Andrea Rottach, Heinrich Leonhardt and Jürgen Ruland designed the study. Susanne Roth, Andrea Rottach, Amelie S Lotz-Havla, Verena Laux, Andreas Muschaweckh and Katelynd Vanness did the experiments. Susanne Roth, Andrea Rottach, Amelie S Lotz-Havla, Søren W Gersting, Ania C Muntau, Karl-Peter Hopfner, Ingo Drexler, Heinrich Leonhardt and Jürgen Ruland analyzed the results. Susanne Roth, Andrea Rottach and Amelie S Lotz-Havla generated the figures. Lei Jin and John H J Petrini provided reagents. Susanne Roth and Jürgen Ruland wrote the paper.

**4.2 Vav Proteins Are Key Regulators of Card9 Signaling for Innate Antifungal Immunity**

Syk-coupled CLRs, including Dectin-1, Dectin-2, and Mincle, recognize structures present on a vast array of pathogens, especially fungi, and also detect endogenous damage associated molecules. These PRRs have an essential role in host defense, as well as in immune homeostasis. Activation of Syk-coupled CLRs upon ligand recognition triggers several signaling cascades in parallel, leading to phagocytosis, production of ROS and inflammatory cytokines[18, 19, 20]. ITAM-like motifs within their intracellular region or ITAM-containing signaling chains associated with Syk-coupled CLRs become phosphorylated by Src family kinases and constitute a docking site for the tyrosine kinase Syk. Syk then phosphorylates and thereby activates signaling intermediates, which regulate downstream pathways to MAPK and NF-κB activation for inflammatory responses. The Card9-Bcl10-Malt1 complex, which is regulated by PKCδ, controls Syk-coupled CLR-induced NF-κB activity[4, 18, 19]. Yet, the molecular

mechanisms linking Syk to Card9 signaling are incompletely understood. Here we identified the Vav family of proteins as central signaling intermediates for Syk-coupled CLR-induced NF-κB activation[70]. *C. albicans,* which is detected by Syk-coupled CLRs on myeloid cells, induces tyrosine phosphorylation of Vav1 via Src and Syk kinases. Vav proteins control Syk-coupled CLR-triggered inflammatory responses in vitro and in vivo, and are crucial for anti-fungal host defense[70]. Although distinct Vav isoforms are partially redundant, cells and mice lacking all three Vav family members are almost completely defective in Syk-coupled CLR-induced cytokine production. Excitingly, a *VAV3* single nucleotide polymorphism is associated with candidemia in humans. Mechanistically it seems that Vav proteins control CBM complex activity and NF-κB activation[70]. Together, our results define Vav proteins as central signaling hubs for CLR-induced NF-κB-dependent immune responses.

Susanne Roth and Jürgen Ruland designed the study. Susanne Roth, Hanna Bergmann, Martin Jaeger, Konstantin Neumann, and Paul-Albert Koenig performed experiments. Susanne Roth, Hanna Bergmann, Martin Jaeger, Konstantin Neumann, Paul-Albert Koenig, Mihai Netea, and Jürgen Ruland analyzed the results. Martin Jaeger, Vinod Kumar, Melissa Johnson, and Mihai Netea conducted patient sample collection and clinical data analyses. Assa Yeroslaviz and Bianca Habermann performed bioinformatic analyses. Susanne Roth, Martin Jaeger, and Assa Yeroslaviz generated the figures. Clarissa Prazeres da Costa, Lesley Vanes, Mauricio Menacho-Márquez, Victor L Tybulewicz, and Xosé R. Bustelo provided critical reagents. Susanne Roth and Jürgen Ruland wrote the paper.

## 4.3 Interferon-β Production via Dectin-1-Syk-IRF5 Signaling in Dendritic Cells Is Crucial for Immunity to *C. albicans*

Type I interferons are best known for their essential role in antiviral immunity by regulating anti-viral mechanisms within infected cells and by orchestrating adaptive immune responses. Several PRRs in different cellular compartments have been shown to induce IFNα/β expression mainly via IRF3/7 transcription factors[98, 99]. Recently fungi, especially Candida, have been identified to also induce type I interferon production. Depending on the fungal species or strain, type I interferons seem to have beneficial or detrimental effects on host protection[107, 108, 109]. However, the molecular events regulating fungal-induced IFN responses remain unclear. In the present study we discovered a new signaling pathway leading to type I interferon production upon recognition of fungi by myeloid cells[73]. In dendritic cells, *C.*

*albicans*-triggered IFNβ expression was mainly dependent on Dectin-1 and Dectin-2[73]. Thereby our data expand the class of type I IFN-inducing PRRs by Syk-coupled CLRs. Using the specific Dectin-1 ligand curdlan we further mapped the corresponding pathway. Dectin-1-induced IFNβ responses involved Syk-Card9-IRF5 signaling, and were independent of the transcription factors IRF3 and IRF7. IFNβ production was largely impaired in Dectin-1, Syk, Card9, or IRF5-deficient dendritic cells in response to curdlan or *C. albicans*, while it was intact in cells lacking IRF3, or IRF7. Interestingly, type I interferon receptor-deficient mice rapidly succumbed after systemic *C. albicans* infection, indicating a protective role of type I interferon responses in anti-fungal host defense[73]. Thus, our data describe a Dectin-1-Syk-Card9-IRF5 signaling pathway regulating type I interferon production, which is essential for anti-fungal immunity.

Susanne Roth had discovered in independent experiments that Dectin-1 activation induces type I interferon responses in a Card9-dependent manner. After being contacted by Carlos Ardavín we contributed our results to a joint manuscript. Susanne Roth performed experiments, analyzed results and contributed to design and writing of the study.

## 5. References

1.  Janeway CA, Jr. Approaching the asymptote? Evolution and revolution in immunology. *Cold Spring Harb Symp Quant Biol* 1989, **54 Pt 1:** 1-13.

2.  Medzhitov R. Approaching the asymptote: 20 years later. *Immunity* 2009, **30**(6)**:** 766-775.

3.  Takeuchi O, Akira S. Pattern recognition receptors and inflammation. *Cell* 2010, **140**(6)**:** 805-820.

4.  Roth S, Ruland J. Caspase recruitment domain-containing protein 9 signaling in innate immunity and inflammation. *Trends Immunol* 2013, **34**(6)**:** 243-250.

5.  Dinarello CA, Simon A, van der Meer JW. Treating inflammation by blocking interleukin-1 in a broad spectrum of diseases. *Nat Rev Drug Discov* 2012, **11**(8)**:** 633-652.

6.  Paludan SR, Bowie AG. Immune sensing of DNA. *Immunity* 2013, **38**(5)**:** 870-880.

7.  Strowig T, Henao-Mejia J, Elinav E, Flavell R. Inflammasomes in health and disease. *Nature* 2012, **481**(7381)**:** 278-286.

8.  Rotem Z, Cox RA, Isaacs A. Inhibition of virus multiplication by foreign nucleic acid. *Nature* 1963, **197:** 564-566.

9.  Hemmi H, Takeuchi O, Kawai T, Kaisho T, Sato S, Sanjo H*, et al.* A Toll-like receptor recognizes bacterial DNA. *Nature* 2000, **408**(6813)**:** 740-745.

10. Dempsey A, Bowie AG. Innate immune recognition of DNA: A recent history. *Virology* 2015, **479-480:** 146-152.

11. Ishikawa H, Barber GN. STING is an endoplasmic reticulum adaptor that facilitates innate immune signalling. *Nature* 2008, **455**(7213)**:** 674-678.

12. Ishikawa H, Ma Z, Barber GN. STING regulates intracellular DNA-mediated, type I interferon-dependent innate immunity. *Nature* 2009, **461**(7265)**:** 788-792.

13. Tanaka Y, Chen ZJ. STING specifies IRF3 phosphorylation by TBK1 in the cytosolic DNA signaling pathway. *Sci Signal* 2012, **5**(214)**:** ra20.

14. Sun L, Wu J, Du F, Chen X, Chen ZJ. Cyclic GMP-AMP synthase is a cytosolic DNA sensor that activates the type I interferon pathway. *Science* 2013, **339**(6121)**:** 786-791.

15. Wu J, Sun L, Chen X, Du F, Shi H, Chen C*, et al.* Cyclic GMP-AMP is an endogenous second messenger in innate immune signaling by cytosolic DNA. *Science* 2013, **339**(6121)**:** 826-830.

16.    Li XD, Wu J, Gao D, Wang H, Sun L, Chen ZJ. Pivotal roles of cGAS-cGAMP signaling in antiviral defense and immune adjuvant effects. *Science* 2013, **341**(6152)**:** 1390-1394.

17.    Zhang Z, Yuan B, Bao M, Lu N, Kim T, Liu YJ. The helicase DDX41 senses intracellular DNA mediated by the adaptor STING in dendritic cells. *Nat Immunol* 2011, **12**(10)**:** 959-965.

18.    Kerrigan AM, Brown GD. Syk-coupled C-type lectin receptors that mediate cellular activation via single tyrosine based activation motifs. *Immunol Rev* 2010, **234**(1)**:** 335-352.

19.    Sancho D, Sousa CRE. Signaling by Myeloid C-Type Lectin Receptors in Immunity and Homeostasis. *Annual Review of Immunology, Vol 30* 2012, **30:** 491-529.

20.    Kerrigan AM, Brown GD. Syk-coupled C-type lectins in immunity. *Trends Immunol* 2011, **32**(4)**:** 151-156.

21.    van den Berg LM, Gringhuis SI, Geijtenbeek TB. An evolutionary perspective on C-type lectins in infection and immunity. *Ann N Y Acad Sci* 2012, **1253:** 149-158.

22.    Ishikawa E, Ishikawa T, Morita YS, Toyonaga K, Yamada H, Takeuchi O*, et al.* Direct recognition of the mycobacterial glycolipid, trehalose dimycolate, by C-type lectin Mincle. *J Exp Med* 2009, **206**(13)**:** 2879-2888.

23.    Schoenen H, Bodendorfer B, Hitchens K, Manzanero S, Werninghaus K, Nimmerjahn F*, et al.* Cutting edge: Mincle is essential for recognition and adjuvanticity of the mycobacterial cord factor and its synthetic analog trehalose-dibehenate. *J Immunol* 2010, **184**(6)**:** 2756-2760.

24.    Werninghaus K, Babiak A, Gross O, Holscher C, Dietrich H, Agger EM*, et al.* Adjuvanticity of a synthetic cord factor analogue for subunit Mycobacterium tuberculosis vaccination requires FcRgamma-Syk-Card9-dependent innate immune activation. *J Exp Med* 2009, **206**(1)**:** 89-97.

25.    Chen ST, Lin YL, Huang MT, Wu MF, Cheng SC, Lei HY*, et al.* CLEC5A is critical for dengue-virus-induced lethal disease. *Nature* 2008, **453**(7195)**:** 672-676.

26.    Ritter M, Gross O, Kays S, Ruland J, Nimmerjahn F, Saijo S*, et al.* Schistosoma mansoni triggers Dectin-2, which activates the Nlrp3 inflammasome and alters adaptive immune responses. *Proc Natl Acad Sci U S A* 2010, **107**(47)**:** 20459-20464.

27.    Ahrens S, Zelenay S, Sancho D, Hanc P, Kjaer S, Feest C*, et al.* F-actin is an evolutionarily conserved damage-associated molecular pattern recognized by DNGR-1, a receptor for dead cells. *Immunity* 2012, **36**(4)**:** 635-645.

28.    Zhang JG, Czabotar PE, Policheni AN, Caminschi I, Wan SS, Kitsoulis S*, et al.* The dendritic cell receptor Clec9A binds damaged cells via exposed actin filaments. *Immunity* 2012, **36**(4)**:** 646-657.

29.    Osorio F, Reis e Sousa C. Myeloid C-type lectin receptors in pathogen recognition and host defense. *Immunity* 2011, **34**(5)**:** 651-664.

30. Goodridge HS, Reyes CN, Becker CA, Katsumoto TR, Ma J, Wolf AJ, *et al.* Activation of the innate immune receptor Dectin-1 upon formation of a 'phagocytic synapse'. *Nature* 2011, **472**(7344)**:** 471-475.

31. Gross O, Poeck H, Bscheider M, Dostert C, Hannesschlager N, Endres S, *et al.* Syk kinase signalling couples to the Nlrp3 inflammasome for anti-fungal host defence. *Nature* 2009, **459**(7245)**:** 433-436.

32. Mocsai A, Ruland J, Tybulewicz VL. The SYK tyrosine kinase: a crucial player in diverse biological functions. *Nat Rev Immunol* 2010, **10**(6)**:** 387-402.

33. Gross O, Gewies A, Finger K, Schafer M, Sparwasser T, Peschel C, *et al.* Card9 controls a non-TLR signalling pathway for innate anti-fungal immunity. *Nature* 2006, **442**(7103)**:** 651-656.

34. Strasser D, Neumann K, Bergmann H, Marakalala MJ, Guler R, Rojowska A, *et al.* Syk Kinase-Coupled C-type Lectin Receptors Engage Protein Kinase C-delta to Elicit Card9 Adaptor-Mediated Innate Immunity. *Immunity* 2012.

35. Gringhuis SI, Wevers BA, Kaptein TM, van Capel TM, Theelen B, Boekhout T, *et al.* Selective C-Rel activation via Malt1 controls anti-fungal T(H)-17 immunity by dectin-1 and dectin-2. *PLoS Pathog* 2011, **7**(1)**:** e1001259.

36. Gringhuis SI, den Dunnen J, Litjens M, van der Vlist M, Wevers B, Bruijns SC, *et al.* Dectin-1 directs T helper cell differentiation by controlling noncanonical NF-kappaB activation through Raf-1 and Syk. *Nat Immunol* 2009, **10**(2)**:** 203-213.

37. Bertin J, Guo Y, Wang L, Srinivasula SM, Jacobson MD, Poyet JL, *et al.* CARD9 is a novel caspase recruitment domain-containing protein that interacts with BCL10/CLAP and activates NF-kappa B. *J Biol Chem* 2000, **275**(52)**:** 41082-41086.

38. Hara H, Saito T. CARD9 versus CARMA1 in innate and adaptive immunity. *Trends Immunol* 2009, **30**(5)**:** 234-242.

39. Bezbradica JS, Medzhitov R. Role of ITAM signaling module in signal integration. *Curr Opin Immunol* 2012, **24**(1)**:** 58-66.

40. LeibundGut-Landmann S, Gross O, Robinson MJ, Osorio F, Slack EC, Tsoni SV, *et al.* Syk- and CARD9-dependent coupling of innate immunity to the induction of T helper cells that produce interleukin 17. *Nat Immunol* 2007, **8**(6)**:** 630-638.

41. Robinson MJ, Osorio F, Rosas M, Freitas RP, Schweighoffer E, Gross O, *et al.* Dectin-2 is a Syk-coupled pattern recognition receptor crucial for Th17 responses to fungal infection. *J Exp Med* 2009, **206**(9)**:** 2037-2051.

42. Saijo S, Ikeda S, Yamabe K, Kakuta S, Ishigame H, Akitsu A, *et al.* Dectin-2 recognition of alpha-mannans and induction of Th17 cell differentiation is essential for host defense against Candida albicans. *Immunity* 2010, **32**(5)**:** 681-691.

43. Wells CA, Salvage-Jones JA, Li X, Hitchens K, Butcher S, Murray RZ, *et al.* The macrophage-inducible C-type lectin, mincle, is an essential component of the innate immune response to Candida albicans. *J Immunol* 2008, **180**(11)**:** 7404-7413.

44.    Dorhoi A, Desel C, Yeremeev V, Pradl L, Brinkmann V, Mollenkopf HJ*, et al.* The adaptor molecule CARD9 is essential for tuberculosis control. *J Exp Med* 2010, **207**(4)**:** 777-792.

45.    Saleh M. The machinery of Nod-like receptors: refining the paths to immunity and cell death. *Immunol Rev* 2011, **243**(1)**:** 235-246.

46.    Hsu YM, Zhang Y, You Y, Wang D, Li H, Duramad O*, et al.* The adaptor protein CARD9 is required for innate immune responses to intracellular pathogens. *Nat Immunol* 2007, **8**(2)**:** 198-205.

47.    Wu J, Chen ZJ. Innate immune sensing and signaling of cytosolic nucleic acids. *Annu Rev Immunol* 2014, **32:** 461-488.

48.    Poeck H, Bscheider M, Gross O, Finger K, Roth S, Rebsamen M*, et al.* Recognition of RNA virus by RIG-I results in activation of CARD9 and inflammasome signaling for interleukin 1 beta production. *Nat Immunol* 2010, **11**(1)**:** 63-69.

49.    Abdullah Z, Schlee M, Roth S, Mraheil MA, Barchet W, Bottcher J*, et al.* RIG-I detects infection with live Listeria by sensing secreted bacterial nucleic acids. *EMBO J* 2012, **31**(21)**:** 4153-4164.

50.    Perez de Diego R, Sanchez-Ramon S, Lopez-Collazo E, Martinez-Barricarte R, Cubillos-Zapata C, Ferreira Cerdan A*, et al.* Genetic errors of the human caspase recruitment domain-B-cell lymphoma 10-mucosa-associated lymphoid tissue lymphoma-translocation gene 1 (CBM) complex: Molecular, immunologic, and clinical heterogeneity. *J Allergy Clin Immunol* 2015.

51.    Glocker EO, Hennigs A, Nabavi M, Schaffer AA, Woellner C, Salzer U*, et al.* A homozygous CARD9 mutation in a family with susceptibility to fungal infections. *N Engl J Med* 2009, **361**(18)**:** 1727-1735.

52.    Cunha C, Di Ianni M, Bozza S, Giovannini G, Zagarella S, Zelante T*, et al.* Dectin-1 Y238X polymorphism associates with susceptibility to invasive aspergillosis in hematopoietic transplantation through impairment of both recipient- and donor-dependent mechanisms of antifungal immunity. *Blood* 2010, **116**(24)**:** 5394-5402.

53.    Ferwerda B, Ferwerda G, Plantinga TS, Willment JA, van Spriel AB, Venselaar H*, et al.* Human dectin-1 deficiency and mucocutaneous fungal infections. *N Engl J Med* 2009, **361**(18)**:** 1760-1767.

54.    Plantinga TS, van der Velden WJ, Ferwerda B, van Spriel AB, Adema G, Feuth T*, et al.* Early stop polymorphism in human DECTIN-1 is associated with increased candida colonization in hematopoietic stem cell transplant recipients. *Clin Infect Dis* 2009, **49**(5)**:** 724-732.

55.    Van Limbergen J, Wilson DC, Satsangi J. The genetics of Crohn's disease. *Annu Rev Genomics Hum Genet* 2009, **10:** 89-116.

56.    Beaugerie L, Itzkowitz SH. Cancers complicating inflammatory bowel disease. *N Engl J Med* 2015, **372**(15)**:** 1441-1452.

57. Zhernakova A, Festen EM, Franke L, Trynka G, van Diemen CC, Monsuur AJ*, et al.* Genetic analysis of innate immunity in Crohn's disease and ulcerative colitis identifies two susceptibility loci harboring CARD9 and IL18RAP. *Am J Hum Genet* 2008, **82**(5)**:** 1202-1210.

58. Franke A, McGovern DP, Barrett JC, Wang K, Radford-Smith GL, Ahmad T*, et al.* Genome-wide meta-analysis increases to 71 the number of confirmed Crohn's disease susceptibility loci. *Nat Genet* 2010, **42**(12)**:** 1118-1125.

59. McGovern DP, Gardet A, Torkvist L, Goyette P, Essers J, Taylor KD*, et al.* Genome-wide association identifies multiple ulcerative colitis susceptibility loci. *Nat Genet* 2010, **42**(4)**:** 332-337.

60. Cooke J, Zhang H, Greger L, Silva AL, Massey D, Dawson C*, et al.* Mucosal genome-wide methylation changes in inflammatory bowel disease. *Inflamm Bowel Dis* 2012, **18**(11)**:** 2128-2137.

61. Lamas B, Richard ML, Leducq V, Pham HP, Michel ML, Da Costa G*, et al.* CARD9 impacts colitis by altering gut microbiota metabolism of tryptophan into aryl hydrocarbon receptor ligands. *Nat Med* 2016, **22**(6)**:** 598-605.

62. Rivas MA, Beaudoin M, Gardet A, Stevens C, Sharma Y, Zhang CK*, et al.* Deep resequencing of GWAS loci identifies independent rare variants associated with inflammatory bowel disease. *Nat Genet* 2011, **43**(11)**:** 1066-1073.

63. Sokol H, Conway KL, Zhang M, Choi M, Morin B, Cao Z*, et al.* Card9 mediates intestinal epithelial cell restitution, T-helper 17 responses, and control of bacterial infection in mice. *Gastroenterology* 2013, **145**(3)**:** 591-601 e593.

64. Iliev ID, Funari VA, Taylor KD, Nguyen Q, Reyes CN, Strom SP*, et al.* Interactions between commensal fungi and the C-type lectin receptor Dectin-1 influence colitis. *Science* 2012, **336**(6086)**:** 1314-1317.

65. Janse M, Lamberts LE, Franke L, Raychaudhuri S, Ellinghaus E, Muri Boberg K*, et al.* Three ulcerative colitis susceptibility loci are associated with primary sclerosing cholangitis and indicate a role for IL2, REL, and CARD9. *Hepatology* 2011, **53**(6)**:** 1977-1985.

66. Evans DM, Spencer CC, Pointon JJ, Su Z, Harvey D, Kochan G*, et al.* Interaction between ERAP1 and HLA-B27 in ankylosing spondylitis implicates peptide handling in the mechanism for HLA-B27 in disease susceptibility. *Nat Genet* 2011, **43**(8)**:** 761-767.

67. Pointon JJ, Harvey D, Karaderi T, Appleton LH, Farrar C, Stone MA*, et al.* Elucidating the chromosome 9 association with AS; CARD9 is a candidate gene. *Genes Immun* 2010, **11**(6)**:** 490-496.

68. Reveille JD. Genetics of spondyloarthritis--beyond the MHC. *Nat Rev Rheumatol* 2012, **8**(5)**:** 296-304.

69. Roth S, Rottach A, Lotz-Havla AS, Laux V, Muschaweckh A, Gersting SW*, et al.* Rad50-CARD9 interactions link cytosolic DNA sensing to IL-1beta production. *Nat Immunol* 2014, **15**(6)**:** 538-545.

70. Roth S, Bergmann H, Jaeger M, Yeroslaviz A, Neumann K, Koenig PA*, et al.* Vav Proteins Are Key Regulators of Card9 Signaling for Innate Antifungal Immunity. *Cell Rep* 2016, **17**(10)**:** 2572-2583.

71. Biondo C, Signorino G, Costa A, Midiri A, Gerace E, Galbo R*, et al.* Recognition of yeast nucleic acids triggers a host-protective type I interferon response. *Eur J Immunol* 2011, **41**(7)**:** 1969-1979.

72. Bourgeois C, Majer O, Frohner IE, Lesiak-Markowicz I, Hildering KS, Glaser W*, et al.* Conventional dendritic cells mount a type I IFN response against Candida spp. requiring novel phagosomal TLR7-mediated IFN-beta signaling. *J Immunol* 2011, **186**(5)**:** 3104-3112.

73. del Fresno C, Soulat D, Roth S, Blazek K, Udalova I, Sancho D*, et al.* Interferon-beta production via Dectin-1-Syk-IRF5 signaling in dendritic cells is crucial for immunity to C. albicans. *Immunity* 2013, **38**(6)**:** 1176-1186.

74. Stracker TH, Petrini JH. The MRE11 complex: starting from the ends. *Nat Rev Mol Cell Biol* 2011, **12**(2)**:** 90-103.

75. Petrini JH, Stracker TH. The cellular response to DNA double-strand breaks: defining the sensors and mediators. *Trends Cell Biol* 2003, **13**(9)**:** 458-462.

76. Maser RS, Monsen KJ, Nelms BE, Petrini JH. hMre11 and hRad50 nuclear foci are induced during the normal cellular response to DNA double-strand breaks. *Mol Cell Biol* 1997, **17**(10)**:** 6087-6096.

77. Chaurushiya MS, Weitzman MD. Viral manipulation of DNA repair and cell cycle checkpoints. *DNA Repair (Amst)* 2009, **8**(9)**:** 1166-1176.

78. Kondo T, Kobayashi J, Saitoh T, Maruyama K, Ishii KJ, Barber GN*, et al.* DNA damage sensor MRE11 recognizes cytosolic double-stranded DNA and induces type I interferon by regulating STING trafficking. *Proc Natl Acad Sci U S A* 2013, **110**(8)**:** 2969-2974.

79. Epperson ML, Lee CA, Fremont DH. Subversion of cytokine networks by virally encoded decoy receptors. *Immunol Rev* 2012, **250**(1)**:** 199-215.

80. Smith GL, Benfield CT, Maluquer de Motes C, Mazzon M, Ember SW, Ferguson BJ*, et al.* Vaccinia virus immune evasion: mechanisms, virulence and immunogenicity. *J Gen Virol* 2013.

81. Ben-Sasson SZ, Caucheteux S, Crank M, Hu-Li J, Paul WE. IL-1 acts on T cells to enhance the magnitude of in vivo immune responses. *Cytokine* 2011, **56**(1)**:** 122-125.

82. Staib C, Kisling S, Erfle V, Sutter G. Inactivation of the viral interleukin 1beta receptor improves CD8+ T-cell memory responses elicited upon immunization with modified vaccinia virus Ankara. *J Gen Virol* 2005, **86**(Pt 7)**:** 1997-2006.

83.     Zimmerling S, Waibler Z, Resch T, Sutter G, Schwantes A. Interleukin-1beta receptor expressed by modified vaccinia virus Ankara interferes with interleukin-1beta activity produced in various virus-infected antigen-presenting cells. *Virol J* 2013, **10:** 34.

84.     Lilley CE, Schwartz RA, Weitzman MD. Using or abusing: viruses and the cellular DNA damage response. *Trends Microbiol* 2007, **15**(3)**:** 119-126.

85.     Stracker TH, Carson CT, Weitzman MD. Adenovirus oncoproteins inactivate the Mre11-Rad50-NBS1 DNA repair complex. *Nature* 2002, **418**(6895)**:** 348-352.

86.     Boswell JM, Yui MA, Burt DW, Kelley VE. Increased tumor necrosis factor and IL-1 beta gene expression in the kidneys of mice with lupus nephritis. *J Immunol* 1988, **141**(9)**:** 3050-3054.

87.     Dombrowski Y, Peric M, Koglin S, Kammerbauer C, Goss C, Anz D*, et al.* Cytosolic DNA triggers inflammasome activation in keratinocytes in psoriatic lesions. *Sci Transl Med* 2011, **3**(82)**:** 82ra38.

88.     Popovic K, Ek M, Espinosa A, Padyukov L, Harris HE, Wahren-Herlenius M*, et al.* Increased expression of the novel proinflammatory cytokine high mobility group box chromosomal protein 1 in skin lesions of patients with lupus erythematosus. *Arthritis Rheum* 2005, **52**(11)**:** 3639-3645.

89.     Enoch DA, Ludlam HA, Brown NM. Invasive fungal infections: a review of epidemiology and management options. *J Med Microbiol* 2006, **55**(Pt 7)**:** 809-818.

90.     Gow NA, van de Veerdonk FL, Brown AJ, Netea MG. Candida albicans morphogenesis and host defence: discriminating invasion from colonization. *Nat Rev Microbiol* 2012, **10**(2)**:** 112-122.

91.     Shah VB, Ozment-Skelton TR, Williams DL, Keshvaraa L. Vav1 and PI3K are required for phagocytosis of beta-glucan and subsequent superoxide generation by microglia. *Mol Immunol* 2009, **46**(8-9)**:** 1845-1853.

92.     Turner M, Billadeau DD. VAV proteins as signal integrators for multi-subunit immune-recognition receptors. *Nature Reviews Immunology* 2002, **2**(7)**:** 476-486.

93.     Tybulewicz VL. Vav-family proteins in T-cell signalling. *Curr Opin Immunol* 2005, **17**(3)**:** 267-274.

94.     Graham DB, Stephenson LM, Lam SK, Brim K, Lee HM, Bautista J*, et al.* An ITAM-signaling pathway controls cross-presentation of particulate but not soluble antigens in dendritic cells. *Journal of Experimental Medicine* 2007, **204**(12)**:** 2889-2897.

95.     Li X, Utomo A, Cullere X, Choi MM, Milner DA, Jr., Venkatesh D*, et al.* The beta-glucan receptor Dectin-1 activates the integrin Mac-1 in neutrophils via Vav protein signaling to promote Candida albicans clearance. *Cell Host Microbe* 2011, **10**(6)**:** 603-615.

96.     Strijbis K, Tafesse FG, Fairn GD, Witte MD, Dougan SK, Watson N*, et al.* Bruton's Tyrosine Kinase (BTK) and Vav1 contribute to Dectin1-dependent phagocytosis of Candida albicans in macrophages. *PLoS Pathog* 2013, **9**(6)**:** e1003446.

97.     Vautier S, MacCallum DM, Brown GD. C-type lectin receptors and cytokines in fungal immunity. *Cytokine* 2012, **58**(1)**:** 89-99.

98.     Trinchieri G. Type I interferon: friend or foe? *J Exp Med* 2010, **207**(10)**:** 2053-2063.

99.     McNab F, Mayer-Barber K, Sher A, Wack A, O'Garra A. Type I interferons in infectious disease. *Nat Rev Immunol* 2015, **15**(2)**:** 87-103.

100.    Romani L. Immunity to fungal infections. *Nature Reviews Immunology* 2011, **11**(4)**:** 275-288.

101.    Saijo S, Fujikado N, Furuta T, Chung SH, Kotaki H, Seki K*, et al.* Dectin-1 is required for host defense against Pneumocystis carinii but not against Candida albicans. *Nat Immunol* 2007, **8**(1)**:** 39-46.

102.    Taylor PR, Tsoni SV, Willment JA, Dennehy KM, Rosas M, Findon H*, et al.* Dectin-1 is required for beta-glucan recognition and control of fungal infection. *Nat Immunol* 2007, **8**(1)**:** 31-38.

103.    Ford E, Thanos D. The transcriptional code of human IFN-beta gene expression. *Biochim Biophys Acta* 2010, **1799**(3-4)**:** 328-336.

104.    Gratz N, Hartweger H, Matt U, Kratochvill F, Janos M, Sigel S*, et al.* Type I interferon production induced by Streptococcus pyogenes-derived nucleic acids is required for host protection. *PLoS Pathog* 2011, **7**(5)**:** e1001345.

105.    Pandey AK, Yang Y, Jiang Z, Fortune SM, Coulombe F, Behr MA*, et al.* NOD2, RIP2 and IRF5 play a critical role in the type I interferon response to Mycobacterium tuberculosis. *PLoS Pathog* 2009, **5**(7)**:** e1000500.

106.    Lopez-Pelaez M, Lamont DJ, Peggie M, Shpiro N, Gray NS, Cohen P. Protein kinase IKKbeta-catalyzed phosphorylation of IRF5 at Ser462 induces its dimerization and nuclear translocation in myeloid cells. *Proc Natl Acad Sci U S A* 2014, **111**(49)**:** 17432-17437.

107.    Biondo C, Midiri A, Gambuzza M, Gerace E, Falduto M, Galbo R*, et al.* IFN-alpha/beta signaling is required for polarization of cytokine responses toward a protective type 1 pattern during experimental cryptococcosis. *J Immunol* 2008, **181**(1)**:** 566-573.

108.    Majer O, Bourgeois C, Zwolanek F, Lassnig C, Kerjaschki D, Mack M*, et al.* Type I interferons promote fatal immunopathology by regulating inflammatory monocytes and neutrophils during Candida infections. *PLoS Pathog* 2012, **8**(7)**:** e1002811.

109.    Smeekens SP, Ng A, Kumar V, Johnson MD, Plantinga TS, van Diemen C*, et al.* Functional genomics identifies type I interferon pathway as central for host defense against Candida albicans. *Nat Commun* 2013, **4:** 1342.

**Appendices**

A. *Nature Immunology* 2014, **15**(6)**:** 538-545

Roth S, Rottach A, Lotz-Havla AS, Laux V, Muschaweckh A, Gersting SW*, et al.* Rad50-CARD9 interactions link cytosolic DNA sensing to IL-1beta production. *Nat Immunol* 2014, **15**(6)**:** 538-545.

B. *Cell Reports* 2016, **17**(10)**:** 2572-2583

Roth S, Bergmann H, Jaeger M, Yeroslaviz A, Neumann K, Koenig PA*, et al.* Vav Proteins Are Key Regulators of Card9 Signaling for Innate Antifungal Immunity. *Cell Rep* 2016, **17**(10)**:** 2572-2583.

C. *Immunity* 2013, **38**(6)**:** 1176-1186

del Fresno C, Soulat D, Roth S, Blazek K, Udalova I, Sancho D*, et al.* Interferon-beta production via Dectin-1-Syk-IRF5 signaling in dendritic cells is crucial for immunity to C. albicans. *Immunity* 2013, **38**(6)**:** 1176-1186.

# Rad50-CARD9 interactions link cytosolic DNA sensing to IL-1β production

**Susanne Roth**[1], **Andrea Rottach**[2], **Amelie S. Lotz-Havla**[3], **Verena Laux**[1], **Andreas Muschaweckh**[4], **Søren W. Gersting**[3], **Ania C. Muntau**[3], **Karl-Peter Hopfner**[5], **Lei Jin**[6], **Katelynd Vanness**[7], **John H. J. Petrini**[7], **Ingo Drexler**[4,8], **Heinrich Leonhardt**[2], and **Jürgen Ruland**[1]

[1]Institut für Klinische Chemie und Pathobiochemie, Klinikum rechts der Isar, Technische Universität München, Ismaninger Str. 22, 81675 Munich, Germany

[2]Department Biology II and Center for integrated Protein Science Munich (CiPSM), Ludwig-Maximilians-Universität München, Großhaderner Str. 2-4, 82152 Martinsried, Germany

[3]Kinderklinik und Kinderpoliklinik im Dr. von Haunersches Kinderspital, Ludwig-Maximilians-Universität, Lindwurmstrasse 4, 80337 Munich, Germany

[4]Institut für Virologie, Klinikum rechts der Isar, Technische Universität München, and Helmholtz Zentrum München, German Research Centre for Environmental Health, Trogerstr. 30, 81675 Munich, Germany

[5]Gene Center and Center for integrated Protein Science Munich (CiPSM), Department of Biochemistry, Ludwig-Maximilians-Universität, Feodor-Lynen-Straße 25, 81377 Munich, Germany

[6]Center for Immunology and Microbial Disease, Albany Medical College, 47 New Scotland Avenue, Albany, NY 12208, USA

[7]Memorial Sloan-Kettering Cancer Center, 1275 York Avenue, New York, NY 10021, USA

[8]Institut für Virologie, Universitätsklinikum Düsseldorf, Heinrich Heine Universität, Universitätsstr. 1, 40225 Düsseldorf, Germany

## Abstract

Double-stranded DNA (dsDNA) in the cytoplasm triggers interleukin-1β (IL-1β) production as an anti-viral host response, and deregulation of the pathways involved can promote inflammatory disease. Here we report a direct cytosolic interaction between the DNA-damage sensor Rad50 and the innate immune adapter CARD9. Dendritic cell transfection with dsDNA or infection with a DNA virus induces the formation of dsDNA-Rad50-CARD9 signaling complexes for NF-κB activation and pro-IL-1β generation. Primary cells conditionally deficient for Rad50 or lacking

CARD9 consequently exhibit defective DNA-induced IL-1β production, and *Card9*^{−/−} mice have impaired inflammatory responses upon DNA virus infection *in vivo*. These results define a cytosolic DNA recognition pathway for inflammation and a physical and functional connection between a conserved DNA-damage sensor and the innate immune response to pathogens.

---

The appearance of double-stranded DNA (dsDNA) in the cytoplasm, which is normally a DNA-free environment, triggers potent inflammatory pathways that culminate in the production of interleukin-1β (IL-1β) and type 1 interferon (IFN). These innate immune responses alert the host to the presence of danger and are important for the regular defense against viruses and bacteria[1]. To recognize the aberrant localization of DNA, the immune system employs several cytosolic DNA receptors and associated signaling systems, which have in part overlapping and collaborative functions[1]. Central to the anti-viral IFN response is the endoplasmic reticulum-associated adaptor protein STING that is activated by the second messenger cGAMP, generated by the DNA sensor cGAS (cGAMP synthase)[2, 3]. STING subsequently engages the kinase TBK1 to mediate the phosphorylation and activation of IRF3 for IFN gene transcription[4]; in contrast, STING signaling is largely dispensable for IL-1β generation[5, 6].

The highly pro-inflammatory cytokine IL-1β provides additional security checkpoints for anti-viral immunity, particularly under circumstances in which viruses subvert the IFN system[7, 8]. IL-1β also couples innate viral recognition to anti-viral CD8^{+} T cell responses[9, 10], and, as an endogenous pyrogen, IL-1β is responsible for fever reactions during infection. Because aberrant IL-1β production can induce severe pathological conditions, its generation needs to be tightly controlled and involves at least two distinct signals[11]. The first signal for mature IL-1β generation triggers the transcriptional upregulation of pro-IL-1β mRNA, and the second signal results in the proteolytic processing of pro-IL-1β, typically by caspase-1, within inflammasomes. The specific inflammasome for DNA-induced IL-1β processing contains the cytosolic DNA sensor AIM2[1], which engages the common inflammasome adapter protein ASC for caspase-1 activation. The transcription of pro-IL-1β is mediated by NF-κB, which is retained in an inactive form in the cytosol in unstimulated cells by binding to inhibitory IκB proteins. The activation of NF-κB by most stimuli requires the IκB kinase (IKK)-mediated phosphorylation of IκB, resulting in its ubiquitin-mediated degradation and the subsequent translocation of NF-κB dimers to the nucleus[12]. However, the exact mechanism by which the NF-κB signaling module is activated upon cytosolic DNA sensing is not well understood, but assumed to involve STING.

One innate immune cell-specific adapter protein that relays signals from pattern recognition receptors (PRRs) to inflammatory responses is CARD9[13], which possesses an N-terminal caspase recruitment domain (CARD) for the recruitment of downstream effectors as well as a coiled-coil region for protein oligomerization. Similar to most signaling adapters[14], CARD9 is multifunctionally engaged by several receptor systems depending on the specific context. PRRs that connect to CARD9 include the transmembrane Syk-coupled C-type lectin receptors (CLRs) and such cytosolic sensors as RIG-I and Nod2[15, 16, 17, 18, 19].

Here, we report a direct cytosolic interaction between CARD9 and the DNA-binding protein Rad50, which is also prominently involved in the eukaryotic DNA damage response (DDR)[20]. Together with Mre11 and Nbs1, Rad50 can form a DNA receptor complex (the MRN complex) that detects DNA double-strand breaks in the nucleus, subsequently triggering pathways which are required to maintain genome integrity[20]. We found that cytoplasmic dsDNA delivery by DNA transfection or virus infection results in the formation of distinct dsDNA-Rad50-CARD9 complexes, which selectively induce NF-κB signaling for IL-1β production. Our results define a DNA recognition pathway for inflammation and demonstrate a previously unrecognized direct connection between an evolutionarily conserved DNA damage sensor that translocates to the cytoplasm and an innate immune signaling system.

## RESULTS

### CARD9 can directly interact with the DNA binding factor Rad50

To obtain insight into the role of CARD9 in innate immunity, we performed a yeast two-hybrid screen with full-length CARD9 as the bait and searched for interaction partners in a human peripheral blood-derived cDNA library. The screening of $9.9 \times 10^6$ transformants yielded 33 bait-dependent interactors, which were analyzed further. The protein with the most frequent CARD9 yeast two-hybrid interactions was Rad50 (data not shown).

To validate a potential direct CARD9-Rad50 association in a mammalian system, we performed bioluminescence resonance energy transfer (BRET) experiments in COS7 cells. As BRET donor to acceptor energy transfer can only occur within a distance of less than 100 Å, protein-protein interactions can be analyzed within the environment of a living cell[21]. CARD9 and Rad50 fragments were subcloned in-frame with *Renilla reniformis* luciferase (Rluc) as an energy donor or yellow fluorescent protein (YFP) as an energy acceptor fluorophore[21]. In parallel, we generated Rluc and YFP fusion proteins with the CARD9 binding partner Bcl10 as a positive control[19] and also with the inflammasome DNA sensor AIM2[1]. BRET ratios above the method-specific threshold for a binary protein-protein interaction[21] were observed for CARD9-Bcl10 and CARD9-Rad50, but not for CARD9-AIM2 (Fig. 1a). Subsequent saturation experiments revealed a hyperbolic increase in BRET ratios, with increasing acceptor-to-donor ratios for CARD9 and Rad50, thereby excluding random bystander BRET. These biophysical data confirm an association between CARD9 and Rad50 in mammalian cells (Fig. 1b). To identify the region within Rad50 that interacts with CARD9, we created several Rad50 deletion mutants and performed mapping experiments using BRET. The minimal region of Rad50 that is required for CARD9 binding comprises amino acids 628–786, which is the structural domain that includes the zinc hook[20] (Fig. 1a).

Next, we investigated whether endogenous non-tagged CARD9 and Rad50 proteins could bind to each other. Immunoprecipitation experiments in THP-1 cells showed that endogenous Rad50 co-immunoprecipitated with endogenous CARD9 and *vice versa* (Fig. 1c, d). Because Rad50 has DNA binding activity, we tested the possibility that Rad50 could link dsDNA recognition to CARD9 binding. Depletion of Rad50 by repeated treatment (three times) with an antibody against Rad50 in THP-1 cell lysates resulted in the efficient

depletion of Rad50, but did not affect the amount of CARD9 in these lysates (Fig. 1e). To pull down DNA-associated proteins, we immobilized dsDNA containing a genomic sequence from vaccinia virus (VV) to agarose beads. Subsequent precipitations in the presence of Rad50 revealed that CARD9 specifically co-purified with dsDNA-beads, but not with empty control beads (Fig. 1e). CARD9 did not interact with dsDNA in the absence of Rad50 (Fig. 1e), indicating that Rad50 is required for dsDNA binding to CARD9. Together, these results indicate that Rad50 can bridge DNA binding to CARD9 engagement.

## Rad50-CARD9 complexes sense dsDNA in the cytosol

We performed confocal microscopy to visualize the associations between dsDNA, Rad50 and CARD9 in primary immune cells and to investigate the cellular compartments in which these interactions occur (Fig. 2a, b). Fluorescent immunostaining of endogenous proteins revealed that, as expected, Rad50 was mainly localized to the nucleus in unstimulated bone marrow-derived dendritic cells (BMDCs)[22], whereas CARD9 exhibited a cytoplasmic distribution pattern[23] (Fig. 2a). The intracytoplasmic delivery of dsDNA resulted in the recruitment of Rad50 to dsDNA and in the formation of distinct dsDNA-Rad50 foci in the cytosol (Fig. 2a, b); these foci also contained Mre11 and Nbs1, indicating cytoplasmic dsDNA sensing by the entire MRN complex (Fig. 2c and Supplementary Fig. 1a, b). CARD9 was also recruited to the dsDNA-MRN complex aggregates and was specifically co-localized with Rad50 (Fig. 2a, b). Quantitative analysis showed Rad50-CARD9 complexes in all cells that contained cytoplasmic DNA upon transfection (Supplementary Fig. 1c, d). Cytoplasmic dsDNA-Rad50 complexes also formed in BMDCs from CARD9-deficient mice[15] (data not shown and Supplementary Fig. 1e), suggesting that the detection of cytoplasmic dsDNA by Rad50 is CARD9 independent. These findings indicate that CARD9 is secondarily recruited to DNA-sensing Rad50 complexes and suggest that the Rad50-mediated engagement of CARD9 potentially represents a signal for DNA-mediated immune responses.

## CARD9 and Rad50 control DNA-induced IL-1β generation

To test the potential functions of CARD9 complexes in DNA-induced innate immunity, we transfected BMDCs with different forms of DNA and measured cytokine production. The stimulation of wild-type BMDCs with either linear synthetic poly(dA:dT), poly(dG:dC), purified genomic calf thymus DNA (CT-DNA) or circular bacterial plasmid DNA (Plasmid) resulted in a robust production of mature IL-1β and type 1 IFN (Fig. 3a, b). In contrast, BMDCs that lacked CARD9 had severe defects in IL-1β production upon transfection of all these DNA forms (Fig. 3a), though the production of IL-1β induced by Toll-like receptor (TLR) 4 stimulation with LPS or TLR9 stimulation with CpG-DNA was not affected; thus, CARD9-deficient cells are not unspecifically impairment in DNA-induced IL-1β production. Moreover, the IFN responses controlled by the cGAS-STING pathway were also unaffected by the deletion of CARD9 (Fig. 3b), whereas STING-deficient BMDCs produced substantial amounts of IL-1β but no type I IFN, consistent with previously published data (Fig. 3c, d)[5, 6]. We therefore conclude that CARD9 is specifically required for DNA-induced IL-1β responses. This conclusion was supported by additional concentration-response and kinetic studies in dsDNA-stimulated CARD9-deficient cells (Fig. 3e, f).

To study the biological relevance of these results, we transfected CARD9-deficient cells with purified microbial DNA from cowpox virus, VV or *Escherichia coli (E. coli)*. IL-1β responses to microbial genomic DNA were also specifically defective in *Card9−/−* BMDCs, although the IFN responses were intact (Fig. 3f, g, and data not shown), indicating a general role for CARD9 signaling during cytosolic DNA-induced IL-1β generation.

Next, we addressed if Rad50 was required for DNA-induced IL-1β generation. Rad50 is essential for cell viability during division and embryonic or hematopoietic development, and genetic deletion is embryonically lethal[20, 24, 25]. Therefore, we crossed conditional *Rad50Δ/ind* mice, which carry a *Rad50* null allel together with an inducibly depleted *Rad50* allel, and *Rad50+/ind* mice[24], that contain one functional *Rad50* allel, to animals that ubiquitously express a tamoxifen-inducible Cre recombinase (Rosa26-CreERT2), differentiated BMDCs in culture and treated the differentiated, non-dividing BMDCs with tamoxifen to activate Cre-mediated Rad50 gene deletion *in vitro*. This protocol allowed for a substantial depletion of Rad50 from BMDCs, although the protein was not completely absent, presumably due to its long half-life (Fig. 3h). Stimulation of Rad50-depleted BMDCs with either poly(dA:dT), poly(dG:dC) or mammalian genomic DNA resulted in an up to 80% reduction in IL-1β responses compared with control cells, which still contain one functional *Rad50* allel after Cre-mediated depletion of the *Rad50ind* allel. Nonetheless, parallel stimulation of Rad50-depleted cells with CARD9-independent TLR agonists or the CARD9-dependent Dectin-1 ligand curdlan induced regular IL-1β responses (Fig. 3i); thus, the Rad50-depleted cells did not exhibit a general defect in the IL-1β response. Because Rad50 activates the kinase ATM following nuclear DNA damage sensing[20], we also tested the involvement of ATM in cytosolic DNA-induced IL-1β generation. However, the production of IL-1β was not impaired by ATM deficiency[26] (Supplementary Fig. 2). Together, these genetic results establish Rad50 as an innate immune sensor for DNA and reveal that the Rad50- and CARD9-mediated DNA response operates independently of ATM to induce IL-1β.

## Rad50 and CARD9 recruit Bcl10 for NF-κB activation

We next investigated the mechanisms by which the Rad50-CARD9 interaction would mediate IL-1β generation. Because CARD9 is an activator of canonical NF-κB signaling[13], we evaluated the nuclear translocation of the NF-κB subunits RelA (p65) and c-Rel in DNA-transfected *Card9−/−* cells. Using confocal microscopy, we observed that the activation of both NF-κB subunits was defective in *Card9−/−* BMDCs specifically after cytosolic DNA transfection, but not after CpG-DNA-mediated TLR9 stimulation (Fig. 4a-c). Consistent with these findings and the role of NF-κB activation in pro-IL-1β gene transcription, the induction of pro-IL-1β mRNA and the subsequent production of the pro-IL-1β polypeptide were also almost completely abrogated in DNA-transfected *Card9−/−* BMDCs (Fig. 4d and Supplementary Fig. 3). Moreover, cytosolic DNA-induced IL-6 and TNF transcription were also significantly reduced in CARD9-deficient cells (Supplementary Fig. 4a, b). However, and in agreement with the unaffected IFN responses observed above (see Fig. 3), the activation of IRF3 was intact in *Card9−/−* cells, as determined by both IRF3 phosphorylation and IRF3 nuclear translocation (Fig. 4e, f). In contrast, in STING-deficient cells, the activation of IRF3 was abolished (Fig. 4g) and the transcription of IFN-β was

entirely blocked (data not shown). When we transfected *Card9*^{−/−} or STING-deficient BMDCs with cGAMP, which is a strong type 1 IFN inducer that directly activates STING[2, 3] we also observed that STING is essential for the IFN response[2, 3], while CARD9 is dispensable (Supplementary Fig. 5a, b). Next, we investigated the role of STING in DNA-induced IL-1β generation in more detail. Consistent with the almost intact IL-1β production in DNA-stimulated STING-deficient cells (Fig. 3c)[5, 6] the NF-κB dependent transcription of pro-IL-1β was not diminished in *Tmem173*^{−/−} cells, and by confocal microscopy we also detected substantial translocation of both p65 and c-Rel into the nuclei of STING-deficient BMDCs (Fig. 4h, i). Together, these data indicate that CARD9 is essential for a specific pathway that mediates NF-κB activation for pro-IL-1β generation in response to cytosolic DNA sensing. Moreover, although STING contributes to optimal NF-κB responses, it is largely dispensable for the induction of pro-IL-1β gene transcription after DNA detection.

Card9 engages Bcl10 to activate NF-κB upon CLR or RIG-I ligation[15, 16, 18, 19]. Thus, we stimulated *Bcl10*^{−/−} BMDCs with poly(dA:dT), poly(dG:dC), CT-DNA, or circular plasmid DNA to study the involvement of Bcl10 during the DNA-induced innate immune response. Bcl10 was essential for cytosolic dsDNA-induced NF-κB activation and IL-1β generation but not for the IL-1β production induced by TLR4 or TLR9 stimulation (Fig. 5a). Moreover, similar to CARD9, Bcl10 was essential for the upregulation of pro-IL-1β transcription but dispensable for IRF3 signaling and IFN-β synthesis (Fig. 5b, c, Supplementary Fig. 3, and data not shown). To investigate the roles of CARD9 and Bcl10 in inflammasome activation, we also assessed caspase-1 activation in CARD9- or Bcl10-deficient BMDCs. This response, which is mediated by AIM2 and ASC[1], was intact in the absence of CARD9 or Bcl10 (Fig. 5d), indicating that CARD9 and Bcl10 specifically control the signal for pro-IL-1β generation.

Based on the findings that CARD9 and Bcl10 cooperate for NF-κB activation after cytosolic DNA sensing, we next investigated whether Bcl10 was recruited to dsDNA-Rad50 complexes. Using confocal microscopy we observed that endogenous Bcl10 co-localized to dsDNA-Rad50 aggregates upon DNA transfection (Fig. 5e). Moreover, this recruitment of Bcl10 to cytosolic Rad50 was mediated via CARD9, as it was not observed in CARD9-deficient cells. Additionally, CARD9 was regularly recruited to the dsDNA-Rad50 complexes in *Bcl10*^{−/−} cells (Fig. 5e), demonstrating that the initial steps of Rad50-CARD9 complex formation do not require the effector Bcl10. Thus, cytosolic DNA sensing by Rad50 and the subsequent assembly of Rad50/CARD9 complexes result in a further recruitment of Bcl10 for NF-κB activation.

## Rad50-CARD9 complexes sense cytosolic viral DNA upon infection

After having established the critical functions for Rad50, CARD9 and Bcl10 in DNA-induced IL-1β production, we investigated the roles of these factors during virus infection. We used the poxvirus vaccinia virus (VV) as a model because the life cycle of poxviruses includes DNA replication in the cytoplasm[27]. Similar to the DNA transfection experiments described above, the infection of wild-type or *Card9*^{−/−} BMDCs with VV resulted in the localization of Rad50 to the cytoplasmic viral DNA, which confirms that this DNA sensor is able to detect cytosolic viral infection (Fig. 6a, b and data not shown). In wild-type BMDCs,

CARD9 was co-recruited to the viral-dsDNA-Rad50 foci, resulting in the formation of viral-dsDNA-Rad50-CARD9 complexes (Fig. 6a, b) that were morphologically comparable to those observed upon synthetic dsDNA transfection (see Fig. 2). To analyze whether DNA virus sensing also induces CARD9 signaling, we measured inflammatory cytokines after VV infection in wild-type, *Card9*^{−/−} and *Bcl10*^{−/−} BMDCs and found that both *Card9*^{−/−} and *Bcl10*^{−/−} BMDCs demonstrated severely impaired IL-1β production upon VV infection *in vitro*, suggesting VV recognition activated CARD9 signaling (Fig. 6c). Similarly, the VV-induced generation of the NF-κB-controlled cytokines TNF and IL-6 was also severely impaired in *Card9*^{−/−} and *Bcl10*^{−/−} BMDCs (Fig. 6c). Control cell infection with the RNA virus vesicular stomatitis virus (VSV) resulted in defective IL-1β production in *Card9*^{−/−} cells (Supplementary Fig. 6), which is in accord with the function of CARD9 downstream of RIG-I[17, 18, 28, 29].

To investigate the physiological significance of CARD9 in innate immune responses to DNA virus infection *in vivo*, we infected CARD9-deficient mice with VV via an intravenous route. After 6 hours, we measured the serum concentrations of IL-1β using a cytometric bead array (CBA), which revealed that the CARD9-deficient mice exhibited defective IL-1β production upon infection (Fig. 7a). Because IL-1β regulates adaptive anti-viral CD8^{+} T cell responses[9, 10], we investigated the frequency of IFN-γ-producing virus antigen-specific CD8^{+} T cells at 8 days after VV infection in wild-type and CARD9-deficient mice. Consistent with the diminished IL-1β production observed in CARD9-deficient mice, anti-viral CD8^{+} T cell responses were also significantly impaired in the absence of Card9 (Fig. 7b). Thus, the Rad50/CARD9 complexes sense viral cytoplasmic DNA after cell infection and the activation of CARD9 signaling is critical for the subsequent host response *in vivo*.

## DISCUSSION

Understanding cytosolic DNA recognition and downstream signaling has been a focus of intense research for several years. Multiple cytosolic DNA sensors have been described, including AIM2, cGAS, DAI, LRRFIP1, IFI16, DHX9, DDX36, DDX41 and proteins with known functions in the DDR[1, 2, 4]. Although the physiological roles of some of these receptors need to be genetically defined, experiments in gene-deficient mice have revealed the cGAS-STING signaling cascade as the key regulator of the IRF3-mediated IFN response[4, 5, 30]. Nonetheless, the disruption of STING did not affect the generation of IL-1β after DNA virus infection, although it almost completely abolished DNA-induced INF-β production[5], and we also observed that STING is largely dispensable for pro-IL-1β transcription and IL-1β generation.

Data from CARD9-and Bcl10-deficient BMDCs reveal that CARD9-Bcl10 complexes specifically control NF-κB activation and pro-IL-1β gene transcription upon cytosolic DNA sensing. The transcription of the NF-κB dependent cytokines TNF and IL-6 was also significantly reduced in DNA-stimulated CARD9-deficient cells and *Card9*^{−/−} DCs show impaired TNF and IL-6 production upon DNA virus infection. Yet, because TNF and IL-6 generation is not completely defective in *Card9*^{−/−} cells it is possible that STING dependent signals could contribute to the production of certain NF-κB-dependent factors beside from pro-IL-1β. It remains to be determined whether and how distinct NF-κB responses could be

differentially regulated via CARD9 and potentially STING. Because *Card9*^{−/−} cells and *Bcl10*^{−/−} cells exhibit regular IRF3 activation and IFN production, it is highly unlikely that CARD9-Bcl10 complexes would directly influence the cGAS-STING cascade. This hypothesis is supported by the fact that STING triggering with cGAMP induces normal IFN-β production in *Card9*^{−/−} DCs. Thus, the Rad50-CARD9 signaling pathway regulates specifically NF-κB dependent innate immune responses that are required for pro-IL-1β gene transcription. The essential function of AIM2 in DNA-mediated pro-IL-1β cleavage[1] has previously been confirmed[31, 32]. Our findings and these data together provide one comprehensive mechanism for DNA-induced IL-1β generation in which CARD9 complexes can mediate pro-IL-1β generation and the AIM2 inflammasome subsequent pro-IL-1β processing. Because CARD9 is selectively expressed in myeloid cells[13] and because its deletion does not completely abolish IL-1β production, CARD9-independent mechanisms can apparently contribute to IL-1β generation, potentially as a fail-safe mechanism.

Rad50 senses DNA via its N- and C-terminal nucleotide binding domain, which associates with Mre11 and Nbs1 to form a globular DNA binding complex[20]. The Cre-loxP-mediated genetic deletion of Rad50 provides to our knowledge the first clear genetic confirmation of an essential function for Rad50 in innate immune signaling. CARD9 associates directly with Rad50. This association involves the Rad50 Zn-hook region, which is separated from the Rad50 DNA-binding domain by an approx. 50 nm long coiled-coil domain. Bcl10 is also recruited to dsDNA-Rad50 complexes via CARD9. We therefore propose a model in which, together with Mre11 and NBS1, Rad50 detects viral or transfected dsDNA in the cytosol, resulting in the recruitment of CARD9 to the Rad50 Zn-hook region and the subsequent engagement of Bcl10 for inflammatory downstream signal transduction. The identification of the mechanism through which Rad50 localizes to the cytosol requires further investigations. We speculate that these mechanisms could involve modifications on the Nbs1 protein, because this factor controls the subcellular localization of the MRN complex as demonstrated by the finding that in fibroblasts, which contain Nbs1 truncation mutants, nuclear concentrations of Mre11 and Rad50 are reduced compared to normal cells and Mre11 and Rad50 levels increase in the cytoplasm[33].

The MRN complex has previously been reported to co-localize to sites of viral replication and to elicit anti-viral defense mechanisms involving viral DNA concatemerization and, potentially, other pathways including activation of STING[34, 35, 36], although it is still unclear how Rad50 would couple to the cGAS-STING cascade. Additional DNA damage control factors, such as DNA-PK and Ku70[37, 38], were also implicated in cytosolic DNA sensing for innate immunity. Together, these studies demonstrate a more global interaction between the evolutionarily conserved DDR system and the innate immune response to pathogens. By demonstrating a direct physical and functional connection between the damage sensor Rad50 and the pro-inflammatory signaling adapter CARD9, we now provide first mechanistic insight into these interactions.

IL-1β production induced by cytosolic DNA plays a critical role in host defense[31, 32, 39]. Therefore, IL-1β provides an anti-viral selective pressure, which is highlighted by the observation that multiple viruses have evolved strategies to inhibit IL-1β production by interfering with the NF-κB signaling pathway at multiple steps[8] or by inhibiting IL-1β

signaling, for example, through the expression of soluble IL-1β receptors (vIL-1βR) which prevent the fever reaction[7, 8, 10, 40]. Several DNA viruses, such as adenovirus, have also developed strategies to inhibit Rad50 signaling, suggesting that the Rad50 pathway is a potential target for viral subversion[34, 41]. As indicated above, IL-1β is not only important for immune defense but also a significant factor in autoinflammation[11]. Endogenous DNA that is inappropriately cleared can accumulate in cytosolic compartments and drive inflammatory diseases associated with increased IFN and IL-1β levels[42, 43, 44]. These findings indicate that it will be important to investigate the contributions of Rad50-CARD9 signaling to auto-inflammatory conditions associated with cytosolic DNA responses. Ultimately, future studies on the Rad50-CARD9 pathway may lead to selective strategies for dampening DNA-induced IL-1β-driven inflammatory responses without compromising anti-viral IFN production.

# METHODS

## Mice

Mice deficient in CARD9[15], Bcl10[45], STING ($Tmem173^{-/-}$)[46], ATM[26], or ASC ($Pycard^{-/-}$)[47], and $Rad50^{\Delta/ind}$ [24] x Rosa26-CreERT2 and $Rad50^{+/ind}$ [24] x Rosa26-CreERT2 mice were used at 6-12 weeks of age. Animals experiments were approved by Regierung von Oberbayern.

## Media and reagents

All reagents, including Poly(dG-dC) · Poly(dG-dC) acid sodium salt (poly(dG:dC), P9389), calf thymus DNA (CT-DNA, D4764), Poly(dA-dT) · Poly(dA-dT) acid sodium salt (poly(dA:dT), P0883) were purchased from Sigma, if not otherwise stated. cGAMP was obtained from Invivogen (tlrl-cga-s).The pmaxGFP Vector from Lonza was used as the circular plasmid DNA. Cell culture reagents were obtained from Invitrogen, and FCS was obtained from HyClone. Murine recombinant GM-CSF was purchased from PreproTech. CpG 1826 oligonucleotides, ultrapure LPS, and endotoxin-free DNA from *E. coli* K12 were purchased from InvivoGen, and curdlan was purchased from Wako. Poxviral genomic DNA from VV strain CVA and from cowpox virus (isolate 81/01, 5th passage in MA104 cells; originally provided by S. Essbauer, Munich, Germany) was isolated and purified from infected cell cultures, as recently described[48].

## Cell culture and stimulation

COS7 cells, THP-1 cells, and BMDCs were cultured as described[18, 21]. For DNA transfection, Lipofectamine 2000 (Invitrogen) was used according to the manufacturer's protocol. Unless otherwise stated LPS (100 ng/ml), CpG (1 μM), curdlan (200 μg/ml), and ATP (5 mM) were used for stimulation. ATP was added 45 min. prior to the end of the experiment. Bone marrow from $Rad50^{\Delta/ind}$ x Rosa26-CreERT2 and $Rad50^{+/ind}$ x Rosa26-CreERT2 mice was cultured in the presence of GM-CSF for 5 days prior to the addition of 1 μM 4-hydroxy-tamoxifen (4-OHT). These dendritic cells were cultivated for another 4 to 5 days prior to analysis.

## Yeast two-hybrid screen

The yeast two-hybrid screen using CARD9 as the bait was performed by Dualsystems Biotech AG. The bait construct for the yeast two-hybrid screening was generated by subcloning a cDNA encoding human CARD9 isoform 2 into the pLexA-DIR vector, and the bait was co-transformed with a human adult peripheral blood cDNA library into host strain NMY32. A total of $9.9 \times 10^6$ transformants were screened, yielding 96 transformants that grew on selective medium. Positive transformants were tested for β-galactosidase activity using a PXG β-galactosidase assay, and 77 (corresponding to 33 distinct genes) of the 96 initial positives showed β-galactosidase activity and were considered to be true positives. The library plasmids were isolated from positive clones, and the identity of positive interactors was determined by sequencing: 19 of the 77 clones contained Rad50 sequences.

## BRET analysis

BRET measurements were performed in transfected COS7 cells, as described[21]. Briefly, the full-length ORFs of CARD9 (NM_052814), Bcl10 (NM_003921), and AIM2 (NM_004833) and fragments of Rad50 (NM_005732) were introduced into plasmid vectors to express N- and C-terminal fusions with Rluc or YFP. The truncated Rad50 constructs were generated by polymerase chain reaction. All eight possible combinations of the N- or C-terminally tagged Rluc (donor) or YFP (acceptor) fusions were tested for each putative interaction pair at acceptor-to-donor ratios of 3:1, unless otherwise indicated. BRET ratios were calculated based on the equation $R = (I_A/I_D) - cf$, where $R$ is the BRET ratio, $I_A$ is the BRET signal, $I_D$ is the Rluc signal, and $cf$ is a correction factor (($I_A/I_D)_{control}$), with the co-transfection of the donor fusion-protein with YFP in the absence of the second protein of interest used as the control. The method-specific threshold for a positive protein-protein interaction was determined as a BRET ratio of 0.094 for the donor/acceptor combination that resulted in the highest BRET ratio, as previously described[21].

## Co-immunoprecipitation and immunoblot analysis

THP-1 cells were lysed, and immunoprecipitations were performed as described[18]. Cell lysates or cell supernatants were subjected to standard western blotting techniques, as previously described[15]. Proteins in cell-free supernatants were extracted by methanol/chloroform precipitation. Cytosolic and nuclear extracts were prepared as described[45].

## Antibodies

The primary antibodies anti-CARD9 (sc-99054), anti-Rad50 (sc-56209 and sc-74460), anti-caspase-1 p10 (sc-514), anti-Lamin B (sc-6217), anti-NF-κB p65 (sc-372), and anti-cRel (sc-71) were obtained from Santa Cruz, and anti-Bcl10 (#4237), anti-Mre11 (#4895), anti-p95/Nbs1 (#3002), anti-IRF-3 (#4302), and anti-phospho-IRF-3 (Ser396) (#4947) antibodies were obtained from Cell Signaling. Anti-CARD9 (a rabbit polyclonal antibody raised against an N-terminal peptide of CARD9) was kindly provided by Margot Thome. The secondary anti-mouse (donkey) and anti-rabbit antibodies (goat) for immunofluorescence were conjugated to Alexa Fluor 594 and Alexa Fluor 488 (Molecular Probes), respectively.

## Nucleic acid affinity purification

Oligonucleotides (50 bp DNA) containing a partial sequence of the terminal repeats of VV genomic DNA were synthesized by Biomers (sense, 5′-ccatcagaaagaggtttaatatttttgtgagaccatcgaagagagaaaga-3′, and antisense, 5′-tctttctctcttcgatggtctcacaaaaatattaaacctctttctgatgg-3′), annealed to generate dsDNA, and immobilized to Strep-Tactin Superflow (IBA) resin. Nucleic acid affinity purification was performed using THP-1 cell lysates, as described[49]. For the immunodepletion of Rad50, THP-1 lysates were incubated with anti-Rad50 or isotype control antibodies immobilized on sepharose beads for up to three consecutive rounds.

## Immunofluorescence staining and confocal microscopy

Immunofluorescence staining was performed using standard technology, as described[15]. Images were obtained using a TCS SP5 AOBS confocal laser-scanning microscope (Leica) with a 63×/1.4 NA Plan-Apochromat oil immersion objective. For presentation, the images were processed with Image J software http://rsb.info.nih.gov/ij/) using linear contrast enhancement on entire images.

## DNA labeling by nick translation

The direct labeling of double-stranded poly(dG:dC) DNA by incorporating ATTO 647N fluorescently labeled aminoallyl-dUTP nucleotides (Jena Bioscience) was performed by nick translation, as previously described[50].

## Cytokine measurement

Cytokine concentrations were determined by ELISA (BD Biosciences, eBioscience, or PBL Biomedical Laboratories) or Cytometric Bead Array (CBA, BD Biosciences) according to the manufacturer's instructions.

## Real-time PCR

Total RNA was isolated and transcribed using standard methods. The specific primer pairs were as follows: IL-1β, 5′-tgtaatgaaagacggcacacc-3′ and 5′-tcttctttggggtattgcttgg-3′; TNF, 5′-tcttctcattcctgcttgtgg-3′ and 5′-ggtctgggccatagaactga-3′; IL-6 5′-gctaccaaactggatataatcagga-3′ and 5′-ccaggtagctatggtactccagaa-3′; β-actin, 5′-agacctctatgccaacacag-3′ and 5′-tcgtactcctgcttgctgat-3′. The qPCR Core kit for SYBR Green I (Eurogentec) and a LightCycler® 480 Real-Time PCR System were used as indicated by the manufacturer. The relative IL-1β mRNA expression was calculated as the ratio of the real-time PCR signal of IL-1β mRNA to that of the β-actin mRNA and normalized to a WT unstimulated control.

## Viral infections

VV strain CVA and VSV Indiana (Mudd-Summer strain) were used for viral infections. VV was propagated in CV-1 cells and purified twice via ultracentrifugation through 36% sucrose cushions; the viral titers were determined by a plaque assay using CV-1 cells with crystal violet, as described[48]. VSV was propagated in baby hamster kidney (BHK-21) cells, as described[18]. *In vitro* infections were performed at the indicated multiplicities of infection (MOIs) (MOI 0.1 to MOI 10). For *in vivo* experiments, mice were injected intravenously

with $1 \times 10^7$ pfu virus in 200 $\mu$l of PBS. After 6 hours, the serum was collected to determine the IL-1β concentration. Blinding was done for injection and serum collection of mice. Splenocytes from vaccinated mice were isolated at 8 days post-infection and stimulated with the H-2K$^b$-restricted VV-specific peptide B8R(20-27) (TSYKFESV; 1 $\mu$g/ml) or a control peptide, OVA(257-264) (SIINFEKL; 1 $\mu$g/ml), at 37°C for 5 h in the presence of 1 $\mu$g/ml brefeldin A (Sigma-Aldrich). The cells were live/dead-stained with ethidium monoazide bromide (Invitrogen) and blocked with anti-CD16/CD32-Fc-Block (BD Biosciences); the cell surface was stained with an eFluor450-conjugated anti-CD8a antibody (eBioscience). Intracellular staining for IFNγ was performed with a FITC-conjugated anti-IFNγ antibody (BD Biosciences) using the Cytofix/Cytoperm kit (BD Biosciences) according to the manufacturer's instructions. Data were acquired using the FACS Canto II flow cytometer (BD Biosciences) and analyzed with FlowJo software (Tree Star).

### Statistics

P values were determined by Student's two-tailed t test for independent samples using Microsoft Excel.

## Supplementary Material

Refer to Web version on PubMed Central for supplementary material.

## ACKNOWLEDGMENTS

## References

1. Paludan SR, Bowie AG. Immune sensing of DNA. Immunity. 2013; 38(5):870–880. [PubMed: 23706668]

2. Sun L, Wu J, Du F, Chen X, Chen ZJ. Cyclic GMP-AMP synthase is a cytosolic DNA sensor that activates the type I interferon pathway. Science. 2013; 339(6121):786–791. [PubMed: 23258413]

3. Wu J, Sun L, Chen X, Du F, Shi H, Chen C, et al. Cyclic GMP-AMP is an endogenous second messenger in innate immune signaling by cytosolic DNA. Science. 2013; 339(6121):826–830. [PubMed: 23258412]

4. Goubau D, Deddouche S, Reis ESC. Cytosolic sensing of viruses. Immunity. 2013; 38(5):855–869. [PubMed: 23706667]

5. Ishikawa H, Ma Z, Barber GN. STING regulates intracellular DNA-mediated, type I interferon-dependent innate immunity. Nature. 2009; 461(7265):788–792. [PubMed: 19776740]

6. Zhang Z, Yuan B, Bao M, Lu N, Kim T, Liu YJ. The helicase DDX41 senses intracellular DNA mediated by the adaptor STING in dendritic cells. Nat Immunol. 2011; 12(10):959–965. [PubMed: 21892174]

7. Epperson ML, Lee CA, Fremont DH. Subversion of cytokine networks by virally encoded decoy receptors. Immunol Rev. 2012; 250(1):199–215. [PubMed: 23046131]

8. Smith GL, Benfield CT, Maluquer de Motes C, Mazzon M, Ember SW, Ferguson BJ, et al. Vaccinia virus immune evasion: mechanisms, virulence and immunogenicity. J Gen Virol. 2013

9. Staib C, Kisling S, Erfle V, Sutter G. Inactivation of the viral interleukin 1beta receptor improves CD8+ T-cell memory responses elicited upon immunization with modified vaccinia virus Ankara. J Gen Virol. 2005; 86(Pt 7):1997–2006. [PubMed: 15958679]

10. Zimmerling S, Waibler Z, Resch T, Sutter G, Schwantes A. Interleukin-1beta receptor expressed by modified vaccinia virus Ankara interferes with interleukin-1beta activity produced in various virus-infected antigen-presenting cells. Virol J. 2013; 10:34. [PubMed: 23356675]

11. Dinarello CA, Simon A, van der Meer JW. Treating inflammation by blocking interleukin-1 in a broad spectrum of diseases. Nat Rev Drug Discov. 2012; 11(8):633–652. [PubMed: 22850787]

12. Vallabhapurapu S, Karin M. Regulation and function of NF-kappaB transcription factors in the immune system. Annu Rev Immunol. 2009; 27:693–733. [PubMed: 19302050]

13. Roth S, Ruland J. Caspase recruitment domain-containing protein 9 signaling in innate immunity and inflammation. Trends Immunol. 2013

14. Takeuchi O, Akira S. Pattern recognition receptors and inflammation. Cell. 2010; 140(6):805–820. [PubMed: 20303872]

15. Gross O, Gewies A, Finger K, Schafer M, Sparwasser T, Peschel C, et al. Card9 controls a non-TLR signalling pathway for innate anti-fungal immunity. Nature. 2006; 442(7103):651–656. [PubMed: 16862125]

16. Hara H, Ishihara C, Takeuchi A, Imanishi T, Xue L, Morris SW, et al. The adaptor protein CARD9 is essential for the activation of myeloid cells through ITAM-associated and Toll-like receptors. Nat Immunol. 2007; 8(6):619–629. [PubMed: 17486093]

17. Hsu YM, Zhang Y, You Y, Wang D, Li H, Duramad O, et al. The adaptor protein CARD9 is required for innate immune responses to intracellular pathogens. Nat Immunol. 2007; 8(2):198–205. [PubMed: 17187069]

18. Poeck H, Bscheider M, Gross O, Finger K, Roth S, Rebsamen M, et al. Recognition of RNA virus by RIG-I results in activation of CARD9 and inflammasome signaling for interleukin 1 beta production. Nat Immunol. 2010; 11(1):63–69. [PubMed: 19915568]

19. Strasser D, Neumann K, Bergmann H, Marakalala MJ, Guler R, Rojowska A, et al. Syk Kinase-Coupled C-type Lectin Receptors Engage Protein Kinase C-delta to Elicit Card9 Adaptor-Mediated Innate Immunity. Immunity. 2012

20. Stracker TH, Petrini JH. The MRE11 complex: starting from the ends. Nat Rev Mol Cell Biol. 2011; 12(2):90–103. [PubMed: 21252998]

21. Gersting SW, Lotz-Havla AS, Muntau AC. Bioluminescence resonance energy transfer: an emerging tool for the detection of protein-protein interaction in living cells. Methods Mol Biol. 2012; 815:253–263. [PubMed: 22130997]

22. Maser RS, Monsen KJ, Nelms BE, Petrini JH. hMre11 and hRad50 nuclear foci are induced during the normal cellular response to DNA double-strand breaks. Mol Cell Biol. 1997; 17(10):6087–6096. [PubMed: 9315668]

23. Goodridge HS, Shimada T, Wolf AJ, Hsu YM, Becker CA, Lin X, et al. Differential use of CARD9 by dectin-1 in macrophages and dendritic cells. J Immunol. 2009; 182(2):1146–1154. [PubMed: 19124758]

24. Adelman CA, De S, Petrini JH. Rad50 is dispensable for the maintenance and viability of postmitotic tissues. Mol Cell Biol. 2009; 29(2):483–492. [PubMed: 19001091]

25. Luo G, Yao MS, Bender CF, Mills M, Bladl AR, Bradley A, et al. Disruption of mRad50 causes embryonic stem cell lethality, abnormal embryonic development, and sensitivity to ionizing radiation. Proc Natl Acad Sci U S A. 1999; 96(13):7376–7381. [PubMed: 10377422]

26. Barlow C, Hirotsune S, Paylor R, Liyanage M, Eckhaus M, Collins F, et al. Atm-deficient mice: a paradigm of ataxia telangiectasia. Cell. 1996; 86(1):159–171. [PubMed: 8689683]

27. Roberts KL, Smith GL. Vaccinia virus morphogenesis and dissemination. Trends Microbiol. 2008; 16(10):472–479. [PubMed: 18789694]

28. Abdullah Z, Schlee M, Roth S, Mraheil MA, Barchet W, Bottcher J, et al. RIG-I detects infection with live Listeria by sensing secreted bacterial nucleic acids. EMBO J. 2012; 31(21):4153–4164. [PubMed: 23064150]

29. Kok KH, Lui PY, Ng MH, Siu KL, Au SW, Jin DY. The double-stranded RNA-binding protein PACT functions as a cellular activator of RIG-I to facilitate innate antiviral response. Cell Host Microbe. 2011; 9(4):299–309. [PubMed: 21501829]

30. Li XD, Wu J, Gao D, Wang H, Sun L, Chen ZJ. Pivotal roles of cGAS-cGAMP signaling in antiviral defense and immune adjuvant effects. Science. 2013; 341(6152):1390–1394. [PubMed: 23989956]

31. Fernandes-Alnemri T, Yu JW, Juliana C, Solorzano L, Kang S, Wu J, et al. The AIM2 inflammasome is critical for innate immunity to Francisella tularensis. Nat Immunol. 2010; 11(5): 385–393. [PubMed: 20351693]

32. Rathinam VA, Jiang Z, Waggoner SN, Sharma S, Cole LE, Waggoner L, et al. The AIM2 inflammasome is essential for host defense against cytosolic bacteria and DNA viruses. Nat Immunol. 2010; 11(5):395–402. [PubMed: 20351692]

33. Carney JP, Maser RS, Olivares H, Davis EM, Le Beau M, Yates JR 3rd, et al. The hMre11/hRad50 protein complex and Nijmegen breakage syndrome: linkage of double-strand break repair to the cellular DNA damage response. Cell. 1998; 93(3):477–486. [PubMed: 9590181]

34. Lilley CE, Schwartz RA, Weitzman MD. Using or abusing: viruses and the cellular DNA damage response. Trends Microbiol. 2007; 15(3):119–126. [PubMed: 17275307]

35. Weitzman MD, Carson CT, Schwartz RA, Lilley CE. Interactions of viruses with the cellular DNA repair machinery. DNA Repair (Amst). 2004; 3(8-9):1165–1173. [PubMed: 15279805]

36. Kondo T, Kobayashi J, Saitoh T, Maruyama K, Ishii KJ, Barber GN, et al. DNA damage sensor MRE11 recognizes cytosolic double-stranded DNA and induces type I interferon by regulating STING trafficking. Proc Natl Acad Sci U S A. 2013; 110(8):2969–2974. [PubMed: 23388631]

37. Ferguson BJ, Mansur DS, Peters NE, Ren H, Smith GL. DNA-PK is a DNA sensor for IRF-3-dependent innate immunity. Elife. 2012; 1:e00047. [PubMed: 23251783]

38. Zhang X, Brann TW, Zhou M, Yang J, Oguariri RM, Lidie KB, et al. Cutting edge: Ku70 is a novel cytosolic DNA sensor that induces type III rather than type I IFN. J Immunol. 2011; 186(8): 4541–4545. [PubMed: 21398614]

39. Saiga H, Kitada S, Shimada Y, Kamiyama N, Okuyama M, Makino M, et al. Critical role of AIM2 in Mycobacterium tuberculosis infection. Int Immunol. 2012; 24(10):637–644. [PubMed: 22695634]

40. Alcami A, Smith GL. A mechanism for the inhibition of fever by a virus. Proc Natl Acad Sci U S A. 1996; 93(20):11029–11034. [PubMed: 8855303]

41. Stracker TH, Carson CT, Weitzman MD. Adenovirus oncoproteins inactivate the Mre11-Rad50-NBS1 DNA repair complex. Nature. 2002; 418(6895):348–352. [PubMed: 12124628]

42. Boswell JM, Yui MA, Burt DW, Kelley VE. Increased tumor necrosis factor and IL-1 beta gene expression in the kidneys of mice with lupus nephritis. J Immunol. 1988; 141(9):3050–3054. [PubMed: 3262676]

43. Dombrowski Y, Peric M, Koglin S, Kammerbauer C, Goss C, Anz D, et al. Cytosolic DNA triggers inflammasome activation in keratinocytes in psoriatic lesions. Sci Transl Med. 2011; 3(82):82ra38.

44. Popovic K, Ek M, Espinosa A, Padyukov L, Harris HE, Wahren-Herlenius M, et al. Increased expression of the novel proinflammatory cytokine high mobility group box chromosomal protein 1 in skin lesions of patients with lupus erythematosus. Arthritis Rheum. 2005; 52(11):3639–3645. [PubMed: 16255056]

45. Ruland J, Duncan GS, Elia A, del Barco Barrantes I, Nguyen L, Plyte S, et al. Bcl10 is a positive regulator of antigen receptor-induced activation of NF-kappaB and neural tube closure. Cell. 2001; 104(1):33–42. [PubMed: 11163238]

46. Jin L, Hill KK, Filak H, Mogan J, Knowles H, Zhang B, et al. MPYS is required for IFN response factor 3 activation and type I IFN production in the response of cultured phagocytes to bacterial second messengers cyclic-di-AMP and cyclic-di-GMP. J Immunol. 2011; 187(5):2595–2601. [PubMed: 21813776]

47. Mariathasan S, Newton K, Monack DM, Vucic D, French DM, Lee WP, et al. Differential activation of the inflammasome by caspase-1 adaptors ASC and Ipaf. Nature. 2004; 430(6996): 213–218. [PubMed: 15190255]

48. Gasteiger G, Kastenmuller W, Ljapoci R, Sutter G, Drexler I. Cross-priming of cytotoxic T cells dictates antigen requisites for modified vaccinia virus Ankara vector vaccines. J Virol. 2007; 81(21):11925–11936. [PubMed: 17699574]

49. Burckstummer T, Baumann C, Bluml S, Dixit E, Durnberger G, Jahn H, et al. An orthogonal proteomic-genomic screen identifies AIM2 as a cytoplasmic DNA sensor for the inflammasome. Nat Immunol. 2009; 10(3):266–272. [PubMed: 19158679]

50. Cremer M, Grasser F, Lanctot C, Muller S, Neusser M, Zinner R, et al. Multicolor 3D fluorescence in situ hybridization for imaging interphase chromosomes. Methods Mol Biol. 2008; 463:205–239. [PubMed: 18951171]
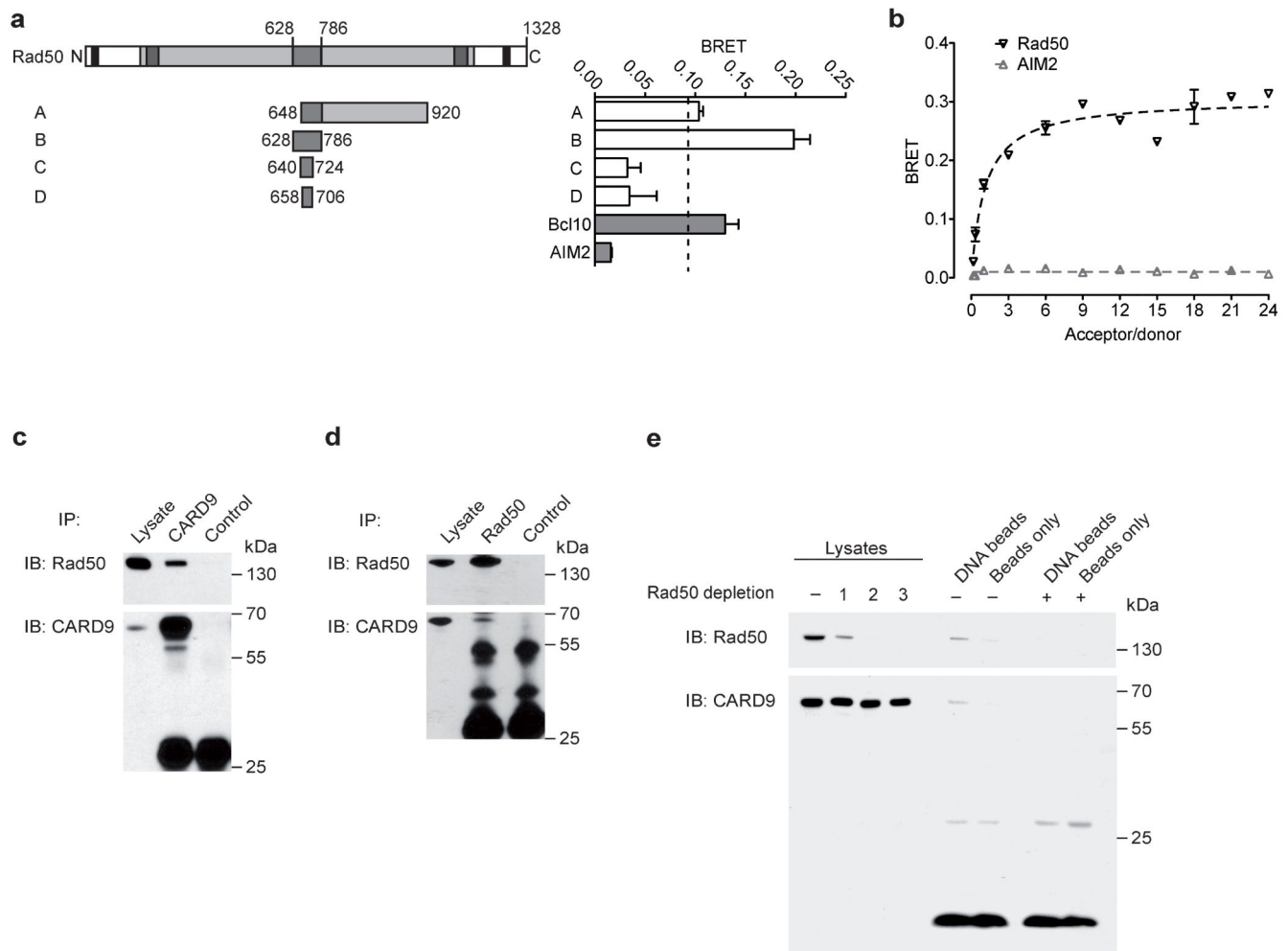
**Figure 1. CARD9 interacts with Rad50**

(**a**) BRET assays of binary interactions of CARD9 with Rad50 fragments, Bcl10 or AIM2 as Rluc and YFP fusion proteins in COS7 cells. The BRET ratios are given as the means + SEMs of two independent experiments. The dashed line indicates the method-specific threshold for a positive protein-protein interaction. (**b**) BRET saturation experiments using co-transfected fusions of CARD9 with Rad50 zinc hook (fragment B) orAIM2 at the indicated acceptor-to-donor ratio. The specific interaction of CARD9 with Rad50 is demonstrated by the hyperbolic behavior of BRET ratios as a function of the acceptor-to-donor ratio. (**c, d**) THP1 cell lysates were immunoprecipitated (IP) with anti-CARD9 (**c**), anti-Rad50 (**d**), or the respective isotype control antibodies. Immunoprecipitates were separated on one gel and transferred onto a single membrane, which was subsequently cut and used for immunoblot (IB) analysis with anti-Rad50 or CARD9 antibody, as indicated. (**e**) THP-1 cell lysates were left untreated (−) or were immunodepleted for Rad50 1, 2, or 3 times. Subsequently, bead-immobilized dsDNA (DNA beads) or empty streptavidin beads (Beads only) were incubated with THP-1 cell lysates that were either not treated, or immunodepleted for Rad50 three times. The beads were precipitated, and bound proteins were separated on a gel and blotted onto a single membrane. The membrane was cut and

used for western blot analysis with anti-Rad50 or CARD9 antibody, as indicated. The data are representative of at least three independent experiments (**c-e**).
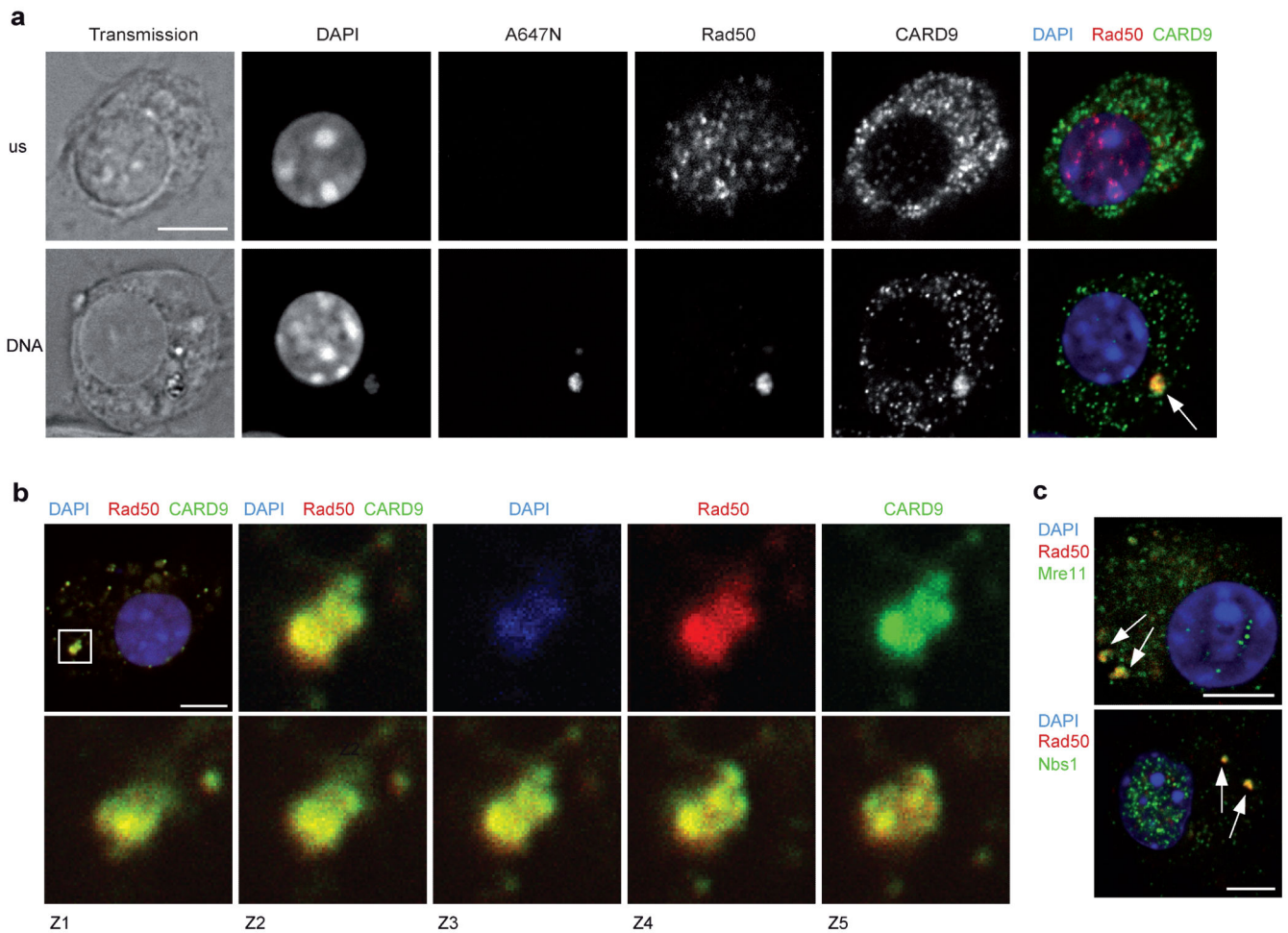
**Figure 2. CARD9 is recruited to cytoplasmic dsDNA-sensing Rad50 complexes**
(**a-c**) Confocal microscopy analysis. (**a**) BMDCs were left unstimulated (us) or were transfected with ATTO 647N (A647N) fluorescently labeled poly(dG:dC) (DNA) (2.5 µg/ml) for 2 hours and then stained with DAPI as a DNA counterstain and antibodies against Rad50 and CARD9. The arrow in the merged picture indicates a representative cytosolic dsDNA/Rad50/CARD9 complex. (**b**) BMDCs were transfected with dsDNA, stained, and analyzed as in (**a**). A dsDNA/Rad50/CARD9 complex (upper left picture, box) was visualized at higher magnifications and in different z-layers (z1 – z5). (**c**) BMDCs were transfected with dsDNA as in (**a**) and stained with DAPI and antibodies against Rad50 and Mre11 or Nbs1. Cytosolic dsDNA/Rad50/Mre11 or dsDNA/Rad50/Nbs1 complexes are indicated by arrows. Scale bars represent 5 µm, and the data are representative of at least three independent experiments in which at least 50 individual cells were analyzed per experiment and assay point.
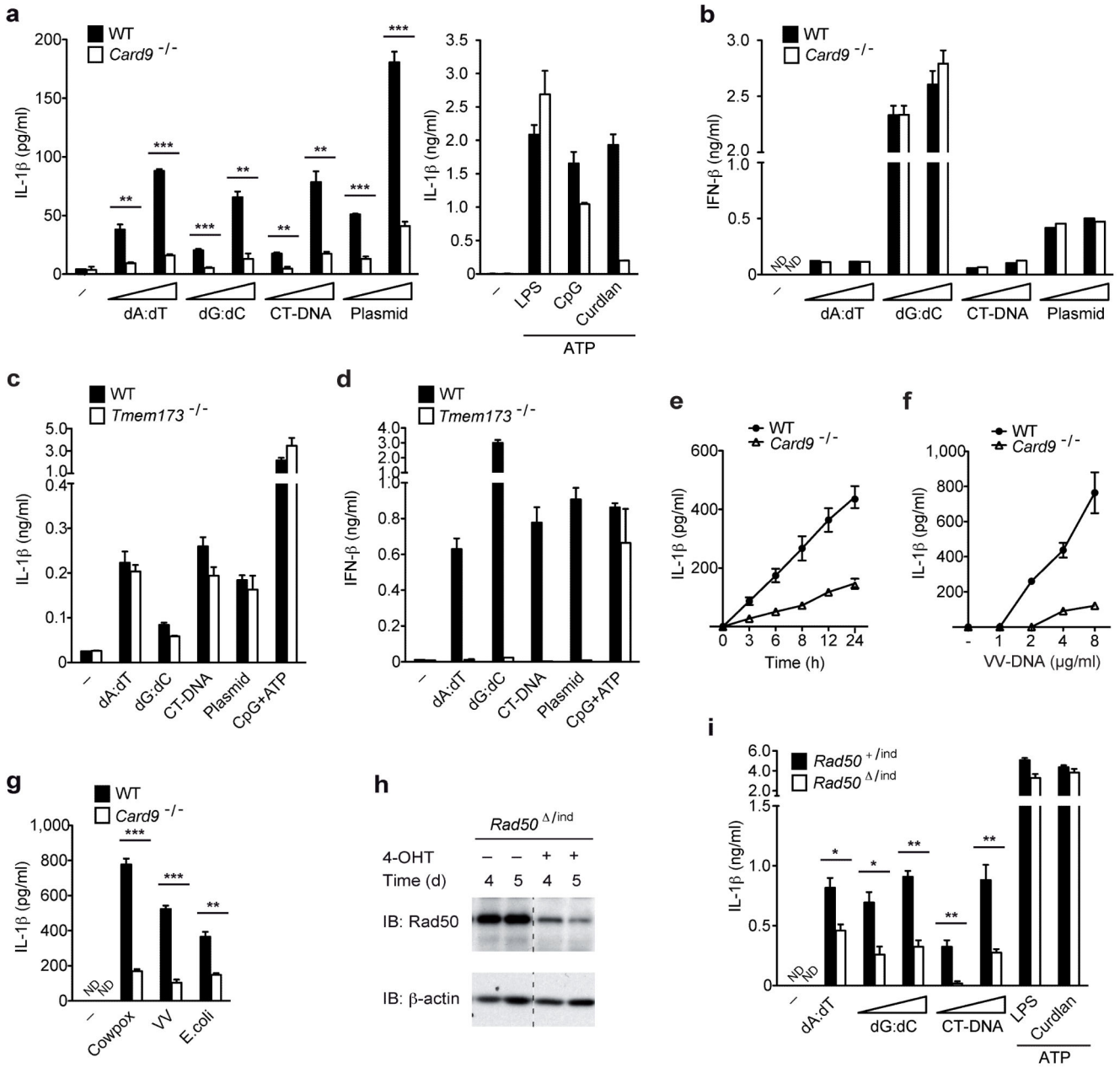
**Figure 3. CARD9 and Rad50 are essential for DNA-induced IL-1β production**
(**a, b**) BMDCs from WT and *Card9−/−* mice were transfected with dsDNA (1 - 4 *μ*g/ml) of different origins, or stimulated with LPS, CpG, and curdlan plus ATP for 6 hours. IL-1β (**a**) and IFN-β (**b**) concentrations in the supernatants were determined. (**c, d**) BMDCs from WT and *Tmem173−/−* mice were transfected with dsDNA or stimulated with CpG + ATP as in (**a, b**). IL-1β (**c**) and IFN-β (**d**) concentrations were determined in the supernatants. (**e**) BMDCs were transfected with poly(dG:dC) (4 *μ*g/ml) for the indicated time period. (**f**) BMDCs were transfected with increasing amounts of purified dsDNA from vaccinia virus (VV-DNA) for 16 hours. (**g**) BMDCs were transfected with the indicated microbial DNA for 16 hours, and the IL-1β levels in the supernatants were determined. (**h, i**) Dendritic cells were

differentiated from murine bone marrow of the indicated genotype; 4-hydroxy-tamoxifen (4-OHT) was added on culture day 5. (**h**) BMDCs (with or without 4-OHT treatment) were lysed at the indicated time after the addition of 4-OHT. The Rad50 and β-actin protein levels in the cellular lysates were analyzed by western blotting. (**i**) At 5 days after the addition of 4-OHT, BMDCs were transfected with dsDNA (1 - 4 $\mu$g/ml) or stimulated with LPS + ATP and curdlan + ATP, and IL-1β concentrations in the supernatants were determined. The data are represented as the mean + SEM of triplicates. One representative of at least three independent experiments is shown. *$p < 0.05$, **$p < 0.01$, ***$p < 0.01$, Student's t-test. ND, not detectable.
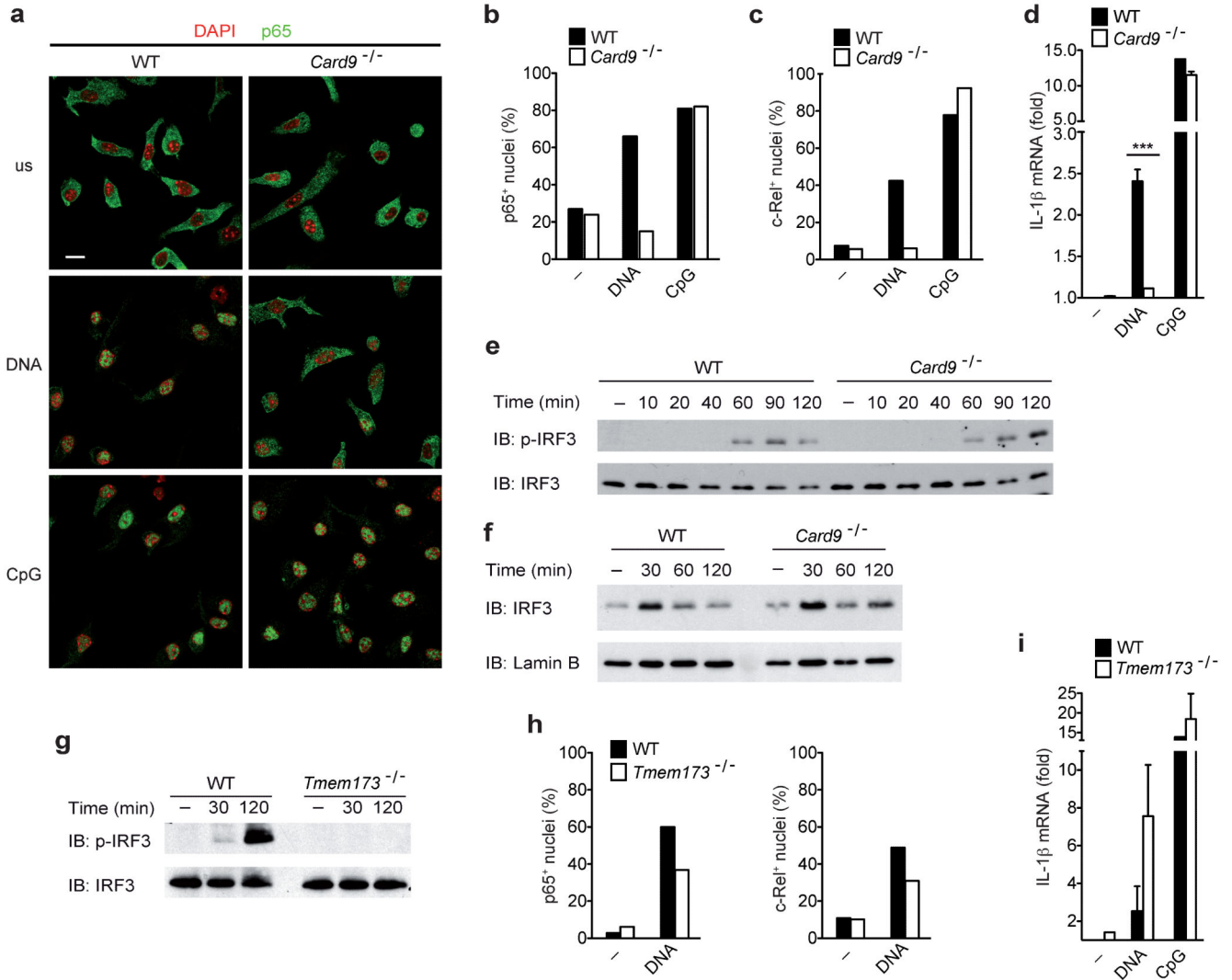
**Figure 4. CARD9 controls dsDNA-mediated NF-κB activity**

(**a-c**) BMDCs from WT or *Card9*$^{-/-}$ mice were left untreated (us), transfected with poly(dG:dC) (DNA) (2.5 μg/ml), or stimulated with CpG for 1 hour, and subsequently fixed and stained with DAPI and an anti-p65 or anti-c-Rel antibody. p65 and c-Rel translocation into the nucleus was monitored by confocal microscopy and quantified by determining the frequency of p65- or c-Rel-positive nuclei in at least 100 individual cells. The scale bar represents 5 μm. (**d**) BMDCs were left untreated, transfected with poly(dG:dC) (DNA) (2.5 μg/ml), or stimulated with CpG for 4 hours, and IL-1β transcript levels were measured by quantitative real-time PCR and normalized to β-actin mRNA levels. The data are shown as the mean + SEM. ***p < 0.001, Student's t-test. (**e, f**) WT or *Card9*$^{-/-}$ BMDCs were transfected with dsDNA for the indicated time. (**e**) Immunoblot analysis of cytosolic extracts. The blots were probed with an antibody against phospho-IRF3 (Ser396) or IRF3. (**f**) Nuclear extracts were immunoblotted with anti-IRF3 and anti-Lamin B antibodies. (**g**) BMDCs from WT and *Tmem173*$^{-/-}$ mice were stimulated and analysed as in (**e**). (**h**) WT or *Tmem173*$^{-/-}$ BMDCs were left untreated or transfected with dsDNA, and analysed as in (**a-**

**c**). (**i**) BMDCs from WT and *Tmem173*$^{-/-}$ mice were treated and analysed as in (**d**).The data are representative of two (**i**) or three (**a-h**) independent experiments.
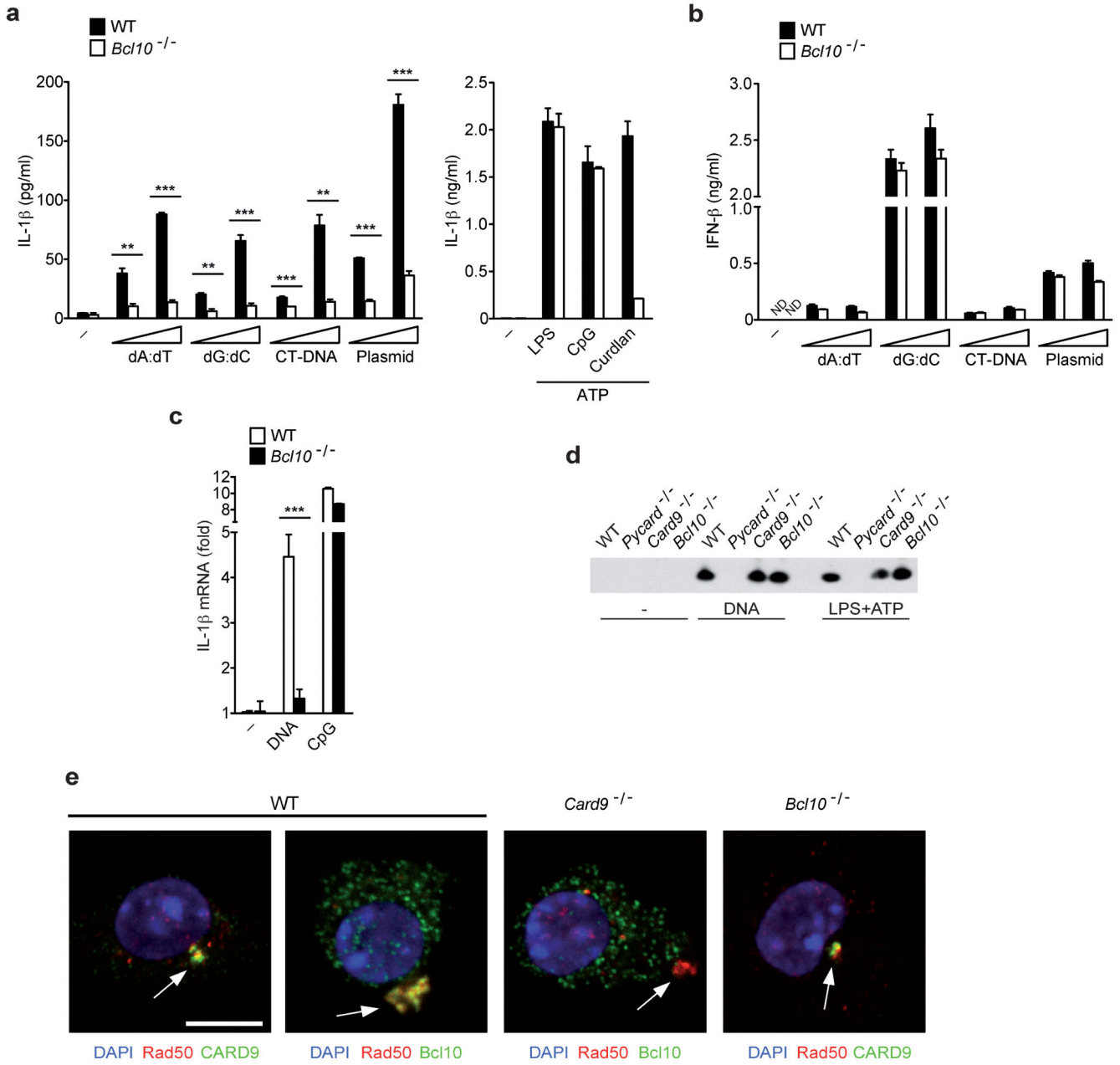
**Figure 5. Rad50/CARD9 interactions recruit Bcl10 for IL-1β responses**

IL-1β (**a**) and IFN-β (**b**) concentrations were measured in the supernatants of BMDCs transfected with dsDNA (1 - 4 μg/ml) of different origins. LPS, CpG, and curdlan plus ATP were used as controls. The data are shown as the mean + SEM. (**c**) BMDCs were left untreated or transfected with poly(dG:dC) (DNA) (2.5 μg/ml) or stimulated with CpG for 4 hours. IL-1β transcript levels were measured by quantitative real-time PCR and normalized to β-actin mRNA levels. The data are shown as the mean + SEM. (**d**) BMDCs of the indicated genotypes were transfected with poly(dG:dC) (DNA), or stimulated with LPS +ATP for 8 hours. Caspase-1 p10 protein levels in the tissue culture supernatants were analysed by immunoblot. (**e**) BMDCs of the indicated genotypes were transfected with

poly(dG:dC) (DNA) for 2 hours and analyzed by confocal microscopy following immunofluorescence staining with antibodies against Rad50 and CARD9 or Bcl10; DNA was stained with DAPI. The merged images are shown; the arrows indicate cytosolic dsDNA/Rad50/CARD9, dsDNA/Rad50/Bcl10, or dsDNA/Rad50 complexes. The scale bar represents 5 $\mu$m. At least 50 individual cells were analyzed per experiment and assay point. All data are representative of at least three independent experiments. ***p < 0.001, Student's t-test. ND, not detectable.
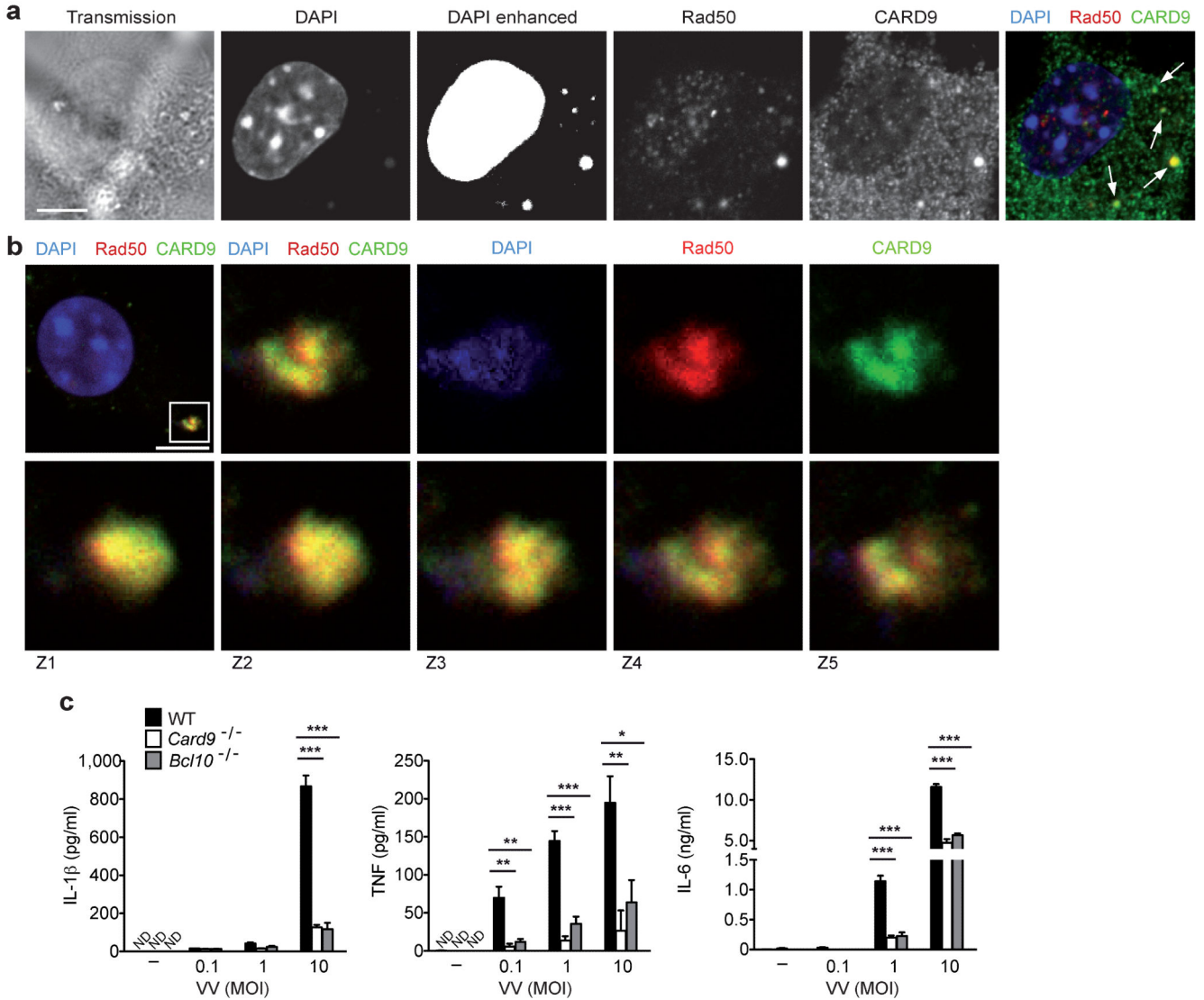
**Figure 6. Recognition of DNA virus infection by Rad50/CARD9 complexes**
(**a, b**) BMDCs were infected with VV, fixed, and stained with antibodies against Rad50 and CARD9. The cells were analyzed using confocal microscopy; dsDNA was stained with DAPI. The arrows indicate viral-dsDNA/Rad50/CARD9 complexes (**a**). In (**b**), the indicated viral-dsDNA/Rad50/CARD9 complex (upper left picture, box) was visualized at higher magnifications and in different z-layers (z1 - z5). Scale bars, 5 $\mu$m. One representative of three independent experiments is shown. (**c**) BMDCs of the indicated genotype were infected with increasing MOIs of VV, and IL-1β, TNF, and IL-6 concentrations were measured in the supernatants. The data are represented as the mean + SEM. *p < 0.05, **p < 0.01, ***p < 0.001, Student's t-test.
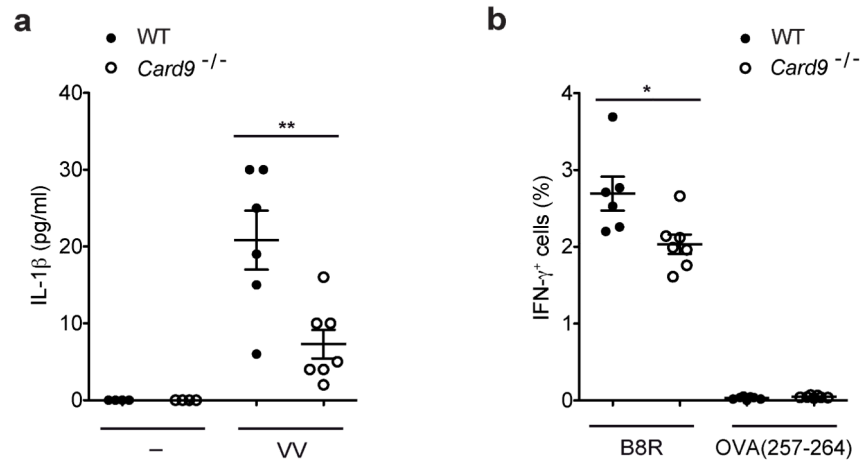
**Figure 7. CARD9 controls DNA virus-induced immune responses *in vivo***
(**a**) WT and *Card9*^{−/−} mice were infected with VV *in vivo*, and the IL-1β concentrations were measured in the serum after 6 hours. (**b**) At 8 days post-infection, splenocytes were isolated and stimulated with a VV-specific peptide (B8R) or a control peptide, OVA(257-264), for 5 hours. The percentage of IFN-γ+ CD8+ T cells was determined by flow cytometry. Circles represent individual mice. The data represent the mean +/− SEM. *p < 0.05, **p < 0.01, Student's t-test.

**Supplementary material:**

**Rad50-CARD9 interactions link cytosolic DNA sensing to IL-1β production**

Susanne Roth, Andrea Rottach, Amelie S. Lotz-Havla, Verena Laux, Andreas Muschaweckh,

Søren W. Gersting, Ania C. Muntau, Karl-Peter Hopfner, Lei Jin, Katelynd Vanness,

John H. J. Petrini, Ingo Drexler, Heinrich Leonhardt, Jürgen Ruland
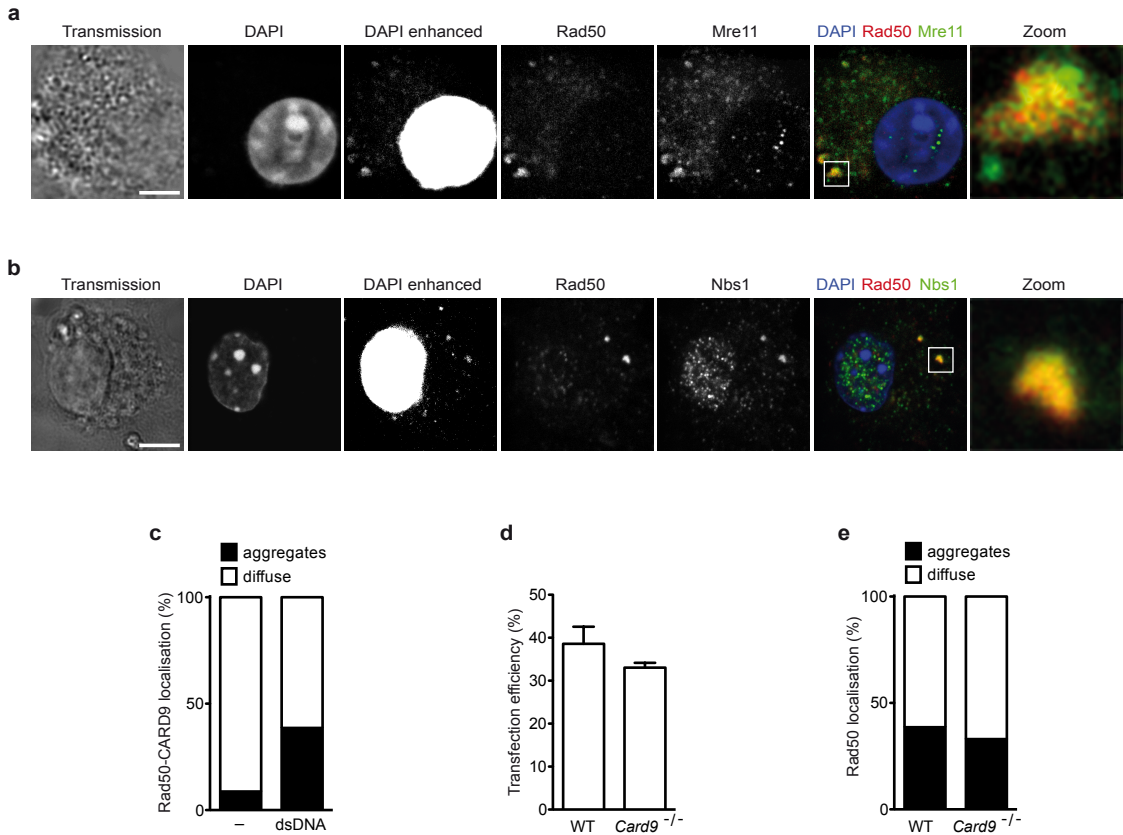
**Supplementary Figure 1** MRN and Rad50-CARD9 complex formation at cytosolic dsDNA. (**a, b**) BMDCs were transfected with dsDNA for 2 hours, stained with DAPI and anti-Rad50 and anti-Mre11 or anti-Nbs1 antibodies, and analyzed using confocal microscopy. The dsDNA/Rad50/Mre11 or dsDNA/Rad50/Nbs1 complexes (boxes) were also visualized at higher magnifications (Zoom). Scale bars represent 5 µm. The data are representative of at least three independent experiments analyzing at least 50 individual cells per experiment and assay point. (**c-d**) BMDCs were left untreated or transfected with poly(dG:dC) (2.5 µg/ml) for 2 hours and analyzed by confocal microscopy following immunofluorescence staining with DAPI and antibodies against Rad50 and CARD9. Localization of dsDNA, Rad50, and CARD9 in 100 cells per assay point was determined. (**c**) Percentages of cells containing Rad50-CARD9 aggregates compared to a diffuse localization of Rad50 and CARD9 are shown. (**d**) Percentages of WT and *Card9*^{-/-} BMDCs containing cytosolic dsDNA at 2 hours after dsDNA transfection are demonstrated. (**e**) BMDCs of WT and *Card9*^{-/-} mice were transfected with dsDNA, the relative number of cells containing Rad50 aggregates and homogenous Rad50 distribution, respectively, is shown. The data are representative of two independent experiments.
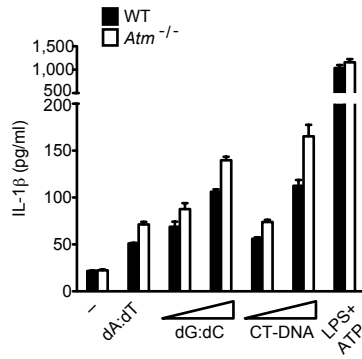
**Supplementary Figure 2** ATM is not involved in dsDNA-induced IL-1β production. BMDCs from WT and *Atm*^{-/-} mice were transfected with dsDNA (1 - 4 μg/ml) of different origins for 16 hours or stimulated with LPS + ATP. The IL-1β concentrations in the supernatants were determined. The data are represented as the mean + SEM of triplicates of three independent experiments.
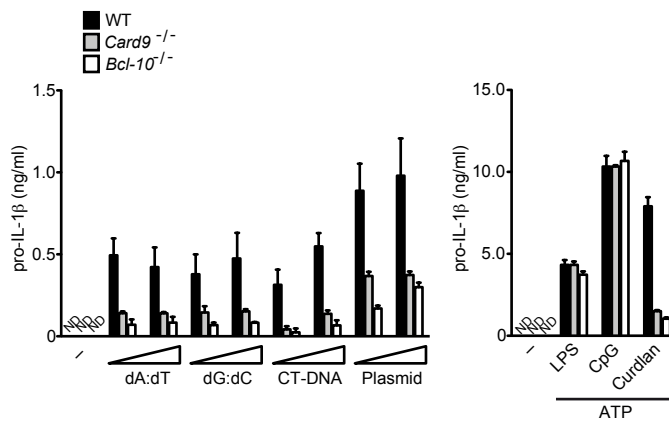
**Supplementary Figure 3** CARD9 and Bcl-10 control pro-IL-1β synthesis. BMDCs from mice of the indicated genotype were transfected with dsDNA (1 - 4 μg/ml) of different origins or stimulated with LPS, CpG, and curdlan plus ATP. The pro-IL-1β concentrations were determined in the cell lysates. The data are represented as the mean + SEM of triplicates. One representative of two independent experiments is shown. ND, not detectable.
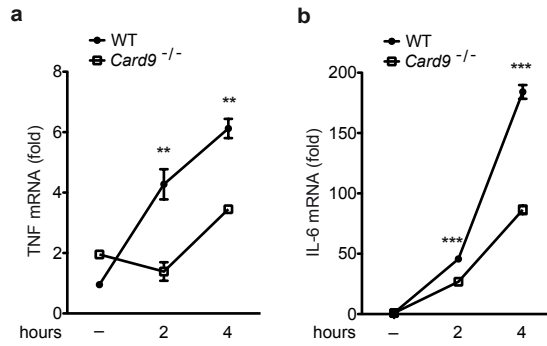
**Supplementary Figure 4** CARD9 regulates DNA-induced transcription of the genes encoding TNF and IL-6. WT and *Card9*$^{-/-}$ BMDCs were transfected with poly(dG:dC) (2.5 $\mu$g/ml) for the indicated time and TNF (**a**) and IL-6 (**b**) transcript levels were measured by quantitative real-time PCR and normalized to $\beta$-actin mRNA levels. The data are shown as the mean + SEM of triplicates. One representative of two independent experiments is shown. \*\*p < 0.01, \*\*\*p < 0.001, Student's t-test.
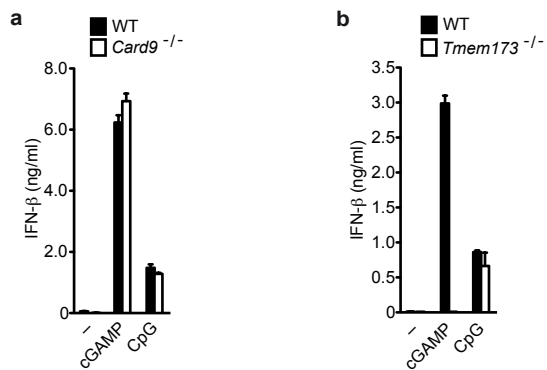
**Supplementary Figure 5** cGAMP-STING signaling is independent of CARD9. BMDCs from WT and *Card9*^{-/-} (**a**), or WT and *Tmem173*^{-/-} (**b**) mice were transfected with the STING activator cGAMP (4 μg/ml) for 6 hours. As control IFN-β production was induced via TLR9 ligation with CpG. IFN-β levels were measured in the supernatant. The data are represented as the mean + SEM of three (**a**), or two (**b**) independent experiments.
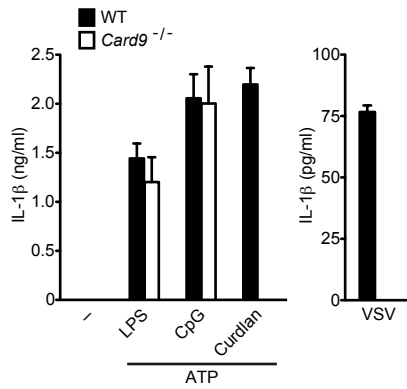
**Supplementary Figure 6** CARD9 is crucial for RNA virus-induced IL-1β generation. WT and *Card9*−/− BMDCs were infected with VSV at MOI 1. LPS, CpG, and curdlan plus ATP were used to investigate CARD9-independent and CARD9-dependent IL-1β production, respectively. The IL-1β concentrations in the supernatants were measured. The data are presented as the mean + SEM. One representative of three independent experiments is shown.

# Vav Proteins Are Key Regulators of Card9 Signaling for Innate Antifungal Immunity

## Graphical Abstract
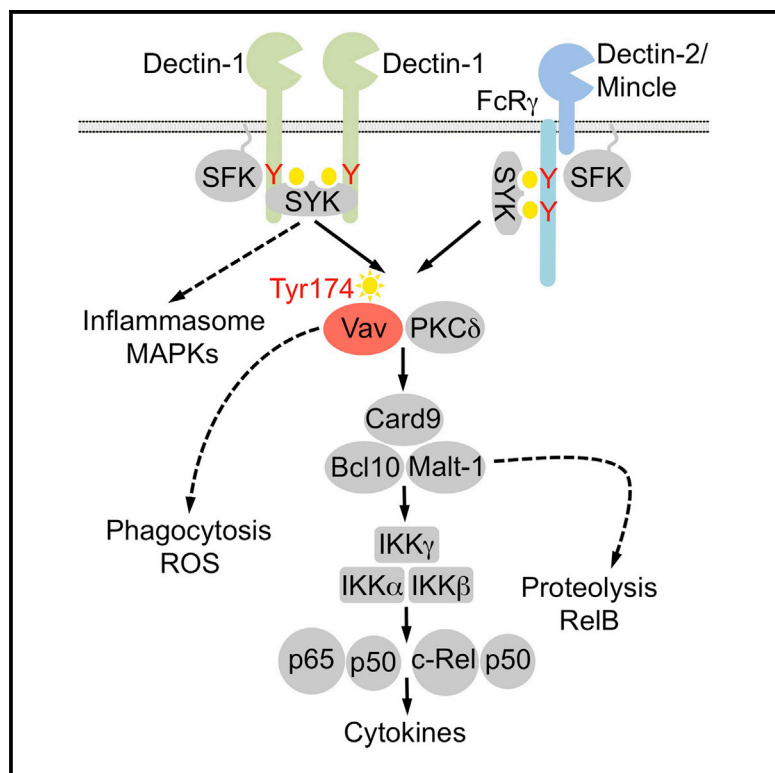


## Authors

Susanne Roth, Hanna Bergmann, Martin Jaeger, ..., Mihai Netea, Xosé R. Bustelo, Jürgen Ruland

## Correspondence

j.ruland@tum.de

## In Brief

CLR/Card9 signaling is essential for antifungal immunity. Roth et al. have identified the Vav family of proteins as key activators of the Card9/NF-kB pathway, essential for CLR-induced inflammatory responses and host defense against fungi.

## Highlights

- Vav proteins control CLR-mediated inflammatory responses
- CLR-induced NF-κB activation is regulated by Vav proteins
- Vav/Card9 signaling is critical for antifungal host defense

## Accession Numbers

GSE83736

CrossMark

**CellPress**

# Vav Proteins Are Key Regulators of Card9 Signaling for Innate Antifungal Immunity

Susanne Roth,[1,2] Hanna Bergmann,[1] Martin Jaeger,[3,4] Assa Yeroslaviz,[5] Konstantin Neumann,[1] Paul-Albert Koenig,[1] Clarissa Prazeres da Costa,[6] Lesley Vanes,[7] Vinod Kumar,[8] Melissa Johnson,[9] Mauricio Menacho-Márquez,[10] Bianca Habermann,[5] Victor L. Tybulewicz,[7,11] Mihai Netea,[3] Xosé R. Bustelo,[10,12] and Jürgen Ruland[1,13,14,15,*]

[1]Institut für Klinische Chemie und Pathobiochemie, Klinikum rechts der Isar, Technische Universität München, 81675 München, Germany
[2]Chirurgische Klinik, Universitätsklinikum Heidelberg, Ruprecht-Karls-Universität, 69120 Heidelberg, Germany
[3]Department of Medicine, Radboud University, Medical Centre, 6500 HB Nijmegen, the Netherlands
[4]Radboud Center for Infectious Diseases, 6500 HB Nijmegen, the Netherlands
[5]Max Planck Institute of Biochemistry, Research Group Computational Biology, 82152 Martinsried, Germany
[6]Institut für Medizinische Mikrobiologie, Immunologie, und Hygiene, Klinikum rechts der Isar, Technische Universität München, 81675 München, Germany
[7]Francis Crick Institute, London NW1 1AT, UK
[8]Department of Genetics, University Medical Center Groningen, University of Groningen, Groningen, 9700 RB, the Netherlands
[9]Duke University Medical Center, Duke Box 102359, Durham, NC 27710, USA
[10]Centro de Investigación del Cáncer, CSIC-University of Salamanca, 37007 Salamanca, Spain
[11]Department of Medicine, Imperial College, London W12 0NN, UK
[12]Centro de Investigacion Biomedica en Red-Oncologia, Carlos III Health Institute, Spain
[13]German Cancer Consortium (DKTK), 69120 Heidelberg, Germany
[14]German Center for Infection Research (DZIF), Partner Site Munich, Munich, Germany
[15]Lead Contact
*Correspondence: j.ruland@tum.de
http://dx.doi.org/10.1016/j.celrep.2016.11.018

## SUMMARY

Fungal infections are major causes of morbidity and mortality, especially in immunocompromised individuals. The innate immune system senses fungal pathogens through Syk-coupled C-type lectin receptors (CLRs), which signal through the conserved immune adaptor Card9. Although Card9 is essential for antifungal defense, the mechanisms that couple CLR-proximal events to Card9 control are not well defined. Here, we identify Vav proteins as key activators of the Card9 pathway. Vav1, Vav2, and Vav3 cooperate downstream of Dectin-1, Dectin-2, and Mincle to engage Card9 for NF-κB control and proinflammatory gene transcription. Although Vav family members show functional redundancy, $Vav1/2/3^{-/-}$ mice phenocopy $Card9^{-/-}$ animals with extreme susceptibility to fungi. In this context, Vav3 is the single most important Vav in mice, and a polymorphism in human *VAV3* is associated with susceptibility to candidemia in patients. Our results reveal a molecular mechanism for CLR-mediated Card9 regulation that controls innate immunity to fungal infections.

## INTRODUCTION

Cells of the innate immune system sense microbial components or cell damage-associated structures via germline-encoded pattern recognition receptors (PRRs) that subsequently signal for host defense and tissue homeostasis (Takeuchi and Akira, 2010). One important family of signaling PRRs on myeloid cells are the Syk-coupled C-type lectin receptors (Kerrigan and Brown, 2011; Sancho and Reis e Sousa, 2012). These PRRs play a broad role in innate immunity and are particularly important for host defense against fungal infections (Ferwerda et al., 2009; Robinson et al., 2009; Saijo et al., 2007, 2010; Sato et al., 2006; Taylor et al., 2007; Wells et al., 2008), which constitute an increasing health threat because of growing numbers of patients at risk mainly because of immunosuppressive medical interventions and AIDS. In the context of antifungal immunity, the C-type lectin receptor (CLR) family member Dectin-1 senses β-glucans in fungal cell walls (Brown and Gordon, 2001), whereas Mincle and Dectin-2 detect α-mannose, glycolipids, and α-mannans, respectively (Sancho and Reis e Sousa, 2012). Agonist binding by Dectin-1 leads to the phosphorylation of immunoreceptor tyrosine-based activation motif (ITAM)-like motifs in its cytoplasmic tail by Src family kinases, resulting in activation of the tyrosine kinase Syk. Likewise, Dectin-2 and Mincle also activate Syk, indicating that these CLR signals engage common effector mechanisms (Mócsai et al., 2010; Sancho and Reis e Sousa, 2012). The innate immune adaptor protein Card9 is critical for CLR signaling. It assembles signaling complexes that also contain Bcl10 and Malt1 (Card9-Bcl10-Malt1 [CBM] complexes) and that serve as scaffolds for activation of the canonical nuclear factor κB (NF-κB) pathway (Roth and Ruland, 2013). This mechanism activates the inhibitor of kappa B (IκB) kinase (IKK) complex, which phosphorylates inhibitory IκBs, leading to their proteasomal degradation and the release of NF-κB dimers to the nucleus to activate gene transcription (Vallabhapurapu and Karin, 2009). Malt1 can also function as a

protease upon CBM complex assembly that cleaves a set of NF-κB regulators, including RelB, to fine-tune immune gene expression (Hailfinger et al., 2011; Jaworski et al., 2014). These Card9 signaling complexes operate downstream of all tested Syk-coupled CLRs (Roth and Ruland, 2013) and are essential for innate antifungal immunity. Indeed, Card9-deficient mice are highly susceptible to infection with *Candida* (Gross et al., 2006; Jia et al., 2014), *Aspergillus* (Jhingran et al., 2012), and *Cryptococcus* (Yamamoto et al., 2014) species. Moreover, loss-of-function mutations in human *CARD9* have been identified as causes of mucocutaneous and invasive fungal infections (Glocker et al., 2009; Pérez de Diego et al., 2015). Nevertheless, despite the critical role for CLR-triggered Card9 signaling in innate immunity and mammalian host defense, the molecular mechanisms that link CLR ligation to Card9-dependent effector mechanisms are not well understood.

Here, we used a mass spectrometry-based proteomic approach and identified Vav proteins as regulators of Card9 signaling. Vav1, Vav2, and Vav3 cooperate downstream of Dectin-1, Dectin-2, and Mincle to engage Card9 complexes for NF-κB control and proinflammatory gene transcription. Like Card9-deficient mice, Vav1/2/3 triple-deficient mice are severely impaired in inflammatory responses to *Candida albicans* infection and host defense against the fungus. Moreover, we report a human polymorphism in *VAV3* that is associated with susceptibility to candidemia. Thus, our results establish Vav proteins as essential regulators of CLR-mediated Card9 control in innate antifungal immunity.

## RESULTS

### Fungal Infection Induces Tyrosine Phosphorylation of Vav in Myeloid Cells

To investigate the mechanisms of Syk-coupled CLR signaling, we stimulated wild-type murine bone marrow-derived dendritic cells (BMDCs), comprising conventional DCs and monocyte-derived macrophages (Helft et al., 2015), for 10 min with zymosan, a yeast cell wall preparation that is highly enriched in Dectin-1 and Dectin-2 agonists, and subsequently affinity-purified tyrosine-phosphorylated proteins for mass spectrometric analysis (Strasser et al., 2012). Under these conditions, we observed signal-induced tyrosine phosphorylation of Vav1 and Vav3, which are cytosolic signaling scaffolds and guanine nucleotide exchange factors that can play context-specific roles in immune receptor pathways (Bustelo, 2014). To validate these findings, we stimulated BMDCs with *C. albicans* hyphae and specifically analyzed Vav1 phosphorylation by western blot analysis. Indeed, Vav1 was tyrosine-phosphorylated after *C. albicans* infection (Figure 1A). These data are in line with previously published results that demonstrated that stimulation with β-glucan or zymosan triggers tyrosine phosphorylation of Vav1 also in microglial cells or neutrophils (Li et al., 2011; Shah et al., 2009). Further analysis with a phosphospecific antibody raised against the regulatory Tyr174 residue of Vav1 additionally revealed that this specific residue is phosphorylated upon *C. albicans* detection, indicating Vav1 activation (Aghazadeh et al., 2000), but not upon LPS stimulation (Figure 1B).

Recent work has demonstrated that Vav phosphorylation downstream of different ITAM-containing receptors is mediated by Src and Syk kinases (Bustelo, 2014). To determine the importance of the CLR-proximal Src and Syk kinases in Vav phosphorylation, we pretreated BMDCs with the Src inhibitor PP2 or the Syk inhibitor R406 prior to the addition of *C. albicans*. Both Src and Syk inhibition blocked Vav1-Tyr174 phosphorylation in a dose-dependent manner, whereas pretreatment with PP3, an inactive analog of PP2, did not affect *C. albicans*-induced phosphorylation of Vav1 at Tyr174 (Figure 1C). Together, these results indicate that Vav1 is activated in myeloid antigen-presenting cells specifically after fungal sensing via an Src and Syk kinase-dependent mechanism.

### CLR-Mediated Inflammatory Responses Are Critically Dependent on Vav Proteins

Next, we studied the functional relevance of Vav proteins in *C. albicans*-induced inflammatory responses. Because dendritic cells express Vav2 (Spurrell et al., 2009) in addition to Vav1 and Vav3, which have partially redundant functions in immune cells (Fujikawa et al., 2003; Tybulewicz, 2005), we investigated BMDCs from mice that lack each individual Vav isoform, two Vav isoforms, or all three Vav family members. Notably, the lack of any one or all Vav molecules did not impair BMDC differentiation (data not shown; Graham et al., 2007; Spurrell et al., 2009). However, BMDCs from Vav1/2/3 triple-deficient mice were severely defective in *C. albicans*-induced TNF production, whereas tumor necrosis factor (TNF) secretion in response to Toll-like receptor (TLR) stimulation with LPS or Pam3CSK4 was unaffected in these cells (Figure 2A). Moreover, the production of interleukin-2 (IL-2) and IL-10 was also defective in BMDCs from *Vav1/2/3$^{-/-}$* mice (Figure 2A). The finding that Vav1, Vav2, or Vav3 single-deficient or *Vav2/3$^{-/-}$* myeloid antigen-presenting cells are only partially impaired in *C. albicans*-induced TNF, IL-2, and IL-10 generation (Figure 2B) indicates redundancy for Vav proteins in fungus-induced cytokine responses.

One important inflammatory cytokine for antifungal immunity is IL-1β (Vonk et al., 2006), the generation of which is controlled by NF-κB-dependent pro-IL-1β gene transcription followed by NLRP3 inflammasome-mediated Caspase-1-dependent pro-IL-1β processing (Gross et al., 2009; Hise et al., 2009). Stimulation of wild-type BMDCs with *C. albicans* induced the robust secretion of mature IL-1β into the culture supernatant (Figure 2C). In contrast, Vav1/2/3-deficient cells were almost completely defective in *Candida*-induced IL-1β production (Figure 2C). This defect was caused by the selective impairment of pro-IL-1β gene transcription in *Vav1/2/3$^{-/-}$* cells (Figure 2D), whereas the deficiency of Vav proteins did not affect NLRP3 inflammasome-dependent Caspase-1 activation (Figure 2E). Together, these experiments demonstrate that Vav proteins are critical for cytokine production by myeloid cells following the detection of whole fungal cells.

Next, we studied the specific requirement of Vav proteins for Dectin-1-, Dectin-2-, and Mincle-induced cytokine responses using selective agonists for each individual receptor. Stimulation of Dectin-1 with curdlan, a purified particulate β-glucan (Leibundgut-Landmann et al., 2007), induced the robust production of TNF in wild-type BMDCs, whereas Vav1/2/3-deficient cells failed to produce TNF in response to Dectin-1 triggering (Figure 2F). Likewise, stimulation of BMDCs with agonistic
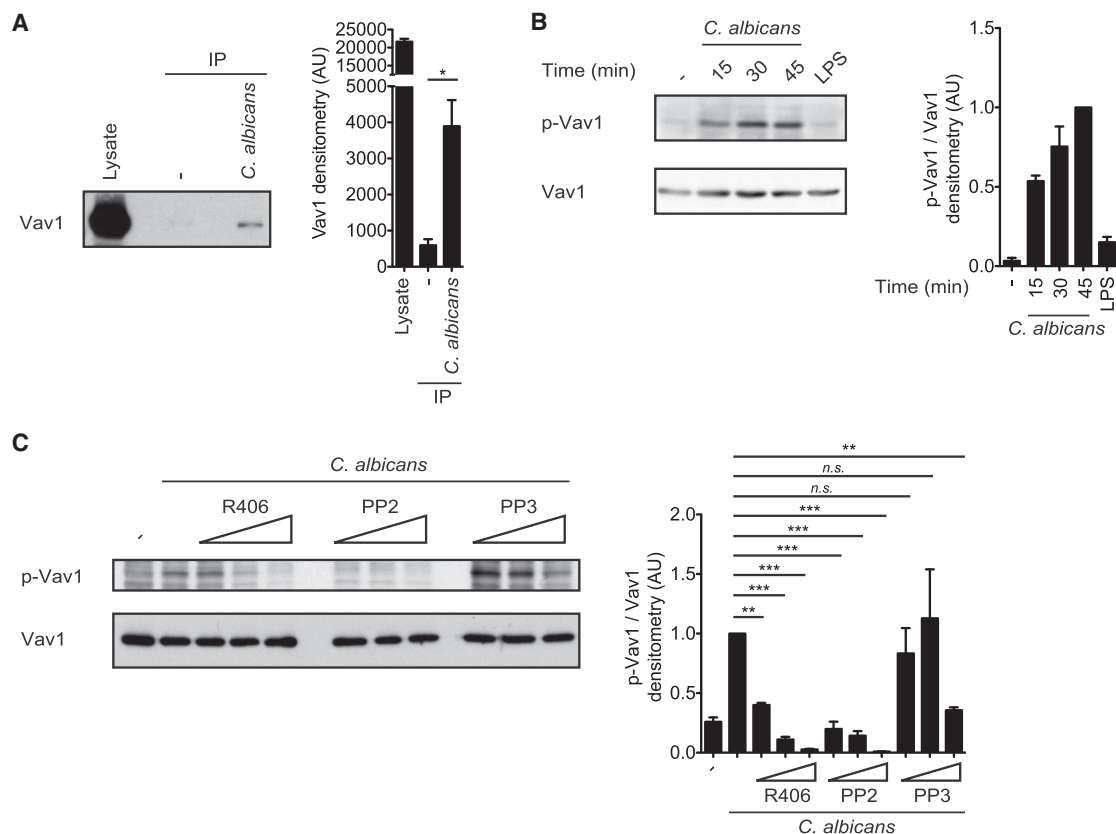
**Figure 1. Vav1 Is Tyrosine-Phosphorylated in Response to *Candida***

(A) BMDCs were untreated (−) or stimulated with *C. albicans* hyphae (MOI 5) for 15 min. Proteins from cell lysates were immunopurified with anti-phospho-tyrosine antibodies and analyzed by immunoblot with a Vav1 antibody (left). Also shown is quantification of Vav1 by densitometry (right).

(B) Immunoblot analysis of BMDCs unstimulated (−), treated with *C. albicans* hyphae (MOI 0.5) for the indicated times, or stimulated with LPS (100 ng/ml) for 45 min and probed with antibodies against phospho-Vav1 (Tyr174) or Vav1 (left). Also shown is densitometrical quantification of phospho-Vav1 relative to total Vav1, normalized to BMDCs treated with *C. albicans* for 45 min (right).

(C) BMDCs were untreated (−) or preincubated with the Syk inhibitor R406 (0.5, 1, and 2 μM) or the Src-kinase inhibitor PP2 (1.5, 3, and 6 μM) or its inactive analog PP3 (1.5, 3, and 6 μM) and then stimulated with *C. albicans* hyphae (MOI 1) for 30 min. Lysates were immunoblotted with anti-phospho-Vav1 (Tyr174) or anti-Vav1 antibodies (left). Also shown is densitometrical quantification of phospho-Vav1 relative to total Vav1, normalized to BMDCs treated with *C. albicans* without any inhibitors (right). Data of at least three independent experiments are shown as mean ± SEM.

*p < 0.05, **p < 0.01, ***p < 0.001; Student's t test (A) and one-way ANOVA and post hoc Tukey-Kramer test (C). n.s., not significant.

antibodies against Dectin-2 or with trehalose-6,6-dibehenate (TDB), a synthetic analog of the mycobacterial cord factor trehalose 6,6′-dimycolate (TDM), which specifically activates Mincle (Lobato-Pascual et al., 2013; Miyake et al., 2013; Schoenen et al., 2010), induced TNF in wild-type cells, but this response was severely impaired in Vav1/2/3-deficient BMDCs (Figure 2F). Therefore, although Vav single- or double-mutant cells exhibited a partially impaired cytokine response upon selective Dectin-1, Dectin-2, or Mincle stimulation (Figure 2G), the Vav family as a whole is essential for cytokine production after Syk-coupled CLR ligation in vitro.

### Vav Proteins Regulate CLR-Induced Inflammatory Responses In Vivo and Are Essential for Antifungal Defense

To investigate the function of Vav proteins in CLR-mediated inflammatory responses in vivo, we intravenously injected the

Mincle ligand TDM (Ishikawa et al., 2009; Miyake et al., 2013) into wild-type and Vav1/2/3−/− mice. Consistent with previously published results (Ishikawa et al., 2009), TDM injection resulted in the strong systemic production of TNF, IL-1β, and IL-10 in wild-type mice (Figure 2H). However, these responses were defective in Vav1/2/3 triple-deficient animals (Figure 2H). Next, we studied the role of Vav proteins in inflammatory cytokine responses after fungal infection in vivo. To this end, we intravenously injected wild-type or Vav1/2/3 triple knockout mice with live *C. albicans* and measured serum TNF and IL-6 levels after 6 hr. Notably, the production of both inflammatory cytokines was almost completely abolished in Vav1/2/3−/− mice (Figure 3A). Subsequently, we studied the importance of individual Vav proteins in host protection against fungi by infecting wild-type or Vav single-, double-, or triple-deficient mice with 1 × 10^{5} colony-forming units (CFUs) of *C. albicans.* Four days later, we assessed intravital fungal growth in the kidneys, the main
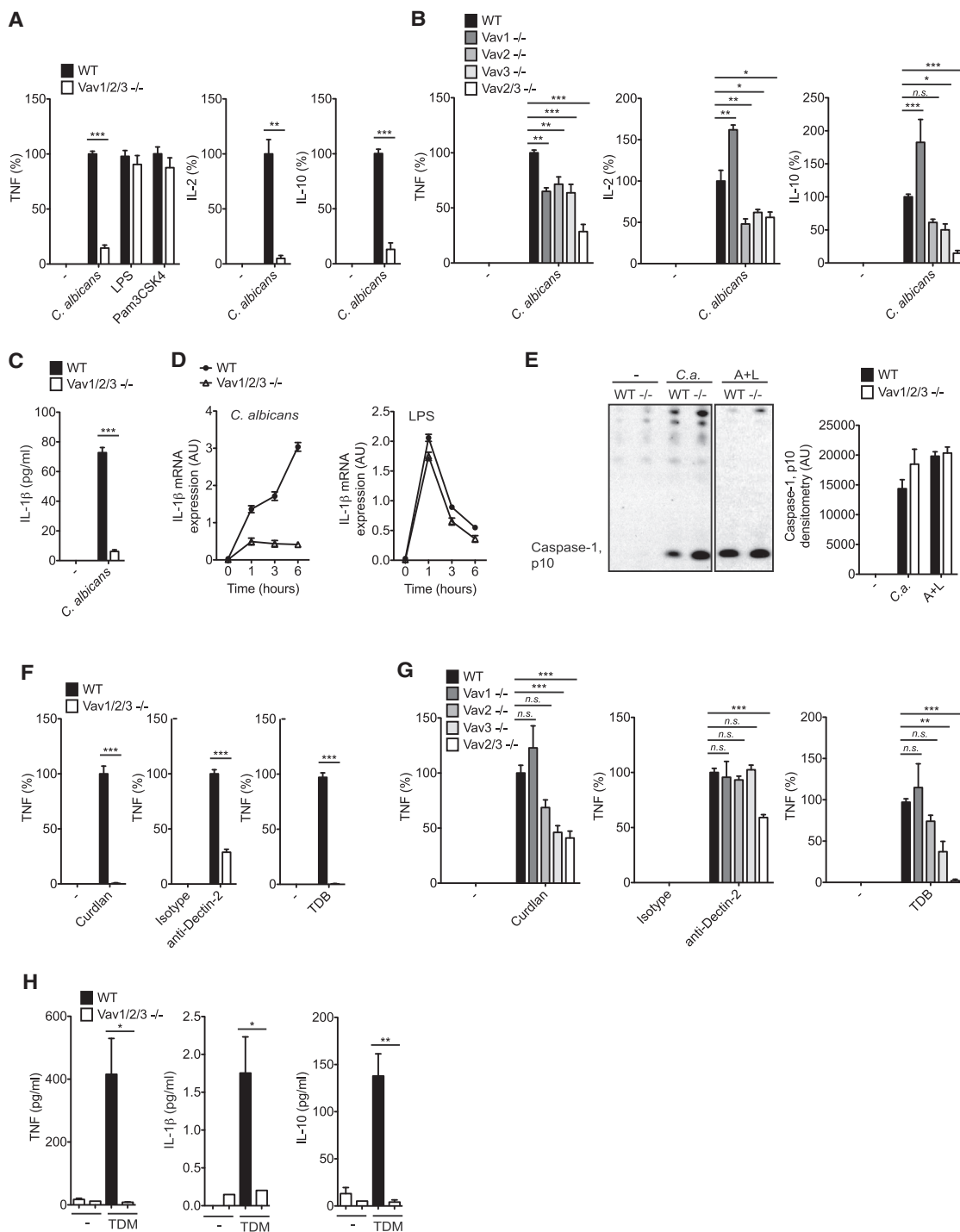
**Figure 2. Vav Proteins Are Essential for Syk-Coupled CLR-Induced Proinflammatory Responses**

(A and B) TNF, IL-2, and IL-10 levels in the supernatants of wild-type (WT) and *Vav1/2/3⁻/⁻* BMDCs (A), or Vav single- or double mutant BMDCs of the indicated genotypes (B) that were untreated (−) or stimulated with *C. albicans* hyphae (MOI 0.3), LPS (500 ng/ml), or Pam3CSK4 (50 ng/ml) for 16 hr were analyzed by ELISA.

(C) IL-1β in the supernatants of WT and *Vav1/2/3⁻/⁻* BMDCs left untreated (−) or stimulated with *C. albicans* hyphae (MOI 1) for 6 hr.

(D) Quantitative real-time PCR analysis of IL-1β transcripts in WT and *Vav1/2/3⁻/⁻* BMDCs left untreated or stimulated with *C. albicans* hyphae (MOI 1) (left) or LPS (100 ng/ml) (right) for the indicated times; results are relative to those of β-actin mRNA.

(E) Immunoblot analysis of mature Caspase-1 (p10) in cell culture supernatants of WT and *Vav1/2/3⁻/⁻* (−/−) BMDCs left untreated (−), stimulated with *C. albicans* hyphae (MOI 1) for 4 hr (C.a.), or pre-stimulated with LPS (50 ng/ml) for 6 hr prior to the addition of ATP (5 mM) for 45 min (A+L). Quantification of mature Caspase-1 p10 by densitometry is shown to the right of the western blot.

*(legend continued on next page)*

target organ of the fungus (Brieland et al., 2001). Although wild-type mice cleared the fungus readily, the kidneys of all investigated $Vav1/2/3^{-/-}$ mice were enlarged and infiltrated with macroscopically visible fungal colonies (Figure 3B). Quantitatively, we detected more than 100-fold higher titers of *C. albicans* in the kidneys of Vav1/2/3 triple-deficient animals compared with the wild-type (Figure 3C), and histopathology confirmed intravital fungal growth (Figure 3D). The fungal burdens in Vav3 single knockout and Vav2/3 double knockout mice were increased by trend compared with the wild-type, but a selective loss of Vav1 or Vav2 did not result in higher fungal titers compared with wild-type mice (Figure 3C). Finally, we studied the role of Vav signaling in the survival of mice after fungal infection. In line with the incapacity to control fungal invasion of the organs, Vav1/2/3-deficient mice died rapidly after injection of $1 \times 10^5$ CFU of *C. albicans,* whereas the wild-type control animals survived this challenge (Figure 3E). These experiments reveal that Vav proteins play essential roles in fungus-induced cytokine production and antifungal immunity in vivo, with Vav3 being the single most important Vav family member for protection against *C. albicans* infection.

## Vav Proteins Are Regulators of CLR-Induced NF-κB Activation

The susceptibility of Vav1/2/3 triple-deficient animals and the failure to induce CLR-mediated cytokine responses are reminiscent of the severe phenotype observed in Card9-deficient mice, suggesting that Vav proteins and Card9 may operate in a common signaling cascade. Because of the partially overlapping functions of the three Vav isoforms, we focused subsequent biochemical studies on Vav1/2/3 triple knockout BMDCs. Upon *C. albicans* stimulation, phosphorylation of the tyrosine kinase Syk and of the Dectin-1 signal transducer PLCγ2 (Xu et al., 2009) did not differ between wild-type and $Vav1/2/3^{-/-}$ BMDCs (Figure 4A), indicating that Vav proteins are not required for the immediate receptor-proximal events. Moreover, because Erk1/2, p38, and Jun N-terminal kinase (JNK) were similarly phosphorylated in *C. albicans*-stimulated wild-type and $Vav1/2/3^{-/-}$ BMDCs (Figure 4B), we conclude that Vavs are not essential for the regulation of mitogen-activated protein kinase (MAPK) signaling after fungal infection. However, activation of protein kinase C δ (PKCδ), which controls Card9 engagement (Strasser et al., 2012), was partially impaired in BMDCs lacking all three Vav isoforms (Figure 4C; Figure S1A). Likewise, PKCδ deficiency partially compromised Vav1 phosphorylation in response to *C. albicans* or curdlan stimulation (Figure S1B). Moreover, although *C. albicans* or curdlan stimulation of wild-type BMDCs induces the rapid activation of the IKK complex, as determined by measuring IKKα/β phosphorylation (Figure 4C; Figures S1A

and S1B), this response is almost completely abolished in the absence of Vav proteins (Figure 4C; Figure S1A) or PKCδ (Figure S1B; Strasser et al., 2012). Consistent with these findings, *C. albicans*-induced nuclear translocation of the transcriptional active NF-κB subunits p65, c-Rel, and RelB were also severely defective in $Vav1/2/3^{-/-}$ BMDCs, as they are in Card9-deficient cells (Figures 4D and 4E; Figures S1C and S1D), demonstrating a critical role for Vav proteins in CLR-dependent NF-κB control.

As indicated above, the activation of the Card9/Bcl10/Malt1 complex not only regulates IKK activation but also induces Malt1 proteolytic activity (Jaworski et al., 2014). Consistently, stimulation of wild-type BMDCs with CLR ligands results in the rapid proteolytic processing of the Malt1 substrate RelB (Figures 4F and 4G; Figures S1E and S1F; Gewies et al., 2014; Hailfinger et al., 2011; Jaworski et al., 2014). Curdlan-induced RelB cleavage was completely defective in BMDCs from $Malt1^{-/-}$ mice and from mice with gene-targeted inactivation of the Malt1 paracaspase function ($Malt1^{PM/-}$) (Gewies et al., 2014; Figure 4F; Figure S1E) and, therefore, can be used as a marker for CBM complex activation. Likewise, Malt1-mediated RelB cleavage upon *C. albicans* stimulation was also defective in Vav1/2/3 triple knockout cells (Figure 4G; Figure S1F), which, together with the defective IKK activation in $Vav1/2/3^{-/-}$ BMDCs, indicates that Vav proteins operate upstream of the Card9/Bcl10/Malt1 signalosome.

Finally, we studied the role of Vav proteins in CLR-induced gene expression in a global manner. To this end, we performed high-throughput cDNA sequencing (RNA sequencing [RNA-seq]) followed by gene set enrichment analysis (GSEA) of curdlan-stimulated and untreated BMDCs. In Dectin-1-stimulated wild-type BMDCs, we detected a significant enrichment of upregulated NF-κB-dependent transcripts compared with $Vav1/2/3^{-/-}$ cells (Figure 4H), which is consistent with the defective IKK activation described above. These results further validate Vav proteins as essential regulators of CLR-mediated NF-κB control.

## A Human Vav3 Polymorphism Is Associated with Susceptibility to Candidemia

After identifying Vav proteins as integral regulators of the Dectin-1/Card9/NF-κB signaling cascade in murine cells, we were interested in the potential roles for Vav molecules in human antifungal immunity. Therefore, we investigated whether genetic variations linked to any of the *VAV* genes correlate with susceptibility to candidemia in patients by studying a previously described cohort of candidemia patients and an appropriate control group (Jaeger et al., 2015). Interestingly, the analysis of SNPs associated with *VAV3* revealed a significant association with candidemia, with the significant SNPs distributed across the linkage

---

(F and G) BMDCs from WT and $Vav1/2/3^{-/-}$ mice (F), or Vav single- or double mutant mice of the indicated genotypes (G) were untreated (−), stimulated with the Dectin-1 ligand curdlan (10 μg/ml), plate-bound anti-Dectin-2 (12.5 μg/ml) or isotype control antibodies (Isotype), or the Mincle ligand TDB (100 μg/ml). TNF levels in the cell culture supernatants were quantified by ELISA.

(H) WT and $Vav1/2/3^{-/-}$ mice were injected intravenously with TDM containing oil-in-water emulsions or with the vehicle control (−). 24 hr post-injection, TNF, IL-1β, and IL-10 levels in sera were determined by CBA.

(A, B, F, and G) Data are expressed as percent of WT ± SEM of three independent experiments.

(C–E and H) Data of at least three independent experiments are presented as mean ± SEM.

*p < 0.05, **p < 0.01, and ***p < 0.001, Student's t test (A, C, F, and H), and one-way ANOVA and post hoc Tukey-Kramer test (B and G).
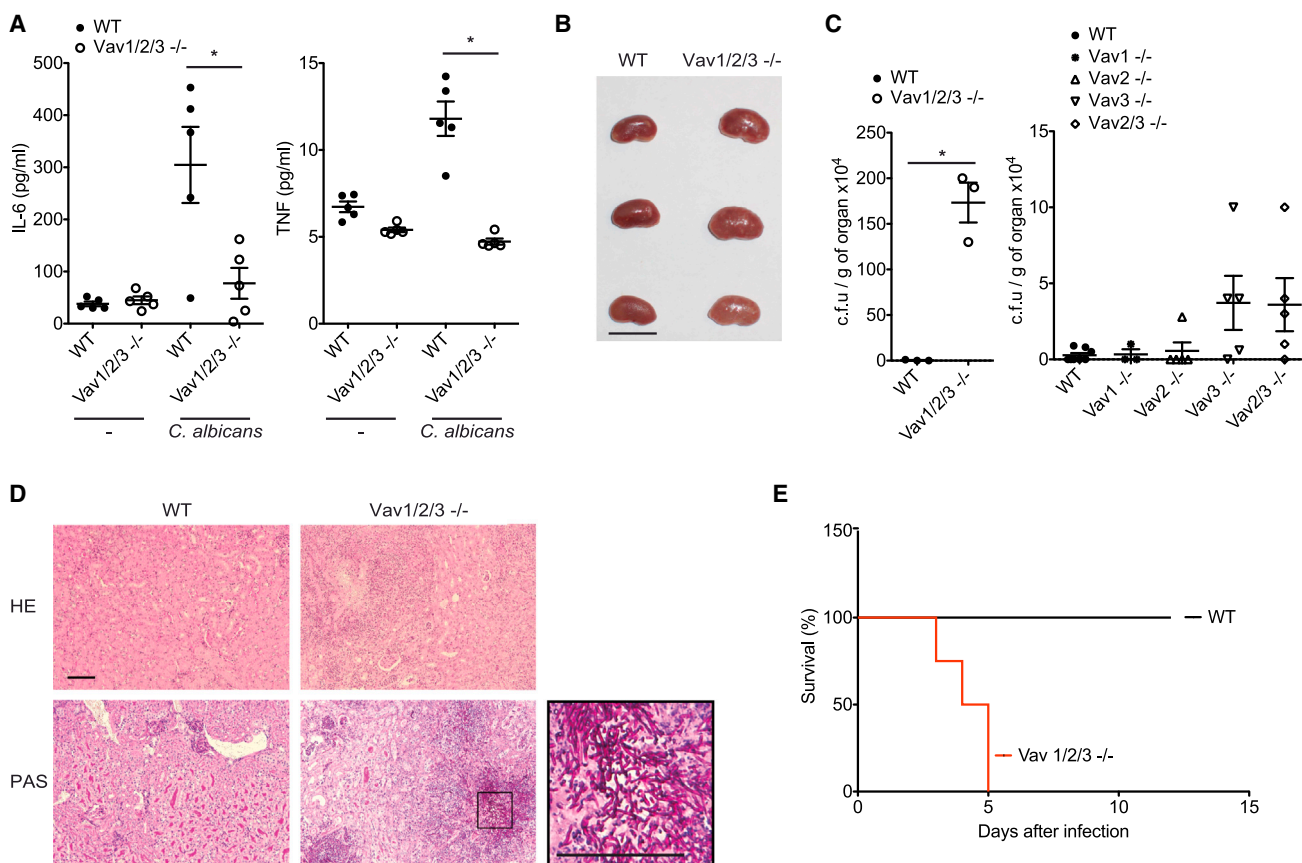
**Figure 3. Vav Proteins Are Required for Systemic Antifungal Host Defense**
(A–E) Mice of the indicated genotypes were intravenously infected with $1 \times 10^5$ CFUs of *C. albicans*.
(A) Serum IL-6 and TNF levels in WT and *Vav1/2/3$^{-/-}$* mice were determined by CBA 6 hr after infection.
(B and C) After 4 days, kidneys were macroscopically examined (B; scale bar, 10 mm), and *C. albicans* titers were determined in the kidneys (C).
(D) Kidney sections from *C. albicans*-infected WT and *Vav1/2/3$^{-/-}$* mice were stained with H&E or periodic acid-Schiff (PAS; scale bars, 100 μm).
(E) WT (n = 5) and *Vav1/2/3$^{-/-}$* (n = 4) mice were monitored daily for health and survival. Statistical survival analyses were performed using the log-rank test ($p < 0.005$).
(A and C) Each symbol represents an individual mouse; small horizontal lines indicate the mean; error bars indicate the SEM. Data of one experiment in each case are presented. *$p < 0.05$, Student's t test (A and C, left) and one-way ANOVA (C, right, $p = 0.06$).

disequilibrium (LD) region of the gene. The association does not extend beyond the LD region, and the strongest association was with the SNP rs4914950 (Figure 5A). The risk genotype of the SNP rs4914950 TT is increased from 10% (control population) to 18% (candidemia patients) (Figure 5B).

## DISCUSSION

Using a complementary approach of immunology, molecular biology, and genetic studies, the results presented in this manuscript define an essential role for Vav proteins in CLR-mediated inflammatory responses and establish these molecules as essential signaling platforms that relay proximal events from Syk-coupled CLRs to the Card9 signaling complex for NF-κB control and antifungal defense (Dambuza and Brown, 2015; Osorio and Reis e Sousa, 2011; Roth and Ruland, 2013). Although individual Vav isoforms can compensate for each other, their combined absence results in a blockade of CLR-

dependent NF-κB activation similar to Card9 deficiency, with Vav3 being the most important family member in this pathway in mice and, presumably, in humans.

When engaged by fungal particles, Syk-coupled CLRs activate various intracellular signaling pathways that regulate phagocytosis, microbicidal activities, and gene transcription. Using *C. albicans* as a clinically relevant model organism that is sensed by multiple CLRs and induces CLR signaling (Robinson et al., 2009; Taylor et al., 2007; Wells et al., 2008), we observed Vav activation downstream of Syk. In addition, using defined agonists of Dectin-1, Dectin-2, and Mincle, we established a general role for Vav proteins in CLR signaling in myeloid antigen-presenting cells. However, our results that CLR-mediated MAPK activation and inflammasome signaling are not impaired in Vav1/2/3 triple-deficient BMDCs reveal that Vav proteins only mediate specific CLR effector mechanisms. Recent studies have indicated the involvement of Vav1 and Vav3 in Dectin-1-mediated zymosan phagocytosis and reactive oxygen
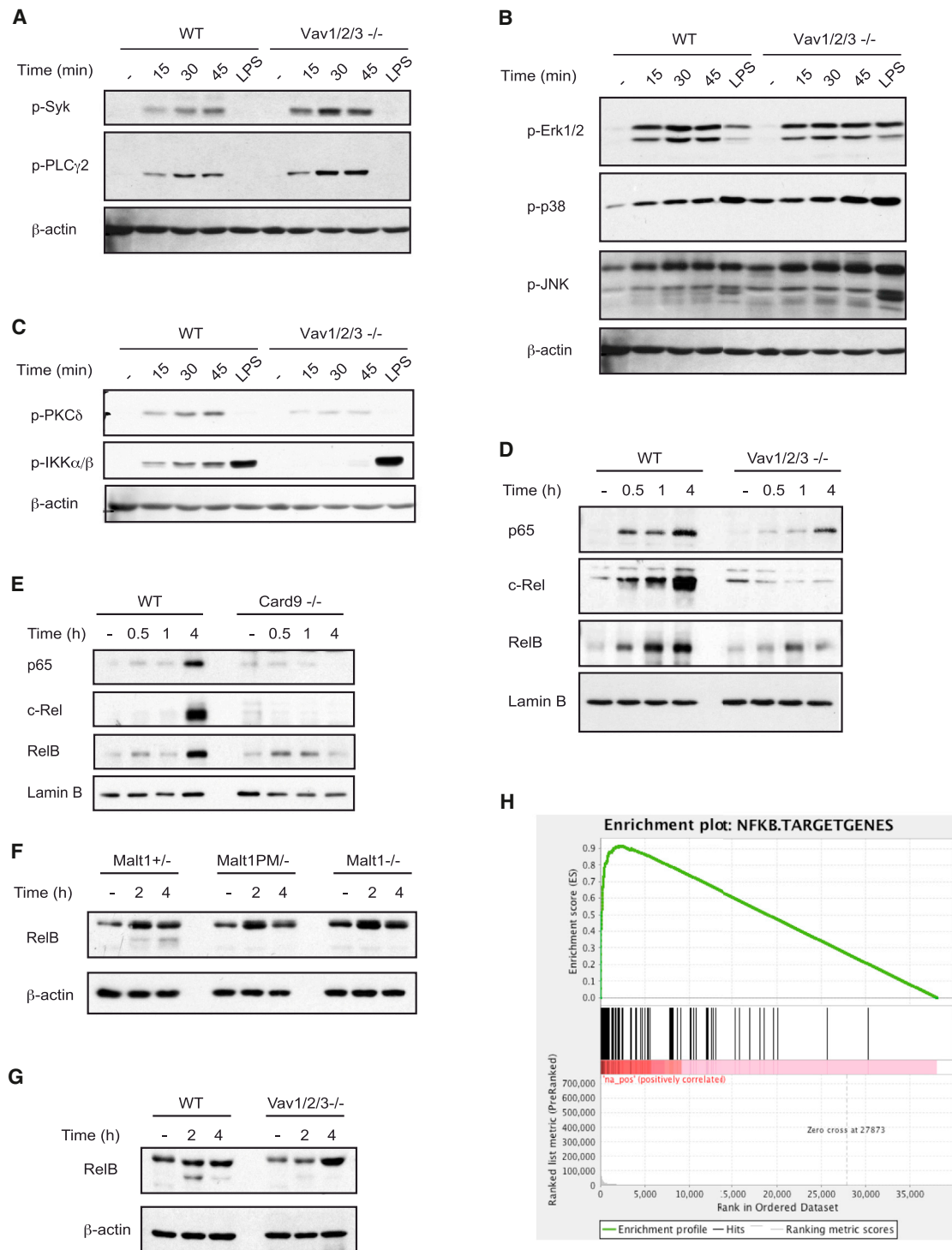
**A**

WT | Vav1/2/3 -/-

Time (min): -, 15, 30, 45, LPS, -, 15, 30, 45, LPS

p-Syk

p-PLCγ2

β-actin

**B**

WT | Vav1/2/3 -/-

Time (min): -, 15, 30, 45, LPS, -, 15, 30, 45, LPS

p-Erk1/2

p-p38

p-JNK

β-actin

**C**

WT | Vav1/2/3 -/-

Time (min): -, 15, 30, 45, LPS, -, 15, 30, 45, LPS

p-PKCδ

p-IKKα/β

β-actin

**D**

WT | Vav1/2/3 -/-

Time (h): -, 0.5, 1, 4, -, 0.5, 1, 4

p65

c-Rel

RelB

Lamin B

**E**

WT | Card9 -/-

Time (h): -, 0.5, 1, 4, -, 0.5, 1, 4

p65

c-Rel

RelB

Lamin B

**F**

Malt1+/- | Malt1PM/- | Malt1-/-

Time (h): -, 2, 4, -, 2, 4, -, 2, 4

RelB

β-actin

**G**

WT | Vav1/2/3-/-

Time (h): -, 2, 4, -, 2, 4

RelB

β-actin

**H**

Enrichment plot: NFKB.TARGETGENES

Enrichment score (ES)

Ranked list metric (PreRanked)

'na_pos' (positively correlated)

Zero cross at 27873

Rank in Ordered Dataset

— Enrichment profile — Hits — Ranking metric scores

**Figure 4. Vav Proteins Control CLR-Triggered NF-κB Activation**

(A–E) BMDCs from the indicated genotypes were stimulated with *C. albicans* hyphae (MOI 0.5) for various times or with LPS (100 ng/ml) for 45 min.

(A) Syk and PLCγ2 phosphorylation was determined in cell lysates by immunoblot with anti-phospho-Syk and anti-phospho-PLCγ2 antibodies.

(B) Activation of the MAP kinases Erk1/2, p38, and JNK was analyzed with anti-phospho-Erk1/2, anti-phospho-p38, and anti-phospho-JNK antibodies.

(C) Cell lysates were analyzed by immunoblot with anti-phospho-PKCδ and anti-phospho-IKKα/β antibodies. β-actin served as a loading control.

(D and E) Nuclear extracts from WT and *Vav1/2/3⁻/⁻* (D), or *Card9⁻/⁻* BMDCs (E) were analyzed by immunoblot with antibodies against the NF-κB subunits p65, c-Rel, and RelB; anti-lamin B antibodies indicate equal protein loading.

*(legend continued on next page)*

species (ROS) production in neutrophils and the recruitment of Vav1 to phagocytic cups for *C. albicans* engulfment by macrophages (Li et al., 2011; Strijbis et al., 2013). Although these effector mechanisms are important during innate immune responses, they are not regulated by the Card9 pathway (Drewniak et al., 2013; Goodridge et al., 2009; Gross et al., 2006). However, the Card9 signaling pathway appears to be the central mammalian host defense mechanism against fungi, given that multiple genetic studies in humans have recently identified that several Card9 loss-of-function defects are causative for several fungal diseases, including various types of mucocutaneous candidiasis; superficial, extensive, and deep dermatophytosis with *Trichophyton* spp.; subcutaneous phaeohyphomycosis; invasive *Candida* infections of the digestive tract and central nervous system; *Candida* endophthalmitis and osteomyelitis; and disseminated *Exophiala* disease of the liver, brain, and lung (Grumach et al., 2015; Pérez de Diego et al., 2015).

We assessed enzymatic Malt1 paracaspase activity as a direct functional marker for Card9 complex activity in Vav-deficient mice. Given that this activity was severely impaired in Vav1/2/3 triple-deficient BMDCs, our results establish Vav molecules as regulators of the Card9/Bcl10/Malt1 complex. Consistent with the essential function of a Vav/Card9-mediated mechanism for CLR-induced NF-κB activation, the NF-κB response is blocked in Vav1/2/3-deficient mice in response to *C. albicans* infection or selective CLR triggering, and Vav1/2/3-deficient animals exhibit dramatically impaired proinflammatory cytokine production in response to *C. albicans* infection and CLR stimulation in vitro and in vivo. Therefore, we propose a mechanistic model in which Syk is engaged by CLRs upon fungal sensing, thereby triggering the phosphorylation and activation of Vav proteins, which subsequently activate the Card9 complex for NF-κB control and antifungal gene transcription.

How Vav proteins are mechanistically coupled to Card9 control remains to be determined. We previously demonstrated that Card9 is phosphorylated by PKCδ at Thr231 to induce Card9 effector function. However, the activation of PKCδ is only partially impaired in Vav-deficient BMDCs, whereas IKK activation is almost completely defective. Similarly, in PKCδ-deficient cells, IKK phosphorylation is abolished, whereas phosphorylation of Vav1 is only slightly compromised, suggesting, together, that Vav and PKCδ operate at the same level upstream of Card9. Because Vav proteins can control cytoskeletal reorganization and serve as scaffolding platforms in other signaling systems (Acton et al., 2012; Bustelo, 2014; Spurrell et al., 2009; Tybulewicz, 2005), we speculate that Vav family members could bring Card9 into the vicinity of key upstream regulators such as PKCδ and potential, still unknown factors to allow Card9 activation. Moreover, because Vav1/2/3 do not only regulate CLR-induced Card9-NF-κB signaling but also control other cellular responses, such as phagocytosis and ROS production (Li et al., 2011; Strijbis et al., 2013), the precise molecular inter-

dependence of these mechanisms should be defined in the future.

In accordance with our molecular model, similar to Card9 deficiency, a complete deficiency in all Vav isoforms results in a massive susceptibility to *C. albicans* infection. Likewise, a conditional deficiency of Syk only in dendritic cells also abolishes innate resistance to acute systemic *C. albicans* infection (Whitney et al., 2014), and Whitney et al. (2014) elegantly demonstrated that the early innate cytokine response is required to orchestrate innate anti-fungal functions, including neutrophil anti-fungal activity. Nevertheless, in our infection models presented here, it must be noted that the Vav mutant mice analyzed were germline Vav-deficient animals and that Vav proteins are not selectively expressed in Syk and Card9-containing innate immune cells, including dendritic cells, macrophages, and neutrophils, but are also expressed in lymphocytes, which signal through Card9-independent mechanisms (Gross et al., 2006; Hara et al., 2007). Still, the rapid death of Vav1/2/3 triple-deficient mice upon fungal infection indicates that an innate immune defect is indeed responsible for the observed phenotype. This hypothesis is also in line with the established roles of Vav1 and Vav3 in mediating phagocytosis and ROS production in macrophages and neutrophils upon fungal sensing (Li et al., 2011; Strijbis et al., 2013). Future studies with conditional Vav mutant mice will further dissect the individual roles of Vav signaling in dendritic cells, macrophages, and neutrophils as well as in adaptive immune subsets during complex fungal infection scenarios in vivo. In addition, *in vivo* results in individual Vav1-, 2-, and 3-deficient animals also revealed that, although there is functional redundancy among the three Vav family members in infection control, Vav3 is the single most important Vav family member for antifungal defense in mice. This finding is consistent with our results in patients who link a polymorphism in the *VAV3* gene to susceptibility to *Candida* infection, suggesting that the function of Vav molecules is similar to Card9 function conserved between mice and men.

In addition to fungal components, CLRs also recognize structures present on mycobacteria (Ishikawa et al., 2009; Lobato-Pascual et al., 2013; Miyake et al., 2013; Schoenen et al., 2010), viruses such as dengue virus (Chen et al., 2008), and parasites such as *Schistosoma mansoni* (Ritter et al., 2010), as well as endogenous ligands under sterile inflammatory conditions (Roth and Ruland, 2013). We therefore believe that our findings have implications beyond antifungal immunity. Consistent with this hypothesis, *Vav1/2/3−/−* mice were almost completely impaired in systemic inflammatory responses upon innate immune stimulation with the mycobacterial pathogen-associated molecular patterns (PAMP) analog TDM, implying that, like Card9 (Dorhoi et al., 2010), Vav proteins might also be critical for innate anti-mycobacterial immune responses. In addition, accumulating evidence indicates important roles for CLR/Card9 signaling in inflammatory disorders. Several independent studies have shown an

---

(F and G) BMDCs from mice of the indicated genotypes were pretreated with the proteasome inhibitor MG132 for 30 min and then stimulated with curdlan (0.5 mg/ml) (F) or *C. albicans* hyphae (MOI 1) (G) for 2 or 4 hr. Cell lysates were analyzed by immunoblot using antibodies against RelB and β-actin.

(H) WT and *Vav1/2/3−/−* BMDCs were stimulated with curdlan (0.2 mg/ml) for 3 hr. Shown is the GSEA enrichment score of NF-κB target genes differentially expressed in curdlan-stimulated wild-type cells compared with Vav1/2/3-deficient BMDCs.

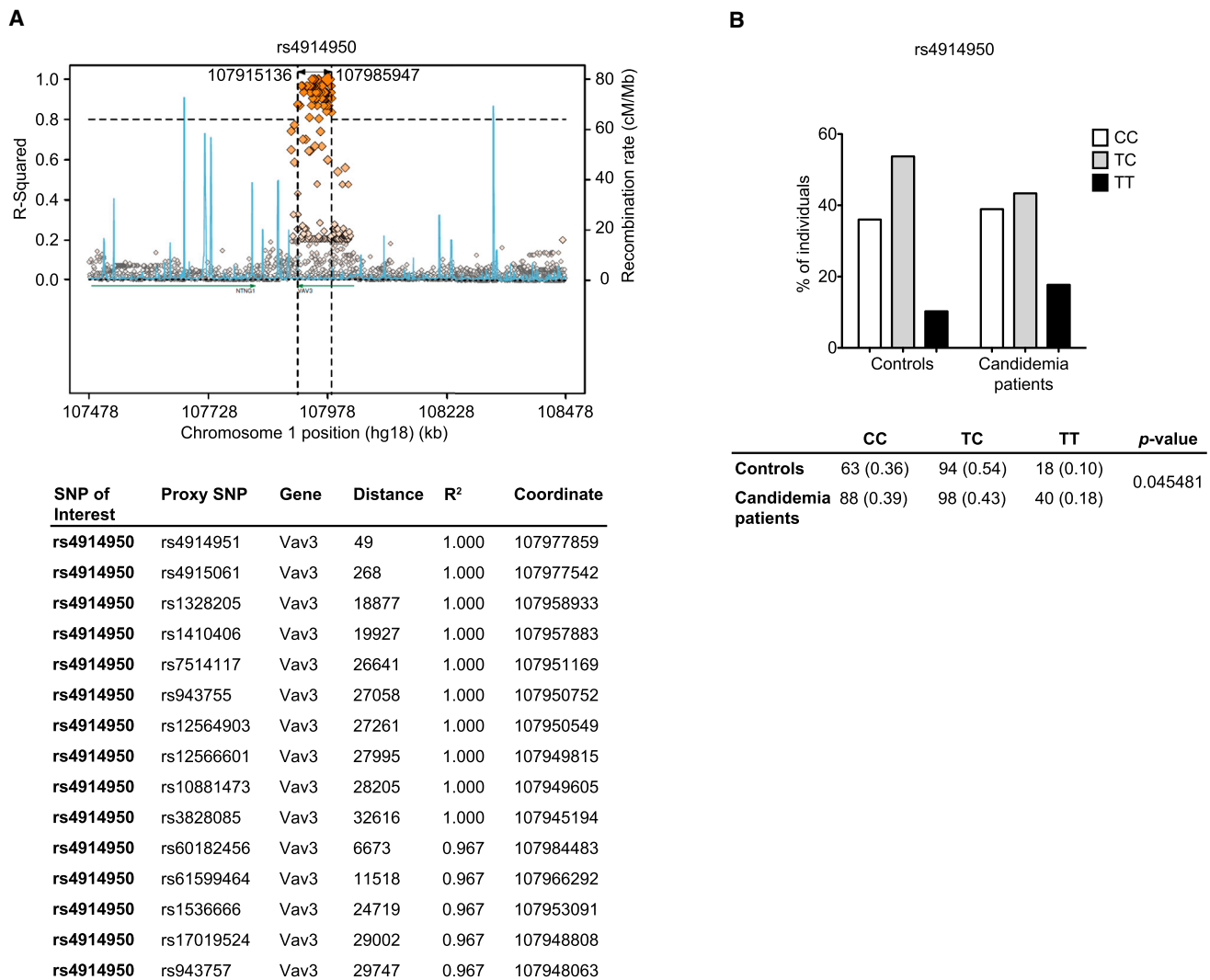Data are representative of at least three independent experiments. See also Figure S1.

**Figure 5. A *VAV3* Polymorphism Is Associated with Increased Susceptibility to Candidemia**

(A) Polymorphisms associated with candidemia were investigated in a group of 227 patients with *Candida*-positive blood cultures and compared with 176 patients from the same clinical wards without infection. SNPs associated with the *VAV3* locus revealed a significant association with candidemia, with the significant SNPs distributed across the LD region of the gene. The *VAV3* gene region on chromosome 1 is shown. Using the SNAP server, the SNP of interest (rs4914950) (biggest orange diamond) was plotted with all annotated polymorphisms in this gene (other diamonds). $R^2$ and recombination rate are indicated on the left and right y axis, respectively. Diamonds on the same horizontal line as the SNP of interest (biggest orange diamond) are in complete linkage disequilibrium ($R^2 = 1$) with this SNP and have the same disease association values. Diamonds below this line have a lower LD value with the SNP of interest and, therefore, differ in the association with the disease. The table below shows the top 15 polymorphisms that are linked to rs4914950.

(B) Genotype frequencies for the rs4914950 SNP that showed the strongest association with candidemia. The table below shows the total numbers and percentages (in parentheses) of genotypes in *Candida*-infected (candidemia patients) and non-infected (controls) individuals. Statistical comparisons of genotype frequencies between the two groups were made using $\chi^2$ test.

association between Card9 polymorphisms and ulcerative colitis and Crohn's disease (Roth and Ruland, 2013), which are supported by a recent study in mice demonstrating a protective role for Card9 in intestinal inflammation (Sokol et al., 2013). Deep resequencing of inflammatory bowel disease genome-wide association study (GWAS) loci confirmed an association between Card9 and ulcerative colitis and Crohn's disease (Beaudoin et al., 2013; Hong et al., 2016). Moreover, additional genome-wide association studies in humans have identified significant associations between *CARD9* and *VAV3* gene loci and immunoglobulin A (IgA)

nephropathy (Kiryluk et al., 2014). In conjunction with the results presented here, these data suggest that the described Vav/Card9-dependent signaling mechanism could also play a role in sterile inflammatory diseases.

**EXPERIMENTAL PROCEDURES**

**Mice**

*Vav1*^{−/−} (Turner et al., 1997), *Vav2*^{−/−} (Doody et al., 2001), *Vav3*^{−/−} (Sauzeau et al., 2006), *Card9*^{−/−} (Gross et al., 2006), *Prkcd*^{−/−} (Leitges et al., 2001),

*Malt1*$^{-/-}$ (Ruland et al., 2003), and *Malt1*$^{PM/-}$ (Gewies et al., 2014) mice were described previously. Vav double-deficient (*Vav2/3*$^{-/-}$) and triple-deficient (*Vav1/2/3*$^{-/-}$) mice were generated by intercrossings of Vav single knockout animals and were provided by X.R.B. and V.L.T.. All animal work was conducted in accordance with German federal animal protection laws and approved by the Institutional Animal Care and Use Committee at the Technical University of Munich. Animals were used at 8–16 weeks of age.

## Cell Culture and Stimulation

BMDCs were derived from bone marrow as described previously (Gross et al., 2006) and stimulated with curdlan (Wako Pure Chemicals Industries), LPS (ultrapure, from *Escherichia coli* strain K12, InvivoGen), Pam3CSK4 (InvivoGen), Dectin-2 monoclonal antibody (AbD Serotec), Rat IgG2a isotype control (R&D Systems), TDB (Avanti Polar Lipids), or *C. albicans* strain SC5314 as indicated. For tyrosine kinase or proteasome inhibition, the Syk inhibitor R406 (Rigel), the Src kinase inhibitor PP2 or its inactive analog PP3 (both from Calbiochem), or MG132 (Sigma) were used. Cell culture reagents were purchased from Invitrogen, and fetal calf serum (FCS) was purchased from HyClone. Mouse recombinant granulocyte-macrophage colony-stimulating factor was purchased from PeproTech.

## Cytokine Measurement

Cytokine levels were measured by ELISA (BD Biosciences and eBioscience) or by cytometric bead array (CBA; BD Biosciences) according to the manufacturer's instructions.

## Immunoprecipitation and Immunoblot Analysis

Cell lysates or cell supernatants were subjected to standard immunoblot analysis techniques as described previously (Strasser et al., 2012). Cytosolic and nuclear extracts were prepared as described previously (Ferch et al., 2007). For immunoprecipitation experiments, BMDCs were left unstimulated or stimulated with *C. albicans* as indicated and lysed in an NP-40-containing buffer. Lysates were pre-cleared by incubation with protein G Sepharose (GE Healthcare 4 Fast Flow) and then incubated with anti-phospho-tyrosine antibodies. Immune complexes were precipitated with protein G Sepharose and subjected to protein immunoblotting as indicated. Quantification of immunoblots was performed by densitometry using ImageJ software. Densitometry data were expressed relative to levels of appropriate loading controls and normalized to specific treatment conditions.

## Statistical Analysis

Data were analyzed and graphed using Excel (Microsoft Office) and Prism (GraphPad). For comparison between two groups, two-tailed Student's t test was used. Analysis across more than two groups on a single dataset was performed using one-way ANOVA and post hoc Tukey-Kramer test. Survival data were analyzed using the log-rank test. Genotype frequencies between controls and candidemia patients were compared using the $\chi^2$ test. The level of significance was defined as *$p < 0.05$, **$p < 0.01$, and ***$p < 0.001$.

## ACCESSION NUMBERS

The accession number for the gene expression profiling raw data reported in this paper is NCBI GEO: GSE83736.

## SUPPLEMENTAL INFORMATION

Supplemental Information includes Supplemental Experimental Procedures and one figure and can be found with this article online at http://dx.doi.org/10.1016/j.celrep.2016.11.018.

## AUTHOR CONTRIBUTIONS

S.R. and J.R. designed the study. S.R., H.B., M.J., K.N., and P.A.K. performed experiments. S.R., H.B., M.J., K.N., P.A.K., M.N., and J.R. analyzed the results. M.J., V.K., M.J., and M.N. conducted patient sample collection and clinical data analyses. A.Y. and B.H. performed bioinformatic analyses. S.R., M.J.,

and A.Y. generated the figures. C.P.C., L.V., M.M.M., V.L.T., and X.R.B. provided critical reagents. S.R. and J.R. wrote the paper.

## REFERENCES

Acton, S.E., Astarita, J.L., Malhotra, D., Lukacs-Kornek, V., Franz, B., Hess, P.R., Jakus, Z., Kuligowski, M., Fletcher, A.L., Elpek, K.G., et al. (2012). Podoplanin-rich stromal networks induce dendritic cell motility via activation of the C-type lectin receptor CLEC-2. Immunity *37*, 276–289.

Aghazadeh, B., Lowry, W.E., Huang, X.Y., and Rosen, M.K. (2000). Structural basis for relief of autoinhibition of the Dbl homology domain of proto-oncogene Vav by tyrosine phosphorylation. Cell *102*, 625–633.

Beaudoin, M., Goyette, P., Boucher, G., Lo, K.S., Rivas, M.A., Stevens, C., Alikashani, A., Ladouceur, M., Ellinghaus, D., Törkvist, L., et al.; Quebec IBD Genetics Consortium; NIDDK IBD Genetics Consortium; International IBD Genetics Consortium (2013). Deep resequencing of GWAS loci identifies rare variants in CARD9, IL23R and RNF186 that are associated with ulcerative colitis. PLoS Genet. *9*, e1003723.

Brieland, J., Essig, D., Jackson, C., Frank, D., Loebenberg, D., Menzel, F., Arnold, B., DiDomenico, B., and Hare, R. (2001). Comparison of pathogenesis and host immune responses to Candida glabrata and Candida albicans in systemically infected immunocompetent mice. Infect. Immun. *69*, 5046–5055.

Brown, G.D., and Gordon, S. (2001). Immune recognition. A new receptor for beta-glucans. Nature *413*, 36–37.

Bustelo, X.R. (2014). Vav family exchange factors: an integrated regulatory and functional view. Small GTPases *5*, 9.

Chen, S.T., Lin, Y.L., Huang, M.T., Wu, M.F., Cheng, S.C., Lei, H.Y., Lee, C.K., Chiou, T.W., Wong, C.H., and Hsieh, S.L. (2008). CLEC5A is critical for dengue-virus-induced lethal disease. Nature *453*, 672–676.

Dambuza, I.M., and Brown, G.D. (2015). C-type lectins in immunity: recent developments. Curr. Opin. Immunol. *32*, 21–27.

Doody, G.M., Bell, S.E., Vigorito, E., Clayton, E., McAdam, S., Tooze, R., Fernandez, C., Lee, I.J., and Turner, M. (2001). Signal transduction through Vav-2 participates in humoral immune responses and B cell maturation. Nat. Immunol. *2*, 542–547.

Dorhoi, A., Desel, C., Yeremeev, V., Pradl, L., Brinkmann, V., Mollenkopf, H.J., Hanke, K., Gross, O., Ruland, J., and Kaufmann, S.H. (2010). The adaptor molecule CARD9 is essential for tuberculosis control. J. Exp. Med. *207*, 777–792.

Drewniak, A., Gazendam, R.P., Tool, A.T., van Houdt, M., Jansen, M.H., van Hamme, J.L., van Leeuwen, E.M., Roos, D., Scalais, E., de Beaufort, C., et al. (2013). Invasive fungal infection and impaired neutrophil killing in human CARD9 deficiency. Blood *121*, 2385–2392.

Ferch, U., zum Büschenfelde, C.M., Gewies, A., Wegener, E., Rauser, S., Peschel, C., Krappmann, D., and Ruland, J. (2007). MALT1 directs B cell

receptor-induced canonical nuclear factor-kappaB signaling selectively to the c-Rel subunit. Nat. Immunol. 8, 984–991.

Ferwerda, B., Ferwerda, G., Plantinga, T.S., Willment, J.A., van Spriel, A.B., Venselaar, H., Elbers, C.C., Johnson, M.D., Cambi, A., Huysamen, C., et al. (2009). Human dectin-1 deficiency and mucocutaneous fungal infections. N. Engl. J. Med. 361, 1760–1767.

Fujikawa, K., Miletic, A.V., Alt, F.W., Faccio, R., Brown, T., Hoog, J., Fredericks, J., Nishi, S., Mildiner, S., Moores, S.L., et al. (2003). Vav1/2/3-null mice define an essential role for Vav family proteins in lymphocyte development and activation but a differential requirement in MAPK signaling in T and B cells. J. Exp. Med. 198, 1595–1608.

Gewies, A., Gorka, O., Bergmann, H., Pechloff, K., Petermann, F., Jeltsch, K.M., Rudelius, M., Kriegsmann, M., Weichert, W., Horsch, M., et al. (2014). Uncoupling Malt1 threshold function from paracaspase activity results in destructive autoimmune inflammation. Cell Rep. 9, 1292–1305.

Glocker, E.O., Hennigs, A., Nabavi, M., Schäffer, A.A., Woellner, C., Salzer, U., Pfeifer, D., Veelken, H., Warnatz, K., Tahami, F., et al. (2009). A homozygous CARD9 mutation in a family with susceptibility to fungal infections. N. Engl. J. Med. 361, 1727–1735.

Goodridge, H.S., Shimada, T., Wolf, A.J., Hsu, Y.M., Becker, C.A., Lin, X., and Underhill, D.M. (2009). Differential use of CARD9 by dectin-1 in macrophages and dendritic cells. J. Immunol. 182, 1146–1154.

Graham, D.B., Stephenson, L.M., Lam, S.K., Brim, K., Lee, H.M., Bautista, J., Gilfillan, S., Akilesh, S., Fujikawa, K., and Swat, W. (2007). An ITAM-signaling pathway controls cross-presentation of particulate but not soluble antigens in dendritic cells. J. Exp. Med. 204, 2889–2897.

Gross, O., Gewies, A., Finger, K., Schäfer, M., Sparwasser, T., Peschel, C., Förster, I., and Ruland, J. (2006). Card9 controls a non-TLR signalling pathway for innate anti-fungal immunity. Nature 442, 651–656.

Gross, O., Poeck, H., Bscheider, M., Dostert, C., Hannesschläger, N., Endres, S., Hartmann, G., Tardivel, A., Schweighoffer, E., Tybulewicz, V., et al. (2009). Syk kinase signalling couples to the Nlrp3 inflammasome for anti-fungal host defence. Nature 459, 433–436.

Grumach, A.S., de Queiroz-Telles, F., Migaud, M., Lanternier, F., Filho, N.R., Palma, S.M., Constantino-Silva, R.N., Casanova, J.L., and Puel, A. (2015). A homozygous CARD9 mutation in a Brazilian patient with deep dermatophytosis. J. Clin. Immunol. 35, 486–490.

Hailfinger, S., Nogai, H., Pelzer, C., Jaworski, M., Cabalzar, K., Charton, J.E., Guzzardi, M., Décaillet, C., Grau, M., Dörken, B., et al. (2011). Malt1-dependent RelB cleavage promotes canonical NF-kappaB activation in lymphocytes and lymphoma cell lines. Proc. Natl. Acad. Sci. USA 108, 14596–14601.

Hara, H., Ishihara, C., Takeuchi, A., Imanishi, T., Xue, L., Morris, S.W., Inui, M., Takai, T., Shibuya, A., Saijo, S., et al. (2007). The adaptor protein CARD9 is essential for the activation of myeloid cells through ITAM-associated and Toll-like receptors. Nat. Immunol. 8, 619–629.

Helft, J., Böttcher, J., Chakravarty, P., Zelenay, S., Huotari, J., Schraml, B.U., Goubau, D., and Reis e Sousa, C. (2015). GM-CSF Mouse Bone Marrow Cultures Comprise a Heterogeneous Population of CD11c(+)MHCII(+) Macrophages and Dendritic Cells. Immunity 42, 1197–1211.

Hise, A.G., Tomalka, J., Ganesan, S., Patel, K., Hall, B.A., Brown, G.D., and Fitzgerald, K.A. (2009). An essential role for the NLRP3 inflammasome in host defense against the human fungal pathogen Candida albicans. Cell Host Microbe 5, 487–497.

Hong, S.N., Park, C., Park, S.J., Lee, C.K., Ye, B.D., Kim, Y.S., Lee, S., Chae, J., Kim, J.I., and Kim, Y.H.; IBD Study Group of the Korean Association for the Study of Intestinal Diseases (KASID) (2016). Deep resequencing of 131 Crohn's disease associated genes in pooled DNA confirmed three reported variants and identified eight novel variants. Gut 65, 788–796.

Ishikawa, E., Ishikawa, T., Morita, Y.S., Toyonaga, K., Yamada, H., Takeuchi, O., Kinoshita, T., Akira, S., Yoshikai, Y., and Yamasaki, S. (2009). Direct recognition of the mycobacterial glycolipid, trehalose dimycolate, by C-type lectin Mincle. J. Exp. Med. 206, 2879–2888.

Jaeger, M., van der Lee, R., Cheng, S.C., Johnson, M.D., Kumar, V., Ng, A., Plantinga, T.S., Smeekens, S.P., Oosting, M., Wang, X., et al. (2015). The RIG-I-like helicase receptor MDA5 (IFIH1) is involved in the host defense against Candida infections. Eur. J. Clin. Microbiol. Infect. Dis. 34, 963–974.

Jaworski, M., Marsland, B.J., Gehrig, J., Held, W., Favre, S., Luther, S.A., Perroud, M., Golshayan, D., Gaide, O., and Thome, M. (2014). Malt1 protease inactivation efficiently dampens immune responses but causes spontaneous autoimmunity. EMBO J. 33, 2765–2781.

Jhingran, A., Mar, K.B., Kumasaka, D.K., Knoblaugh, S.E., Ngo, L.Y., Segal, B.H., Iwakura, Y., Lowell, C.A., Hamerman, J.A., Lin, X., and Hohl, T.M. (2012). Tracing conidial fate and measuring host cell antifungal activity using a reporter of microbial viability in the lung. Cell Rep. 2, 1762–1773.

Jia, X.M., Tang, B., Zhu, L.L., Liu, Y.H., Zhao, X.Q., Gorjestani, S., Hsu, Y.M., Yang, L., Guan, J.H., Xu, G.T., and Lin, X. (2014). CARD9 mediates Dectin-1-induced ERK activation by linking Ras-GRF1 to H-Ras for antifungal immunity. J. Exp. Med. 211, 2307–2321.

Kerrigan, A.M., and Brown, G.D. (2011). Syk-coupled C-type lectins in immunity. Trends Immunol. 32, 151–156.

Kiryluk, K., Li, Y., Scolari, F., Sanna-Cherchi, S., Choi, M., Verbitsky, M., Fasel, D., Lata, S., Prakash, S., Shapiro, S., et al. (2014). Discovery of new risk loci for IgA nephropathy implicates genes involved in immunity against intestinal pathogens. Nat. Genet. 46, 1187–1196.

LeibundGut-Landmann, S., Gross, O., Robinson, M.J., Osorio, F., Slack, E.C., Tsoni, S.V., Schweighoffer, E., Tybulewicz, V., Brown, G.D., Ruland, J., and Reis e Sousa, C. (2007). Syk- and CARD9-dependent coupling of innate immunity to the induction of T helper cells that produce interleukin 17. Nat. Immunol. 8, 630–638.

Leitges, M., Mayr, M., Braun, U., Mayr, U., Li, C., Pfister, G., Ghaffari-Tabrizi, N., Baier, G., Hu, Y., and Xu, Q. (2001). Exacerbated vein graft arteriosclerosis in protein kinase Cdelta-null mice. J. Clin. Invest. 108, 1505–1512.

Li, X., Utomo, A., Cullere, X., Choi, M.M., Milner, D.A., Jr., Venkatesh, D., Yun, S.H., and Mayadas, T.N. (2011). The β-glucan receptor Dectin-1 activates the integrin Mac-1 in neutrophils via Vav protein signaling to promote Candida albicans clearance. Cell Host Microbe 10, 603–615.

Lobato-Pascual, A., Saether, P.C., Fossum, S., Dissen, E., and Daws, M.R. (2013). Mincle, the receptor for mycobacterial cord factor, forms a functional receptor complex with MCL and FcεRI-γ. Eur. J. Immunol. 43, 3167–3174.

Miyake, Y., Toyonaga, K., Mori, D., Kakuta, S., Hoshino, Y., Oyamada, A., Yamada, H., Ono, K., Suyama, M., Iwakura, Y., et al. (2013). C-type lectin MCL is an FcRγ-coupled receptor that mediates the adjuvanticity of mycobacterial cord factor. Immunity 38, 1050–1062.

Mócsai, A., Ruland, J., and Tybulewicz, V.L. (2010). The SYK tyrosine kinase: a crucial player in diverse biological functions. Nat. Rev. Immunol. 10, 387–402.

Osorio, F., and Reis e Sousa, C. (2011). Myeloid C-type lectin receptors in pathogen recognition and host defense. Immunity 34, 651–664.

Pérez de Diego, R., Sánchez-Ramón, S., López-Collazo, E., Martínez-Barricarte, R., Cubillos-Zapata, C., Ferreira Cerdán, A., Casanova, J.L., and Puel, A. (2015). Genetic errors of the human caspase recruitment domain-B-cell lymphoma 10-mucosa-associated lymphoid tissue lymphoma-translocation gene 1 (CBM) complex: Molecular, immunologic, and clinical heterogeneity. J. Allergy Clin. Immunol. 136, 1139–1149.

Ritter, M., Gross, O., Kays, S., Ruland, J., Nimmerjahn, F., Saijo, S., Tschopp, J., Layland, L.E., and Prazeres da Costa, C. (2010). Schistosoma mansoni triggers Dectin-2, which activates the Nlrp3 inflammasome and alters adaptive immune responses. Proc. Natl. Acad. Sci. USA 107, 20459–20464.

Robinson, M.J., Osorio, F., Rosas, M., Freitas, R.P., Schweighoffer, E., Gross, O., Verbeek, J.S., Ruland, J., Tybulewicz, V., Brown, G.D., et al. (2009). Dectin-2 is a Syk-coupled pattern recognition receptor crucial for Th17 responses to fungal infection. J. Exp. Med. 206, 2037–2051.

Roth, S., and Ruland, J. (2013). Caspase recruitment domain-containing protein 9 signaling in innate immunity and inflammation. Trends Immunol. 34, 243–250.

Ruland, J., Duncan, G.S., Wakeham, A., and Mak, T.W. (2003). Differential requirement for Malt1 in T and B cell antigen receptor signaling. Immunity 19, 749–758.

Saijo, S., Fujikado, N., Furuta, T., Chung, S.H., Kotaki, H., Seki, K., Sudo, K., Akira, S., Adachi, Y., Ohno, N., et al. (2007). Dectin-1 is required for host defense against Pneumocystis carinii but not against Candida albicans. Nat. Immunol. 8, 39–46.

Saijo, S., Ikeda, S., Yamabe, K., Kakuta, S., Ishigame, H., Akitsu, A., Fujikado, N., Kusaka, T., Kubo, S., Chung, S.H., et al. (2010). Dectin-2 recognition of alpha-mannans and induction of Th17 cell differentiation is essential for host defense against Candida albicans. Immunity 32, 681–691.

Sancho, D., and Reis e Sousa, C. (2012). Signaling by myeloid C-type lectin receptors in immunity and homeostasis. Annu. Rev. Immunol. 30, 491–529.

Sato, K., Yang, X.L., Yudate, T., Chung, J.S., Wu, J., Luby-Phelps, K., Kimberly, R.P., Underhill, D., Cruz, P.D., Jr., and Ariizumi, K. (2006). Dectin-2 is a pattern recognition receptor for fungi that couples with the Fc receptor gamma chain to induce innate immune responses. J. Biol. Chem. 281, 38854–38866.

Sauzeau, V., Sevilla, M.A., Rivas-Elena, J.V., de Alava, E., Montero, M.J., López-Novoa, J.M., and Bustelo, X.R. (2006). Vav3 proto-oncogene deficiency leads to sympathetic hyperactivity and cardiovascular dysfunction. Nat. Med. 12, 841–845.

Schoenen, H., Bodendorfer, B., Hitchens, K., Manzanero, S., Werninghaus, K., Nimmerjahn, F., Agger, E.M., Stenger, S., Andersen, P., Ruland, J., et al. (2010). Cutting edge: Mincle is essential for recognition and adjuvanticity of the mycobacterial cord factor and its synthetic analog trehalose-dibehenate. J. Immunol. 184, 2756–2760.

Shah, V.B., Ozment-Skelton, T.R., Williams, D.L., and Keshvara, L. (2009). Vav1 and PI3K are required for phagocytosis of beta-glucan and subsequent superoxide generation by microglia. Mol. Immunol. 46, 1845–1853.

Sokol, H., Conway, K.L., Zhang, M., Choi, M., Morin, B., Cao, Z., Villablanca, E.J., Li, C., Wijmenga, C., Yun, S.H., et al. (2013). Card9 mediates intestinal epithelial cell restitution, T-helper 17 responses, and control of bacterial infection in mice. Gastroenterology 145, 591–601.e3.

Spurrell, D.R., Luckashenak, N.A., Minney, D.C., Chaplin, A., Penninger, J.M., Liwski, R.S., Clements, J.L., and West, K.A. (2009). Vav1 regulates the migration and adhesion of dendritic cells. J. Immunol. 183, 310–318.

Strasser, D., Neumann, K., Bergmann, H., Marakalala, M.J., Guler, R., Rojowska, A., Hopfner, K.P., Brombacher, F., Urlaub, H., Baier, G., et al. (2012). Syk kinase-coupled C-type lectin receptors engage protein kinase C-δ to elicit Card9 adaptor-mediated innate immunity. Immunity 36, 32–42.

Strijbis, K., Tafesse, F.G., Fairn, G.D., Witte, M.D., Dougan, S.K., Watson, N., Spooner, E., Esteban, A., Vyas, V.K., Fink, G.R., et al. (2013). Bruton's Tyrosine Kinase (BTK) and Vav1 contribute to Dectin1-dependent phagocytosis of Candida albicans in macrophages. PLoS Pathog. 9, e1003446.

Takeuchi, O., and Akira, S. (2010). Pattern recognition receptors and inflammation. Cell 140, 805–820.

Taylor, P.R., Tsoni, S.V., Willment, J.A., Dennehy, K.M., Rosas, M., Findon, H., Haynes, K., Steele, C., Botto, M., Gordon, S., and Brown, G.D. (2007). Dectin-1 is required for beta-glucan recognition and control of fungal infection. Nat. Immunol. 8, 31–38.

Turner, M., Mee, P.J., Walters, A.E., Quinn, M.E., Mellor, A.L., Zamoyska, R., and Tybulewicz, V.L. (1997). A requirement for the Rho-family GTP exchange factor Vav in positive and negative selection of thymocytes. Immunity 7, 451–460.

Tybulewicz, V.L. (2005). Vav-family proteins in T-cell signalling. Curr. Opin. Immunol. 17, 267–274.

Vallabhapurapu, S., and Karin, M. (2009). Regulation and function of NF-kappaB transcription factors in the immune system. Annu. Rev. Immunol. 27, 693–733.

Vonk, A.G., Netea, M.G., van Krieken, J.H., Iwakura, Y., van der Meer, J.W., and Kullberg, B.J. (2006). Endogenous interleukin (IL)-1 alpha and IL-1 beta are crucial for host defense against disseminated candidiasis. J. Infect. Dis. 193, 1419–1426.

Wells, C.A., Salvage-Jones, J.A., Li, X., Hitchens, K., Butcher, S., Murray, R.Z., Beckhouse, A.G., Lo, Y.L., Manzanero, S., Cobbold, C., et al. (2008). The macrophage-inducible C-type lectin, mincle, is an essential component of the innate immune response to Candida albicans. J. Immunol. 180, 7404–7413.

Whitney, P.G., Bär, E., Osorio, F., Rogers, N.C., Schraml, B.U., Deddouche, S., LeibundGut-Landmann, S., and Reis e Sousa, C. (2014). Syk signaling in dendritic cells orchestrates innate resistance to systemic fungal infection. PLoS Pathog. 10, e1004276.

Xu, S., Huo, J., Lee, K.G., Kurosaki, T., and Lam, K.P. (2009). Phospholipase Cgamma2 is critical for Dectin-1-mediated Ca2+ flux and cytokine production in dendritic cells. J. Biol. Chem. 284, 7038–7046.

Yamamoto, H., Nakamura, Y., Sato, K., Takahashi, Y., Nomura, T., Miyasaka, T., Ishii, K., Hara, H., Yamamoto, N., Kanno, E., et al. (2014). Defect of CARD9 leads to impaired accumulation of gamma interferon-producing memory phenotype T cells in lungs and increased susceptibility to pulmonary infection with Cryptococcus neoformans. Infect. Immun. 82, 1606–1615.

**Supplemental Information**

# Vav Proteins Are Key Regulators of Card9 Signaling

# for Innate Antifungal Immunity

Susanne Roth, Hanna Bergmann, Martin Jaeger, Assa Yeroslaviz, Konstantin Neumann, Paul-Albert Koenig, Clarissa Prazeres da Costa, Lesley Vanes, Vinod Kumar, Melissa Johnson, Mauricio Menacho-Márquez, Bianca Habermann, Victor L. Tybulewicz, Mihai Netea, Xosé R. Bustelo, and Jürgen Ruland
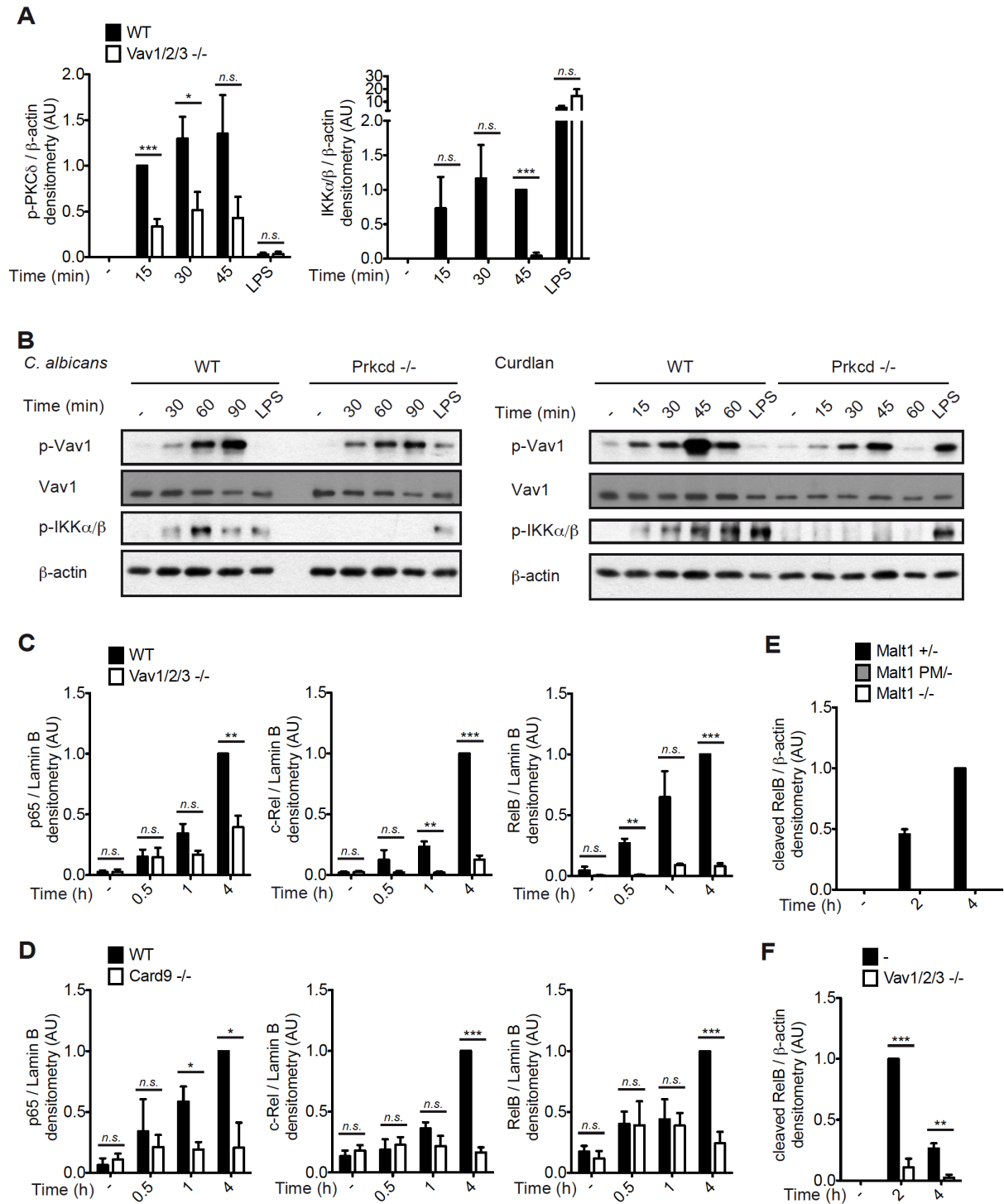
**Figure S 1**



**Figure S 1. Vav proteins control CLR-triggered NF-κB activation, Related to Figure 4.** (A, C, D) BMDCs from the indicated genotypes were stimulated with *C. albicans* hyphae (MOI 0.5) for various times or with LPS (100 ng/ml) for 45 minutes. (A) Cell lysates were analyzed by immunoblot with anti-phospho-PKCδ and anti-phospho-IKKα/β antibodies. Densitometrical quantification of phospho-PKCδ (left) and phospho-IKKα/β (right) relative to β-actin, normalized to WT BMDCs treated with *C. albicans* for 15 minutes (left) or 45 minutes (right). (B) BMDCs from WT or *Prkcd*^{-/-} mice were stimulated with *C. albicans* hyphae (MOI 0.5) (left) or curdlan (0.5 mg/ml) (right) for various times, or with LPS (100 ng/ml) for 30 minutes. Cell lysates were

analyzed by immunoblot with anti-phospho-Vav1 (Tyr174), anti-Vav1, and anti-phospho-IKKα/β antibodies. β-actin serves as a loading control. Representative data of two independent experiments are shown. (C, D) Nuclear extracts were analyzed by immunoblot with antibodies against the NF-κB subunits p65, c-Rel and RelB. Quantification of nuclear p65, c-Rel and RelB by densitometry, relative to Lamin B, normalized to WT BMDCs treated with *C. albicans* hyphae for 4 hours. (E, F) BMDCs from mice of the indicated genotypes were pretreated with the proteasome inhibitor MG132 for 30 minutes, and then stimulated with curdlan (0.5 mg/ml) (E) or *C. albicans* hyphae (MOI 1) (F) for 2 or 4 hours. Cell lysates were analyzed by immunoblot using antibodies against RelB and β-actin. Densitometrical quantification of cleaved RelB relative to β-actin, normalized to WT BMDCs treated with curdlan for 4 hours (E), or with *C. albicans* for 2 hours (F). (A, C-F) Data of at least three independent experiments are shown as means (±s.e.m.). *$p < 0.05$, **$p < 0.01$ and ***$p < 0.001$, Student's *t*-test. Not significant (*n.s.*). Arbitrary units (AU).

**SUPPLEMENTAL EXPERIMENTAL PROCEDURES**

***C. albicans* infections.** Mice were infected with $1\times10^5$ colony-forming units (c.f.u) of *C. albicans* (strain SC5314) as described (Gross et al., 2006) and monitored daily for health and survival according to institutional guidelines. To determine fungal burden, organ homogenates were plated in dilutions on CHROMagar (BD Biosciences). For histological analyses, kidney sections were stained with hematoxylin and eosin (H&E) or periodic acid-Schiff (PAS) according to standard protocols. Six hours after infection, serum was collected to analyze cytokine levels by cytometric bead array (CBA; BD Biosciences).

**Administration of TDM.** Squalane-in-water emulsions containing TDM (Trehalose 6,6′-dimycolate from *Mycobacterium bovis,* Sigma) were prepared by ultrasonic treatment as previously described (Yarkoni and Rapp, 1978). The final concentrations of emulsion components were as follows: 1.5 or 0 mg/ml (vehicle control) TDM, 9% squalane (Sigma), 1% Tween 80 (Sigma), and 90% saline. The TDM emulsions or the squalane-tween-saline vehicle controls were administered to groups of animals via tail vein injection (0.1 ml per mouse). After 24 hours, serum was collected to determine cytokine levels by CBA (BD Biosciences).

**Antibodies.** Primary antibodies anti-Caspase-1, p10 (sc-514), anti-c-Rel (sc-71), anti-lamin B (sc-6217), anti-phospho-Vav (Tyr 174-R, sc-16408-R), and anti-Vav (sc-132) were from Santa Cruz, and anti-NF-κB p65 (4764), anti-phospho-Erk1/2, (Thr202/Tyr204, 9101), anti-phospho-IKKα/β (Ser176/180, 2697), anti-phospho-JNK (Thr183/Tyr185, 9251), anti-phospho-p38 (Thr180/Tyr182, 4511), anti-phospho-PLCγ2 (Tyr759, 3874), anti-phospho-Syk (Tyr525/526, 2711), anti-phospho-PKCδ (Tyr311, 2055), anti-phospho-tyrosine (9411), and anti-RelB (4922) were purchased from Cell Signaling. Anti-β-actin was purchased from Sigma.

**Real-time quantitative PCR.** Total RNA was isolated and transcribed using standard methods. The specific primer pairs were as follows: IL-1β, 5′-TGTAATGAAAGACGGCACACC-3′ and 5′-TCTTCTTTGGGTATTGCTTGG-3′; β-actin, 5′-AGACCTCTATGCCAACACAG-3′ and 5′-TCGTACTCCTGCTTGCTGAT-3′. The qPCR Core kit for SYBR Green I (Eurogentec) and a LightCycler 480 Real-Time PCR System were used as indicated by the manufacturers. IL-1β mRNA expression was calculated as the ratio of the real-time PCR signal for IL-1β mRNA to that of the β-actin mRNA.

**RNA-seq library preparation and data analysis.** Total RNA was purified using TRIzol Reagent (Invitrogen) and the RNeasy Mini kit (QIAGEN) with on-column DNase treatment. Purified RNA was submitted to the Genomics & Proteomics Core Facility at the DKFZ (Heidelberg, Germany) where it was subjected to library preparation using the Illumina TruSeq RNA sample preparation kit v2. Libraries were pooled (three samples per lane) and sequenced on an Illumina HiSeq 2000 (50–base pair single-end reads). The raw data quality of all libraries was analyzed using FastQC (v. 0.11.1). Quality trimming and adapter removal was performed using the FASTX-Toolkit (v. 0.0.14). The fastq files were then mapped to the mouse genome downloaded from Ensembl (genome build NCBI37) using TopHat2 (Kim et al., 2013) (v. 2.4.2a). Mapped reads were processed through featureCount (Liao et al., 2014) (v. 1.4.6-p4) at the gene level to account for the number of reads per gene in all samples. This was followed by differential expression analysis using the DESeq2 (Love et al., 2014) (v. 1.8.2) package of R (v. 3.2.0). Count data were normalized using the size factor to estimate the effective library size (Anders and Huber, 2010). After calculating gene dispersion across all samples, a pair-wise comparison of two different conditions resulted in a list of differentially expressed genes for the stimulated wild-type vs. knockout samples. Genes with an adjusted p-value <= 0.1 were defined as differentially expressed and were used for downstream analyses. The p-values were adjusted for multiple testing to reduce the false discovery rate (FDR). Gene set enrichment analysis (GSEA) for NF-κB was performed as previously described (Subramanian et al., 2005). The NF-κB target gene set was taken from earlier studies (Compagno et al., 2009). GSEA was performed on a pre-ranked gene list based on their normalized mean read counts from the DESeq2 analysis. This list was then compared with the list of 120 NF-κB target genes to compute the GSEA enrichment scores. The algorithm implements weighted scores and was run with 1000 permutation tests.

**Candidemia patients, control volunteer cohorts, and genotyping.** In this study, we included 227 unrelated adult candidemia patients of European genetic background. Patients were enrolled after confirmation of at least one positive blood culture for a *Candida* species. The control cohort of 176 volunteers of European descent consisted of non-*Candida*-infected matched patients from the same clinical departments as the patient cohort. Controls were recruited consecutively from the same hospital wards as infected patients during the study period, with a similar balance of medical, surgical, and oncology patients. Review boards of the involved medical centers approved the study, and patients were enrolled after giving written informed consent (described in detail in (Jaeger et al., 2015)). Patients and control volunteers were genotyped on the Illumina Immunochip SNP array platform, which contains approximately 200,000 SNPs focused on genomic regions known to be involved in immune-mediated diseases (Trynka et al., 2011). After the application of quality control filters, we investigated

whether SNPs in the *VAV* genes influence susceptibility to candidemia in the case-control association. The publicly available SNAP server was used to plot the SNP of interest (rs4914950)(Johnson et al., 2008; Saxena et al., 2007).

**SUPPLEMENTAL REFERENCES**

Anders, S., and Huber, W. (2010). Differential expression analysis for sequence count data. Genome Biol *11*, R106.

Compagno, M., Lim, W.K., Grunn, A., Nandula, S.V., Brahmachary, M., Shen, Q., Bertoni, F., Ponzoni, M., Scandurra, M., Califano, A.*, et al.* (2009). Mutations of multiple genes cause deregulation of NF-kappaB in diffuse large B-cell lymphoma. Nature *459*, 717-721.

Johnson, A.D., Handsaker, R.E., Pulit, S.L., Nizzari, M.M., O'Donnell, C.J., and de Bakker, P.I. (2008). SNAP: a web-based tool for identification and annotation of proxy SNPs using HapMap. Bioinformatics *24*, 2938-2939.

Kim, D., Pertea, G., Trapnell, C., Pimentel, H., Kelley, R., and Salzberg, S.L. (2013). TopHat2: accurate alignment of transcriptomes in the presence of insertions, deletions and gene fusions. Genome Biol *14*, R36.

Liao, Y., Smyth, G.K., and Shi, W. (2014). featureCounts: an efficient general purpose program for assigning sequence reads to genomic features. Bioinformatics *30*, 923-930.

Love, M.I., Huber, W., and Anders, S. (2014). Moderated estimation of fold change and dispersion for RNA-seq data with DESeq2. Genome Biol *15*, 550.

Saxena, R., Voight, B.F., Lyssenko, V., Burtt, N.P., de Bakker, P.I., Chen, H., Roix, J.J., Kathiresan, S., Hirschhorn, J.N., Daly, M.J.*, et al.* (2007). Genome-wide association analysis identifies loci for type 2 diabetes and triglyceride levels. Science *316*, 1331-1336.

Subramanian, A., Tamayo, P., Mootha, V.K., Mukherjee, S., Ebert, B.L., Gillette, M.A., Paulovich, A., Pomeroy, S.L., Golub, T.R., Lander, E.S.*, et al.* (2005). Gene set enrichment analysis: a knowledge-based approach for interpreting genome-wide expression profiles. Proc Natl Acad Sci U S A *102*, 15545-15550.

Trynka, G., Hunt, K.A., Bockett, N.A., Romanos, J., Mistry, V., Szperl, A., Bakker, S.F., Bardella, M.T., Bhaw-Rosun, L., Castillejo, G.*, et al.* (2011). Dense genotyping identifies and localizes multiple common and rare variant association signals in celiac disease. Nat Genet *43*, 1193-1201.

Yarkoni, E., and Rapp, H.J. (1978). Toxicity of emulsified trehalose-6,6'-dimycolate (cord factor) in mice depends on size distribution of mineral oil droplets. Infect Immun *20*, 856-860.

**Immunity**

# Article

**Cell** PRESS

# Interferon-β Production via Dectin-1-Syk-IRF5 Signaling in Dendritic Cells Is Crucial for Immunity to *C. albicans*

Carlos del Fresno,[1,7,8] Didier Soulat,[1,2,7] Susanne Roth,[3] Katrina Blazek,[4] Irina Udalova,[4] David Sancho,[5] Jürgen Ruland,[3,6] and Carlos Ardavín[1,*]

[1]Departamento de Inmunología y Oncología, Centro Nacional de Biotecnología/CSIC, C/ Darwin 3, 28049 Madrid, Spain
[2]Mikrobiologisches Institut – Klinische Mikrobiologie, Immunologie und Hygiene, Universitätsklinikum Erlangen and Friedrich-Alexander-Universität Erlangen-Nürnberg, Wasserturmstraβe 3-5, 91054 Erlangen, Germany
[3]Institut für Klinische Chemie und Pathobiochemie, Klinikum rechts der Isar, Technische Universität München, Ismaninger Straβe. 22, 81675, Munich, Germany
[4]Kennedy Institute of Rheumatology, Nuffield Department of Orthopaedics, Rheumatology and Musculoskeletal Sciences, University of Oxford, London W6 8KH, UK
[5]Centro Nacional de Investigaciones Cardiovasculares Carlos III, C/ Melchor Fernández Almagro 3, 28029 Madrid, Spain
[6]Laboratory of Signaling in the Immune System, Helmholtz Zentrum München – German Research Center for Environmental Health, Ingolstädter Landstraβe 1, 85764, Neuherberg, Germany
[7]These authors contributed equally to this work
[8]Present address: Centro Nacional de Investigaciones Cardiovasculares Carlos III, C/ Melchor Fernández Almagro 3, 28029 Madrid, Spain
*Correspondence: ardavin@cnb.csic.es
http://dx.doi.org/10.1016/j.immuni.2013.05.010

## SUMMARY

**Type I interferon (IFN) is crucial during infection through its antiviral properties and by coordinating the immunocompetent cells involved in antiviral or antibacterial immunity. Type I IFN (IFN-α and IFN-β) is produced after virus or bacteria recognition by cytosolic receptors or membrane-bound TLR receptors following the activation of the transcription factors IRF3 or IRF7. IFN-β production after fungal infection was recently reported, although the underlying mechanism remains controversial. Here we describe that IFN-β production by dendritic cells (DCs) induced by *Candida albicans* is largely dependent on Dectin-1- and Dectin-2-mediated signaling. Dectin-1-induced IFN-β production required the tyrosine kinase Syk and the transcription factor IRF5. Type I IFN receptor-deficient mice had a lower survival after *C. albicans* infection, paralleled by defective renal neutrophil infiltration. IFN-β production by renal infiltrating leukocytes was severely reduced in *C. albicans*-infected mice with Syk-deficient DCs. These data indicate that Dectin-induced IFN-β production by renal DCs is crucial for defense against *C. albicans* infection.**

## INTRODUCTION

The type I interferon (IFN) cytokine family includes IFN-β and 14 members of the IFN-α family (Decker et al., 2005). Type I IFN was originally discovered by its antiviral properties, which rely primarily on its capacity to block gene translation, to inhibit viral replica-

tion, to trigger the production of nucleases degrading viral nucleic acids, and to induce the apoptosis of infected cells (Stetson and Medzhitov, 2006). However, type I IFN was subsequently demonstrated to play also a crucial role during infection by coordinating the function of different immunocompetent cells involved in the induction of defense against viruses and intracellular bacteria. In this regard, type I IFN can license dendritic cells (DCs) for cross-priming-dependent activation of CD8+ T cells, trigger the effector function of cytotoxic CD8+ T cells, activate natural killer (NK) cells through interleukin-15 (IL-15) production, and promote the production of leukocyte-attractant chemokines (González-Navajas et al., 2012). Type I IFN can be produced after recognition of viruses or intracellular bacteria through two categories of receptors: ubiquitously expressed cytosolic receptors such as RIG-I and MDA5 (that sense viral dsRNA), or NOD1 and NOD2 (that sense bacterial peptidoglycans), and membrane-bound Toll-like receptors (TLRs), such as TLR3, TLR4, TLR7, and TLR9 (Trinchieri, 2010). These type I IFN-inducing TLRs that are selectively expressed by specialized immunocompetent cells are located at the cell surface (TLR4, that senses Gram-negative bacteria LPS) or at endosomal compartments (TLR3, TLR7, and TLR9, that sense viral or bacterial nucleic acids). After viral or bacterial infection, the engagement of type I IFN-inducing receptors, except TLR7 and TLR9, leads to the activation of the transcription factor IFN response factor 3 (IRF3) that induces the production of IFN-β and IFN-α4 (Trinchieri, 2010). In contrast, engagement of endosomal TLR7 and TLR9 in DCs leads to the production of IFN-β and all types of IFN-α by a mechanism dependent on the transcription factor IRF7 (Decker et al., 2005; refer to Figure S7 available online for an integrated view of type I IFN-inducing receptors).

Recent studies have revealed that type I IFN can be produced by DCs in response to fungi, particularly to yeasts of the genus *Candida* (Biondo et al., 2011; Bourgeois et al., 2011), which can cause life-threatening infections in immunocompromised

patients (Pfaller and Diekema, 2007). As described for bacterial infections, type I IFN can be beneficial for the immune response to yeast, as described for *Candida albicans* (Biondo et al., 2011), or have a detrimental effect, as reported for *Candida glabrata* infection (Bourgeois et al., 2011). However, the mechanism by which type I IFN is produced during *Candida* infection remains controversial. Activation of DCs after interaction with *C. albicans* has been claimed to result from the engagement of TLR2 and TLR9, and particularly of Dectin-1 (Clec7a; Romani, 2011), a C-type lectin receptor recognizing the complex β-glucan cell wall of *C. albicans*, that is crucial for the induction of protective T helper 17 (Th17) cell responses (LeibundGut-Landmann et al., 2007). Dectin-1 engagement results in the recruitment of Syk, that leads to the activation of PLCγ2 (Xu et al., 2009) and to the assembly of the Card9 complex by a mechanism dependent on PKCδ (Strasser et al., 2012). Dectin-1-triggered Card9 signaling then drives IL-1β, IL-2, IL-6, IL-10, IL-12, IL-23, and tumor necrosis factor-α (TNF-α) production by an NF-κB and NFAT-dependent pathway (Sancho and Reis e Sousa, 2012; refer to Figure S7 for an integrated view of Dectin-1-mediated signaling).

In order to explore the involvement of Dectin-1 in the production of type I IFN during fungal infection, we have analyzed the signaling pathway controlling IFN-β expression by DCs in response to *C. albicans*. Our data have allowed us to describe a pathway leading to IFN-β production by DCs that depends on Dectin-1 and Dectin-2 activation. Dectin-1-induced IFN-β production was dependent on Syk- and Card9-driven signaling and on the transcription factor IRF5 and independent of IRF3 and IRF7. Experiments of in vivo infection with *C. albicans* performed in mice deficient in the IFNAR1 subunit of the type I IFN receptor IFN-α and IFN-β receptor-deficient (*Ifnar1*$^{-/-}$) and CD11c-Cre$^{+/-}$ *Syk*$^{fl/fl}$ mice, in which DCs are not responsive to Syk-dependent signaling, demonstrated that type I IFN exerted a protective role during *C. albicans* infection and that the production of type I IFN by renal leukocytic infiltrates was mainly controlled by DCs through Dectin-1 and Dectin-2 signaling. Taken together, our results support the hypothesis that the production of type I IFN by renal infiltrating DCs, mediated by Dectin-Syk-IRF5 signaling, plays a crucial role in defense against *C. albicans* infection.

## RESULTS

### Dectin-1 Engagement Induces IFN-β Production by Dendritic Cells

In order to address the involvement of Dectin-1 in the production of type I IFN by DCs, we first assessed by real-time PCR the capacity of bone-marrow-derived DCs (BMDCs) to express IFN-β-specific messenger RNA (mRNA) in response to Curdlan (a water-insoluble β-1,3 polysaccharide from *Alcaligenes faecalis* that acts as a Dectin-1 specific ligand), to Zymosan (a complex insoluble preparation from *Saccharomyces cerevisiae* that activates TLR2 and TLR6, TLR9, and Dectin-1), to heat-killed *C. albicans*, strain SC5314 (HKC), and to LPS from *Escherichia coli*, that was used as a control of type I IFN production in response to TLR4. Engagement of TLR4 was characterized by a fast and transient induction of IFN-β mRNA, which peaked 2 hr after LPS stimulation and returned to basal levels along the

next 4 hr. In contrast, Curdlan and Zymosan induced a more sustained expression of IFN-β mRNA, which peaked at 3 hr, was maintained at maximal levels until 5 hr, and was still detectable 8 hr after stimulation (Figure 1A). The kinetics of IFN-β mRNA expression after stimulation with HKC revealed a slower response peaking at 5 hr. This delayed response compared to Curdlan or Zymosan could reflect a reduced exposure of DC-activating *Candida*-associated molecular patterns by HKC, and consequently a less efficient recognition of these ligands by the TLRs and C-type lectin receptors expressed by BMDCs.

One possible explanation for this sustained IFN-β mRNA expression is that IFN-β produced after engagement of Dectin-1 and/or TLRs by yeast compounds present in Curdlan and/or Zymosan triggers, in an autocrine manner, the signaling through the type I IFN receptor (IFNAR) IFN-α and IFN-β receptor (IFNAR1). This would lead to a feed-forward loop of IFN-β production that has been described for TLR7- or TLR-9-activated plasmacytoid DCs (Decker et al., 2005) but that was not operational in BMDCs activated by LPS (Figure S1). However, no differences in IFN-β mRNA expression were observed between *Ifnar1*$^{-/-}$ and wild-type (WT) BMDCs after stimulation with Curdlan or Zymosan (Figure S1). These results indicates that IFNAR signaling did not contribute to a feed-forward loop of IFN-β production in BMDCs under these activation conditions, although the autocrine IFNAR signaling pathway was operational because no expression of mRNA for the IFN-inducible antiviral gene *Mx2* was detected in *Ifnar1*$^{-/-}$ BMDCs (Figure S1). Therefore the sustained IFN-β mRNA expression induced by Curdlan and Zymosan was not due to IFNAR signaling, but most likely to a Dectin-1-specific transcriptional regulation of *Ifnb* gene expression, as discussed below.

As stated before, IRF3-mediated IFN-β production resulting from the recognition of viral or bacterial compounds by type I IFN-inducing cytosolic or TLR receptors has been claimed to be paralleled by IFN-α4 production (Trinchieri, 2010). To address whether this also occurred in response to *C. albicans*, we analyzed IFN-α mRNA expression in BMDCs stimulated with Curdlan or Zymosan by real-time PCR, by using pan-IFN-α primers. IFN-α mRNA expression was not detected in BMDCs stimulated with Curdlan or Zymosan (Figure S2). In contrast, IFN-α mRNA was induced in bone marrow-derived macrophages (BMMs) stimulated with either Curdlan or Zymosan (Figure S2A), indicating that Curdlan-induced signaling can lead to the induction of IFN-α mRNA, although this appears to be cell-type-specific. Interestingly, Curdlan or Zymosan stimulation induced a significantly higher IFN-β mRNA expression in BMDCs than in BMMs (Figure S2B).

To confirm that IFN-β production in response to Curdlan was due to Dectin-1 engagement, the expression of IFN-β mRNA and the production of IFN-β was analyzed by real-time PCR and ELISA, respectively, after stimulation of BMDCs from Dectin-1 deficient (*Clec7a*$^{-/-}$) mice (Figures 1B and 1C). Whereas no difference in the expression of mRNA for IFN-β was observed between WT and *Clec7a*$^{-/-}$ BMDCs stimulated with LPS (Figure 1B), IFN-β mRNA expression was dramatically reduced in *Clec7a*$^{-/-}$ BMDCs after Curdlan stimulation (Figure 1B), and, correspondingly, no IFN-β was detected at the protein level (Figure 1C). This result demonstrates that the production of IFN-β by Curdlan-stimulated BMDCs was dependent

## Immunity

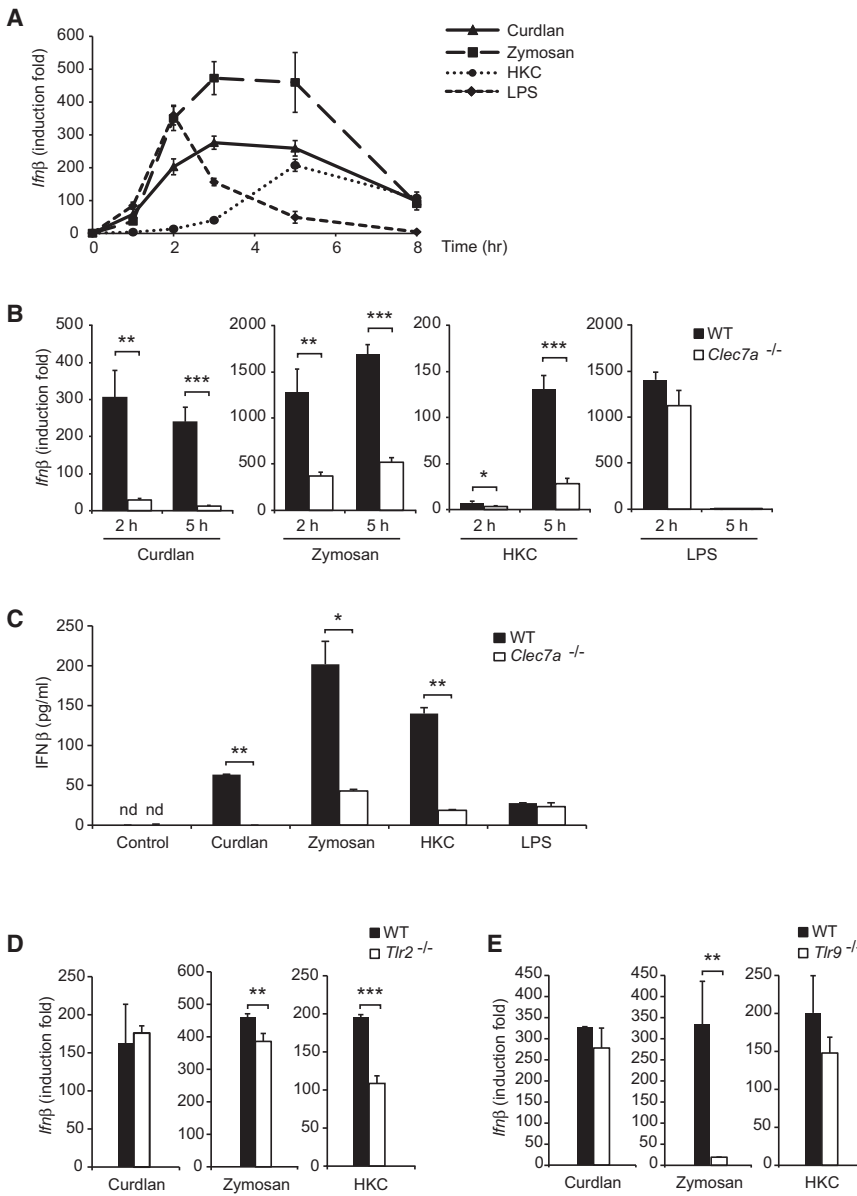### Dectin-1-Syk-IRF5-Dependent IFN-β Production by DCs



**Figure 1. Dectin-1 Engagement Induces IFN-β Production by BMDCs**

(A) Expression of mRNA for IFN-β by BMDCs stimulated for the indicated times with Curdlan, Zymosan, HKC, or LPS was assessed by real-time PCR, normalized to β-actin.

(B) BMDCs from WT or $Clec7a^{-/-}$ mice, unstimulated or stimulated for 2 or 5 hr with Curdlan, Zymosan, HKC, or LPS, were analyzed for the expression of mRNA for IFN-β by real-time PCR, normalized to β-actin.

(C) IFN-β production by BMDCs from WT or $Clec7a^{-/-}$ mice unstimulated (control) or stimulated for 16 hr with Curdlan, Zymosan, HKC, or LPS, was analyzed by ELISA.

(D and E) IFN-β mRNA expression by BMDCs from WT, $Tlr2^{-/-}$ (D), or $Tlr9^{-/-}$ (E) mice stimulated for 5 hr with Curdlan, Zymosan, or HKC was analyzed by real-time PCR, normalized to β-actin. Real-time PCR data are expressed as induction fold relative to unstimulated controls (mean ± SD of triplicates). ELISA data are expressed as mean ± SD of duplicate samples. The values for unstimulated controls were below the detection level of the ELISA kit used in this study (15.6 pg/ml), nd: not detectable. Significant differences, as determined by the unpaired t test, are indicated *p < 0.05; **p < 0.01; ***p < 0.001. Data are representative of at least two independent experiments with similar results. See also Figures S1 and S2.

IFN-β mRNA was reduced around 50% after stimulation of $Tlr2^{-/-}$ BMDCs with HKC compared to their WT counterparts, but was not significantly affected in HKC-stimulated BMDCs from $Tlr9^{-/-}$ mice. This result reflects that *Candida* DNA does not contribute significantly to HKC-mediated IFN-β production and revealed that HKC preparations contained a minimal amount of free *Candida* DNA. In contrast, IFN-β mRNA expression induced by Zymosan was strongly inhibited in $Tlr9^{-/-}$ BMDCs, indicating that yeast DNA from *S. cerevisiae* was readily exposed in Zymosan preparations. Globally, these results reveal that IFN-β production by BMDCs in response to *C. albicans* is mainly driven by Dectin-1 signaling and that IFN-β produced by BMDCs in response to Curdlan is TLR-independent and dependent on Dectin-1.

### IFN-β Production Triggered by Dectin-1 Is Dependent on Syk and Card9

As mentioned above, Dectin-1 engagement results in the recruitment of Syk and Card9, leading to cytokine production by an NF-κB and NFAT-dependent pathway (Sancho and Reis e Sousa, 2012). In order to assess whether Dectin-1-induced IFN-β production was dependent on Syk, IFN-β production was analyzed in BMDCs from CD11c-Cre$^{+/-}$ $Syk^{fl/fl}$ mice, in which Syk deletion is under the control of the promoter for CD11c, an integrin expressed by all mouse DC subtypes. As

on Dectin-1 signaling. After stimulation with Zymosan or HKC, IFN-β mRNA expression was significantly lower in $Clec7a^{-/-}$ that in WT BMDCs (Figure 1B), and, accordingly, IFN-β production was reduced around 80% (Figure 1C). These data suggest that IFN-β production in response to *C. albicans* results, for the most part, from Dectin-1 signaling, and consequently to a lesser extent from TLR-mediated signaling. To further explore the relative contribution of TLR-mediated signaling to IFN-β production in response to *C. albicans*, we analyzed IFN-β mRNA expression by BMDCs from mice deficient in the receptors TLR2 or TLR9 that have been reported to contribute predominantly to TLR-mediated activation of DCs exposed to *C. albicans*, by interacting with *Candida* cell wall mannans and *Candida* DNA, respectively (Romani, 2011). As expected, neither TLR2 nor TLR9 deficiency affected the response of BMDCs to Curdlan stimulation (Figures 1D and 1E). The expression of
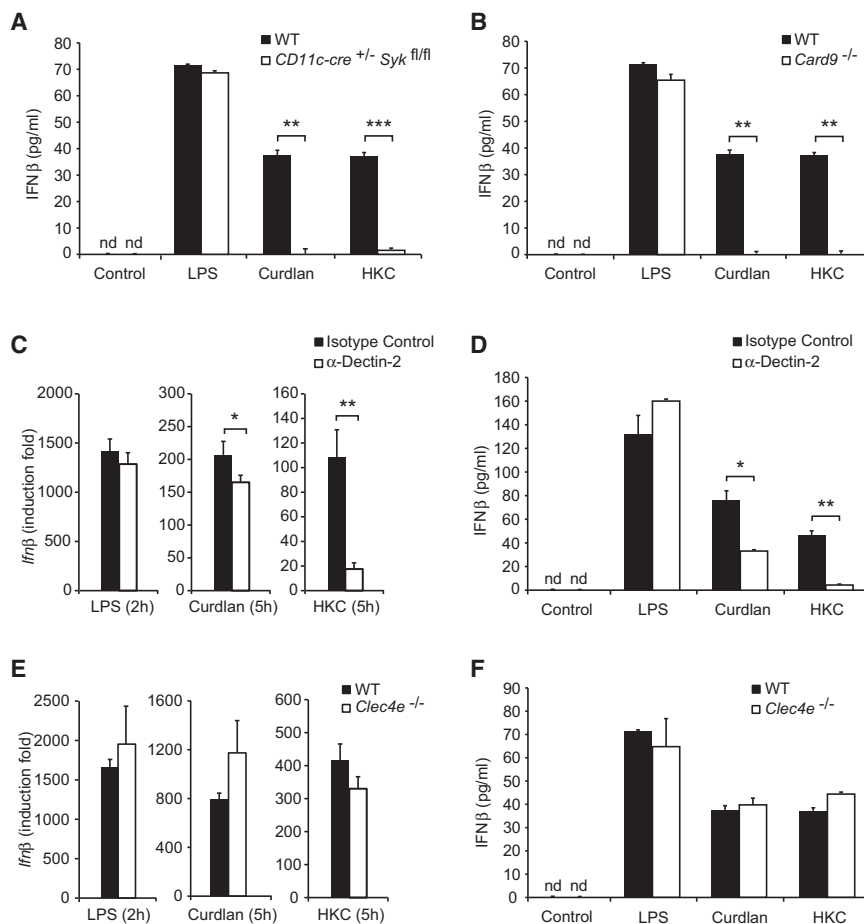
**Figure 2. Contribution of Syk and Card9 Signaling to IFN-β Production by BMDCs in Response to C. albicans**

(A and B) IFN-β production by BMDCs from WT, CD11c-Cre^{+/−} $Syk^{fl/fl}$ (A), or $Card9^{−/−}$ (B) mice unstimulated (control) or stimulated for 16 hr with LPS, Curdlan, or HKC was analyzed by ELISA.

(C) IFN-β mRNA expression by BMDCs treated with anti-Dectin-2 or isotype control antibodies and stimulated for the indicated times with LPS, Curdlan, or HKC was analyzed by real-time PCR, normalized to β-actin.

(D) IFN-β production by BMDCs treated with anti-Dectin-2 or isotype control antibodies and stimulated or not (control) for 16 hr with LPS, Curdlan, or HKC was analyzed by ELISA.

(E) IFN-β mRNA expression by BMDCs from $Clec4e^{−/−}$ mice stimulated for the indicated times with LPS, Curdlan, or HKC was analyzed by real-time PCR, normalized to β-actin.

(F) IFN-β production by BMDCs from $Clec4e^{−/−}$ mice unstimulated (control) or stimulated for 16 hr with LPS, Curdlan, or HKC was analyzed by ELISA. Real-time PCR data are expressed as induction fold relative to unstimulated controls (mean ± SD of triplicates). ELISA data are expressed as mean ± SD of duplicate samples. Significant differences, as determined by the unpaired t test, are indicated *p < 0.05; **p < 0.01; ***p < 0.001. Data are representative of at least two independent experiments with similar results. n.d., not detectable.

shown in Figure 2A, deletion of *Syk* had no effect on the synthesis of IFN-β by BMDCs stimulated by LPS as expected, but completely blocked its production by Curdlan-stimulated BMDCs, confirming the involvement of Syk in Dectin-1-mediated IFN-β production. Because Card9 is involved in NF-κB activation resulting from Dectin-1 engagement (Gross et al., 2006) and NF-κB is required for the transcriptional activation of the *Ifnb* gene (Panne et al., 2007), we hypothesized that Card9 could also control IFN-β production in response to Curdlan. To address this issue, we analyzed BMDCs from *Card9*^{−/−} mice for their ability to produce IFN-β after stimulation with Curdlan or LPS. As expected, Card9 deficiency strongly inhibited the production of IFN-β in response to Curdlan, but not to LPS, confirming that Dectin-1-mediated IFN-β production is dependent on Card9 (Figure 2B). Interestingly, IFN-β production by HKC-stimulated BMDCs from either CD11c-Cre^{+/−} *Syk*^{fl/fl} or *Card9*^{−/−} mice was barely detectable, indicating that production of IFN-β by BMDCs in response to *C. albicans* is essentially dependent on Syk and Card9 signaling.

The fact that the blockade of IFN-β production in response to HKC was even more pronounced in either CD11c-Cre^{+/−} *Syk*^{fl/fl} or *Card9*^{−/−} BMDCs than in *Clec7a*^{−/−} BMDCs, led us to explore the contribution of Dectin-2 and Mincle, the two other C-type lectin receptors recognizing *C. albicans* cell wall mannans and signaling through a Syk-Card9-mediated pathway (Sancho and Reis e Sousa, 2012), to IFN-β production in response to *C. albicans*. The production of IFN-β in response to Curdlan was reduced around 20% and 50% at the mRNA and protein level, respectively, after treatment with the anti-Dectin-2 blocking antibody D2.11E4 (Figures 2C and 2D). This result suggests that in BMDCs Curdlan was recognized by Dectin-2, although less efficiently than by Dectin-1, or alternatively that the Dectin-2 antibody D2.11E4 displayed some cross-reactivity with Dectin-1. Interestingly, HKC-induced production of IFN-β by anti-Dectin-2 treated BMDCs was reduced to a same extent than in *Clec7a*^{−/−} BMDCs. In contrast, Mincle (Clec4e) deficiency had no effect on IFN-β production induced by either Curdlan or HKC (Figures 2E and 2F). These data suggest that Dectin-2, which requires to be associated with the ITAM-bearing adaptor FcRγ to recruit Syk (Sancho and Reis e Sousa, 2012), contributes significantly to IFN-β production in response to *C. albicans*, through a Dectin-2-FcRγ-Syk pathway. Therefore our data support that IFN-β production in response to *C. albicans* results essentially from the combined action of Dectin-1 and Dectin-2 signaling.

## IRF5, but Neither IRF3 Nor IRF7, Controls Dectin-1-Dependent IFN-β Production

To identify the molecular mechanism leading to IFN-β production after Dectin-1 engagement, we analyzed the activation of the main transcriptional activators required for the assembly of the IFN-β enhanceosome: NF-κB, c-Jun, and IRF3. For this purpose, the phosphorylation and nuclear translocation of the RelA subunit of NF-κB, c-Jun, and IRF3 was evaluated by immunoblot
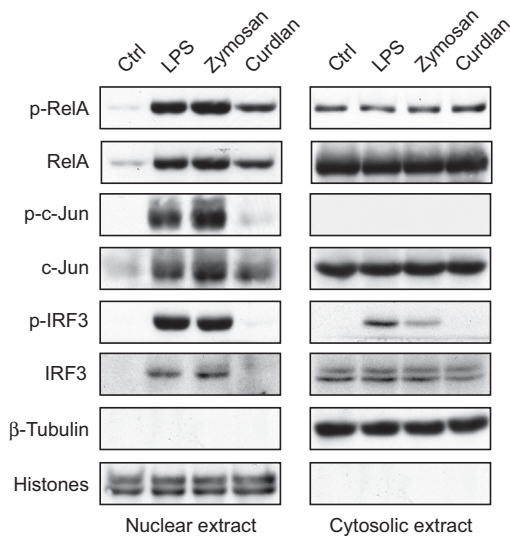
## Immunity

### Dectin-1-Syk-IRF5-Dependent IFN-β Production by DCs

**Cell** PRESS



**Figure 3. Activation of *Ifnb* Gene Transcriptional Activators after Dectin-1 Engagement in BMDCs**

RelA, c-Jun, and IRF3 activation was determined on nuclear and cytosolic protein extracts from BMDCs stimulated with LPS, Zymosan, or Curdlan for 2 hr. Extracts were analyzed by immunoblot by using antibodies against phospho-RelA, phospho-c-Jun, or phospho-IRF3, RelA, c-Jun, and IRF3. Purity of the nuclear and cytosolic cell fractions was assessed by using antibodies against Histones (H1 and core proteins) and β-tubulin, respectively. Data are representative of two independent experiments with similar results.

on cell lysates from the nuclear or cytosolic fractions of Curdlan-, Zymosan-, or LPS-activated BMDCs. Whereas BMDC stimulation with either Curdlan, Zymosan, or LPS led to a correct activation of RelA (Figure 3), the phosphorylation and nuclear translocation of c-Jun was almost undetectable in BMDCs activated with Curdlan, indicating that IFN-β production in response to Curdlan occurred in the absence of a strong c-Jun activation. In contrast, both Zymosan and LPS induced a correct activation of c-Jun. The analysis of IRF3 activation, required for IFN-β production in response to the majority of type I IFN-inducing receptors, including cytosolic receptors as well as TLR3 and TLR4 (Trinchieri, 2010), revealed that IRF3 was not phosphorylated and consequently it was not translocated to the nucleus in response to Curdlan stimulation. In contrast, as expected, these processes occurred correctly in LPS- or Zymosan-activated BMDCs (Figure 3). This finding strongly supports the hypothesis that IRF3 was not required for IFN-β production in response to Curdlan. To confirm this hypothesis, we analyzed BMDCs from $Irf3^{-/-}$ mice for their capacity to produce IFN-β in response to Curdlan or LPS. IRF3 deficiency led to a dramatic reduction in IFN-β production by BMDCs stimulated with LPS, but had no effect on the synthesis of IFN-β in response to Curdlan (Figure 4A), confirming that IRF3 was not involved in Dectin-1-triggered IFN-β production. Given that IFN-β production induced after engagement of TLR7 or TLR9 on DCs has been demonstrated to be dependent on the transcription factor IRF7 (Decker et al., 2005), we used BMDCs from $Irf7^{-/-}$ mice to address whether IRF7 was involved in Dectin-1-mediated IFN-β production. Our data demonstrate that IRF7 was not involved in this process as IFN-β production by Curdlan-stimulated BMDCs was
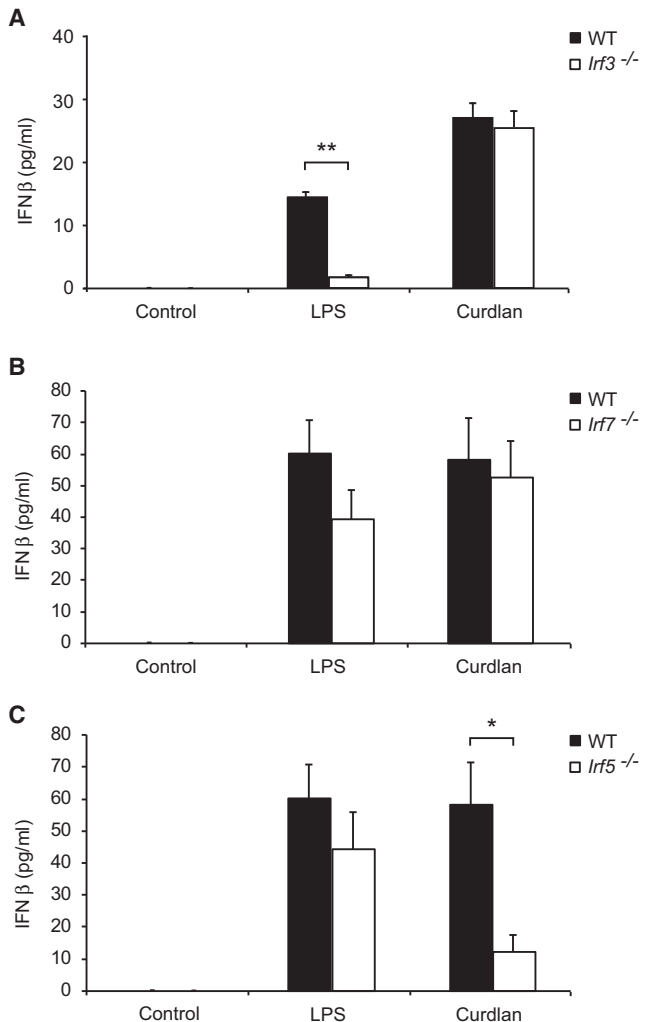


**Figure 4. IRF5, but Neither IRF3 Nor IRF7, Controls Dectin-1-Dependent IFN-β Production**

IFN-β production by BMDCs from wild-type (WT), $Irf3^{-/-}$ (A), $Irf7^{-/-}$ (B) or $Irf5^{-/-}$ (C) mice unstimulated (control) or stimulated for 16 hr with LPS or Curdlan was analyzed by ELISA. Data are expressed as mean ± SD of duplicate samples. Significant differences, as determined by the unpaired t test, are indicated *p < 0.05; **p < 0.01. Data are representative of three (A) or two (B and C) independent experiments with similar results. n.d., not detectable. See also Figure S3.

not affected by IRF7 deficiency (Figure 4B). In conclusion, these experiments confirmed that IFN-β production in response to Curdlan was dependent on neither IRF3 nor IRF7, that in contrast play a crucial role in the control of type I IFN production in response to virus and bacteria through cytosolic or TLR receptors. In search for a member of the IRF family of transcription factors that may control the transcriptional activation of the *Ifnb* gene resulting from Dectin-1 engagement, we explored the possible involvement of IRF5 in this process, based on two recent reports demonstrating a correlation between IRF5 and IFN-β production after bacterial infection (Gratz et al., 2011; Pandey et al., 2009). Interestingly, Dectin-1-mediated IFN-β production was found to be strongly dependent on IRF5, as assessed by analyzing BMDCs from $Irf5^{-/-}$ mice (Figure 4C). Regarding
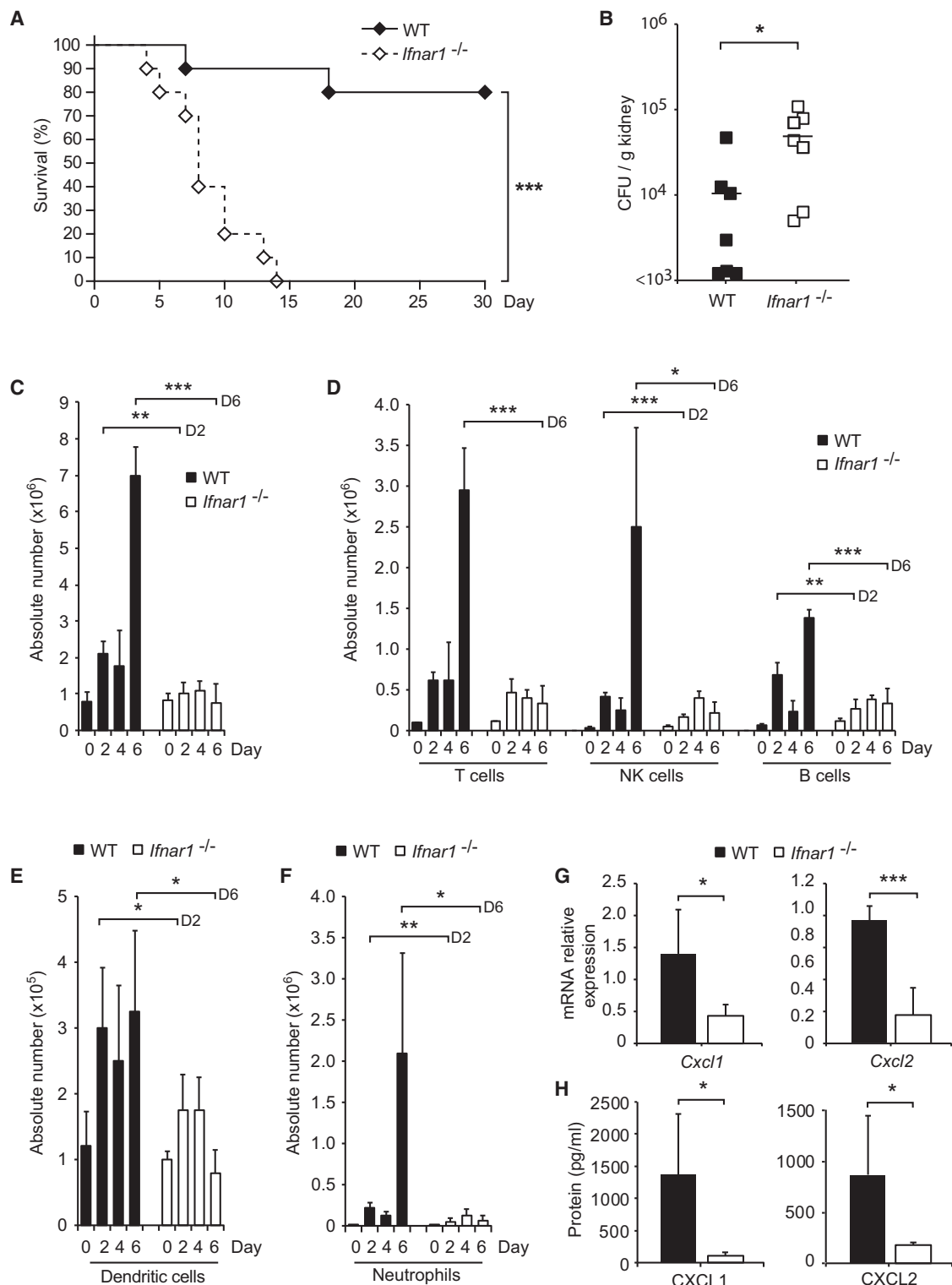
**Figure 5. Type I IFN Produced in Response to *C. albicans* Is Crucial for Defense against Candidiasis**

(A) Survival of WT (n = 12) and *Ifnar1*^{−/−} (n = 12) mice infected intravenously with $1 \times 10^5$ *C. albicans*.

(B) Kidney fungal burden of WT (n = 7) and *Ifnar1*^{−/−} (n = 7) mice at day 6 after infection with $1 \times 10^5$ *C. albicans*. Data are expressed as cfu/g kidney.

(C) Kinetics of infiltrating leukocytes (defined as CD45^{+} cells) after infection with $1 \times 10^5$ *C. albicans* of WT or *Ifnar1*^{−/−} mice. Data are expressed as mean ± SD of four mice per condition.

(D) Absolute number of T, NK, and B cells (defined as CD90^{+}, CD49b^{+}, and CD19^{+} cells, respectively) in the renal leukocyte infiltrates of WT or *Ifnar1*^{−/−} mice at the indicated times after infection with $1 \times 10^5$ *C. albicans*. Data are expressed as mean ± SD of four mice per condition.

*(legend continued on next page)*

these experiments performed with $Irf5^{-/-}$ mice, it is important to point out that a recent report (Purtha et al., 2012) has revealed that, in some cases, $Irf5^{-/-}$ mice harbor a spontaneous mutation in the *Dock2* gene that could interfere with the analysis of IRF5 deficiency. However, as shown in Figure S3, the genotyping of the $Irf5^{-/-}$ mice used in our study confirmed that they had a normal *Dock2* genotype.

In conclusion, our data firmly demonstrate the existence in BMDCs of a Dectin-1-mediated signaling pathway leading to the production of IFN-β that is dependent on the Syk kinase, the NF-κB activator Card9 and on the transcription factor IRF5. Importantly, our results also support that type I IFN production by BMDCs in response to *C. albicans* is mainly controlled by this Dectin-1-dependent pathway.

### Type I IFN Production in Response to *C. albicans* Is Crucial for Defense against Candidiasis

In order to explore the role of IFN-β produced in response to *C. albicans*, we first analyzed the survival of WT versus $Ifnar1^{-/-}$ mice after intravenous injection of LD$_{50}$ dose of $1 \times 10^5$ *C. albicans*. During the 2 first weeks after infection, 100% (12/12) versus 16% (2/12) mice died in $Ifnar1^{-/-}$ and WT strains, respectively. Correspondingly, the survival at day 30 after infection was significantly higher in WT than in $Ifnar1^{-/-}$ mice (75% versus 0%, p value < 0.0001; Figure 5A). Because the kidney is the main target for *C. albicans* infection, we analyzed the renal fungal burden at day 6 after infection, corresponding to the time point when mice started to die. As expected from our survival data, $Ifnar1^{-/-}$ mice had a significantly higher fungal burden than WT mice (p value < 0.05; Figure 5B). In line with our data supporting that type I IFN production by DCs in response to *C. albicans* is essentially dependent on Dectin-Syk-IRF5 signaling, the renal fungal load in *C. albicans*-infected $Irf5^{-/-}$ mice was significantly higher than in their WT counterparts (p value < 0.05; Figure S4). In an attempt to unravel the mechanism by which IFN-β exerted a protective effect after *C. albicans* infection, we analyzed the recruitment to the kidney of the different leukocytic cell types infiltrating the renal parenchyma, in WT and $Ifnar1^{-/-}$ mice, from day 0 to day 6 after infection. The number of renal infiltrating leukocytes, characterized as CD45$^+$ cells, was reduced in $Ifnar1^{-/-}$ mice to 50% and 15% of controls at days 2 and 6 after infection, respectively (Figure 5C). This was paralleled by an average 50% reduction in the number of infiltrating NK cells, B cells, and DCs in $Ifnar1^{-/-}$ mice at day 2 postinfection. At day 6, the lymphoid and DC subsets underwent a more pronounced reduction, to around 30% of controls for B cells and DCs and to around 15% of controls for T cells and NK cells (Figures 5D and 5E). Interestingly, the number of neutrophils present in renal leukocyte infiltrates of $Ifnar1^{-/-}$ mice was reduced to around 25% of controls at day 2 and underwent a dra-

matic 95% reduction at day 6. No reduction was detected in any leukocyte-infiltrating subset at day 4 postinfection in line with previous data revealing the existence of two waves of leukocyte infiltration in the kidney after *C. albicans* infection peaking at days 3 and 5 after infection (Lionakis et al., 2011). To determine whether the impaired neutrophil recruitment to the kidney observed in $Ifnar1^{-/-}$ mice was linked to a defective expression of neutrophil-attractant chemokines, we first analyzed the production of CXCL1 and CXCL2 by CD45$^+$ renal infiltrating leukocytes at the mRNA and protein level, by real-time PCR and Luminex, respectively. In line with the strong reduction in the number of neutrophils observed in the renal infiltrates of $Ifnar1^{-/-}$ mice, the production of CXCL1 and CXCL2 by renal infiltrating leukocytes was also significantly reduced in $Ifnar1^{-/-}$ mice (Figures 5G and 5H). Because nonhematopoietic cells are known to contribute also substantially to the production of these chemokines, we analyzed the expression of CXCL1 and CXCL2 mRNA by the CD45$^-$ nonhematopoietic kidney fraction in *C. albicans*-infected WT and $Ifnar1^{-/-}$ mice. Interestingly, IFNAR1 deficiency did not affect the expression of these chemokines by nonhematopoietic cells (Figure S5). These data suggest that type I IFN promotes neutrophil recruitment to the kidney by a process that involves CXCL1 and CXCL2 production by infiltrating leukocytes. We subsequently explored the mechanism by which type I IFN positively regulates the production of these chemokines in the kidney during *C. albicans* infection. For this purpose we analyzed the effect of IFNAR1 deficiency on the expression of mRNA for CXCL1 and CXCL2 by BMDCs and neutrophils in vitro after stimulation with Curdlan or HKC, because DCs and neutrophils are the main leukocytes subsets potentially responsible for the production of theses chemokines in the kidney after *C. albicans* infection. Our data revealed that whereas no differences in CXCL1 and CXCL2 mRNA expression were found between BMDCs from WT or $Ifnar1^{-/-}$ mice, IFNAR1 deficiency lead to a strong reduction in the expression of mRNA for these chemokines by neutrophils after incubation with either Curdlan or HKC (Figure S6). As expected, no expression of mRNA for CXCL1 or CXCL2 was detected in T or B cells. These data support the idea that *C. albicans*-induced production of CXCL1 and CXCL2 by neutrophils is strongly dependent on type I IFN and suggest that the decreased production of these chemokines by renal infiltrating leukocytes during *C. albicans* infection of $Ifnar1^{-/-}$ mice results from their defective production by neutrophils in the absence of IFNAR signaling.

### IFN-β Production during *C. albicans* Infection Is Controlled by DCs through Dectin and Syk Signaling

Our data from in vivo infection experiments in $Ifnar1^{-/-}$ mice revealed that type I IFN production is crucial for defense against *C. albicans*. In order to determine the contribution of DCs to

(E and F) Absolute number of DCs (E) and neutrophils (F), defined by flow cytometry on the basis of CD11c and Ly-6G expression, respectively, in the renal leukocyte infiltrates of WT or $Ifnar1^{-/-}$ mice, at the indicated times after infection with $1 \times 10^5$ *C. albicans*. Data are expressed as mean ± SD of four mice per condition.

(G) Expression of mRNA for CXCL1 and CXCL2 by purified leukocyte preparations from renal infiltrates obtained from WT or $Ifnar1^{-/-}$ mice at day 4 after infection with $1 \times 10^5$ *C. albicans* was assessed by real-time PCR, normalized to β-actin. Data are expressed as relative expression of each chemokine in $Ifnar1^{-/-}$ versus WT mice, considering as 1 the average expression for WT mice (mean ± SD of four mice per condition).

(H) Production of CXCL1 and CXCL2 by purified leukocyte preparations from renal infiltrates obtained from WT or $Ifnar1^{-/-}$ mice at day 4 after infection with $1 \times 10^5$ *C. albicans*, analyzed by Luminex. Significant differences as determined by the unpaired t test are indicated *p < 0.05; **p < 0.01; ***p < 0.001. Data are representative of at least two independent experiments with similar results. See also Figures S4 to S6.

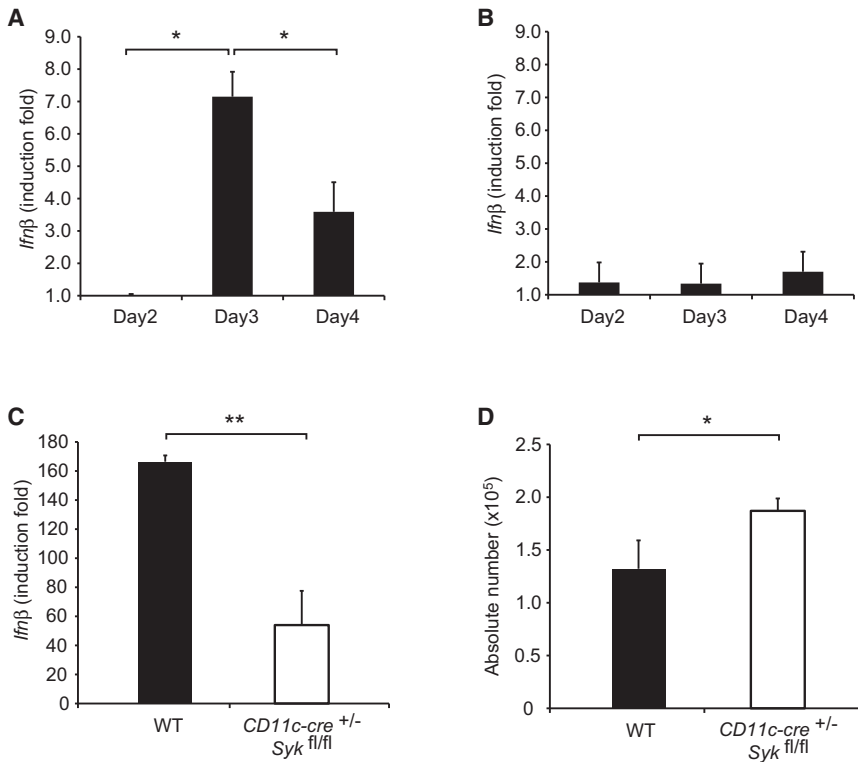**Figure 6. IFN-β Production in *Candida*-Infected CD11c-Cre⁺/⁻ *Syk*^fl/fl Mice**

(A and B) Expression of IFN-β mRNA by purified leukocyte preparations from renal infiltrates (A) or purified splenic DCs (B) obtained at the indicated times after infection with $1 \times 10^5$ *C. albicans* assessed by real-time PCR, normalized to β-actin. Data are expressed as induction fold relative to the expression at day 2 after infection (mean ± SD of triplicates).

(C) Expression of IFN-β mRNA by purified renal infiltrating leukocyte preparations from WT or CD11c-Cre⁺/⁻ *Syk*^fl/fl mice at day 3 after infection assessed by real-time PCR, normalized to β-actin. Data are expressed as induction fold relative to the expression at day 2 post-infection for WT mice (mean ± SD of triplicates).

(D) Absolute number of DCs in the renal leukocyte infiltrates of WT or CD11c-Cre⁺/⁻ *Syk*^fl/fl mice at day 3 after infection. DCs were defined as CD11c⁺ CD11b⁺ cells after gating out cells expressing CD90 (T cells), B220 (B cells), CD49b (NK cells), and Ly-6G (neutrophils). Data are expressed as mean ± SD of three mice per condition. Significant differences as determined by the unpaired t test are indicated *p < 0.05; **p < 0.01. Data are representative of two independent experiments with similar results.

type I IFN production through the Dectin-Syk-IRF5 signaling pathway, *C. albicans* infection experiments were performed in CD11c-Cre⁺/⁻ *Syk*^fl/fl mice, in which DCs are not responsive to Syk-dependent signaling and consequently are impaired in their capacity to produce IFN-β through Dectin and Syk. For this purpose, we first analyzed the kinetics of IFN-β production by renal infiltrating leukocytes after *C. albicans* infection by real-time PCR. Our data revealed that IFN-β production was undetectable at day 2 after infection, peaked at day 3 and was reduced along the next 24 hr (Figure 6A); IFN-β was not detectable on splenic DCs from day 2 to day 4 after infection (Figure 6B). On the basis of these data, we next analyzed IFN-β mRNA expression by renal infiltrating leukocytes at day 3 postinfection in WT and CD11c-Cre⁺/⁻ *Syk*^fl/fl mice. Interestingly, IFN-β production by renal-infiltrating leukocytes was reduced by around 70% in CD11c-Cre⁺/⁻ *Syk*^fl/fl mice (Figure 6C), and this reduction was not paralleled by a decreased number of infiltrating DCs (Figure 6D). In conclusion, our data strongly support the idea that, after *C. albicans* infection, IFN-β production by renal infiltrating leukocytes is controlled primarily by DCs and, importantly, that this production of IFN-β by renal infiltrating DCs is essentially driven by Dectin signaling via Syk.

## DISCUSSION

Type I IFN is produced after engagement of cytosolic receptors or membrane-bound TLR receptors by viral or bacterial compounds through the activation of the transcription factors IRF3 and IRF7 (Trinchieri, 2010), as shown in Figure S7, summarizing the key signaling pathways emerging from the main type I IFN-inducing receptors. Fungi, particularly yeasts of the genus

*Candida*, have also been recently reported to induce IFN-β production (Biondo et al., 2011; Bourgeois et al., 2011), but the mechanism responsible for the transcriptional activation of *Ifnb* gene in DCs, during *C. albicans* infection, is a matter of controversy. In this report we describe a signaling pathway leading to the production of IFN-β after stimulation of BMDCs with Curdlan, a Dectin-1 specific ligand that mimics the interaction of this C-type lectin receptor with β-glucans from *C. albicans* cell wall. IFN-β production triggered by Dectin-1 engagement is dependent on Syk, Card9, and the transcription factor IRF5, and independent of IRF3 and IRF7, as illustrated in Figure S7. To our knowledge, C-type lectin receptors had not been previously demonstrated to trigger the production of type I IFN. In addition, experiments using antibodies against Dectin-2, another Syk and Card9-dependent C-type lectin receptor recognizing *C. albicans* cell wall mannans, revealed that Dectin-2 signaling also contributes significantly to IFN-β production in response to *C. albicans*, a process that therefore results from a dual contribution of Dectin-1 and Dectin-2 signaling, in agreement with previous data demonstrating the cooperation of these receptors in inducing IL-2 and IL-10 production by BMDCs (Robinson et al., 2009). Importantly, our data based on BMDC stimulation with Curdlan and HKC demonstrate that IFN-β production in response to *C. albicans* is mostly controlled by Dectin-1 and Dectin-2 signaling with a minor contribution of TLR2 signaling. Therefore *Candida*-induced IFN-β production essentially results from the recognition of *C. albicans* cell-wall β-glucans by Dectin-1 and cell-wall mannans by Dectin-2 and TLR2. The differential relevance of TLR9 signaling to IFN-β production in response to Zymosan versus HKC reflects that whereas yeast DNA is readily exposed in Zymosan preparations and thus has

a major contribution to Zymosan-induced IFN-β production, *Candida* DNA-mediated TLR9 signaling does not contribute substantially to IFN-β production in response to *C. albicans*.

Our data revealed that Dectin-1-mediated IFN-β production is driven by a Syk-Card9-dependent pathway, that has been demonstrated to activate NF-κB and MAP kinases (Sancho and Reis e Sousa, 2012), supporting the hypothesis that Dectin-1 signaling can lead to the activation of two key transcriptional factors required for the assembly of the IFN-β enhanceosome, NF-κB, and c-Jun (Panne et al., 2007). IRF3 and IRF7 were also demonstrated to contribute to the IFN-β enhanceosome controlling type I IFN production resulting from the activation of cytosolic or TLR receptors (Trinchieri, 2010). However, unexpectedly, Dectin-1-induced transcription of the *Ifnb* gene required neither IRF3 nor IRF7 but the transcription factor IRF5. A link between IRF5 and type I IFN production during viral infections was proposed in studies showing that infection by viruses, such as Newcastle disease virus (NDV), vesicular stomatitis virus (VSV), and herpes simplex virus type 1 (HSV-1), led to the transcription of *Ifna* and *Ifnb* genes, by an IRF5-dependent mechanism (Barnes et al., 2002). Type I IFN production induced in response to the TLR7 ligand R-848 was also found to depend on both IRF7 and IRF5 (Schoenemeyer et al., 2005). More recently, *Mycobacterium tuberculosis*-induced expression of IFN-β mRNA in macrophages has been reported to occur after recognition of a bacterial muramyl dipeptide by the cytosolic receptor NOD2 and was largely dependent on IRF5 (Pandey et al., 2009). In addition, BMDCs were demonstrated to produce IFN-β after recognition of RNA from *Streptococcus pyogenes* by a mechanism dependent on MyD88 and IRF5 (Gratz et al., 2011).

The production of IFN-β by DCs in response to fungi, and particularly to yeasts of the genus *Candida*, has been described in two recent reports that proposed different signaling pathways to explain the transcriptional activation of the *Ifnb* gene induced by yeasts. Bourgeois et al. proposed that IFN-β production in response to *Candida glabrata* was triggered after engagement of TLR-7 by fungal RNA and was not affected by Dectin-1 deficiency; unexpectedly, this process appeared to be independent of IRF3 and IRF7 (Bourgeois et al., 2011). Alternatively, Biondo et al. reported that *C. albicans* 90028 strain induced IFN-β production by BMDCs after recognition of fungal DNA and proposed that this occurred by a mechanism partially dependent on TLR-7 and TLR-9 and on IRF-1, IRF3, and IRF7 (Biondo et al., 2011). In addition, these authors reported that Dectin-1 was not involved in the production of IFN-β in response to *C. albicans* yeast particles. Therefore, these two studies concur in proposing that IFN-β production in response to *Candida* was triggered by the activation of TLR receptors by fungal nucleic acids with no contribution of Dectin-1 signaling. The divergence between these reports and our data, proposing a major role for Dectin-1 in IFN-β production in response to *C. albicans* SC5314 strain (being the contribution of TLR signaling secondary), could be due to differences in the cell-wall composition between the yeast species or strains used in these studies that may dictate their ability to activate Dectin-1 signaling. In this regard, *Candida glabrata* is a nondimorphic yeast that is phylogenetically closer to *Saccharomyces cerevisiae* than to *C. albicans* (Kurtzman and Robnett, 1997), and thus *C. albicans* and *C. glabrata* may differ substantially in their ability to activate Dectin-1 signaling. Interestingly, host defense

against two *C. albicans* strains was found to be differentially dependent on Dectin-1; whereas this receptor was required for the induction of antifungal immunity against the SC5314 strain (Taylor et al., 2007), protective immunity after infection with the IFO1385 strain was independent of Dectin-1 (Saijo et al., 2007).

The physiological relevance of the production of type I IFN in response to *C. albicans* was confirmed by our in vivo studies revealing that *Ifnar1*$^{-/-}$ mice had a lower survival after infection with *C. albicans* that was paralleled by a higher fungal burden in the kidney, the main target after systemic *C. albicans* infection. Our data, demonstrating that type I IFNs contribute to a more efficient immune response against *C. albicans*, confirm two previous reports on *C. albicans* (Biondo et al., 2011) and *Cryptococcus neoformans* (Biondo et al., 2008) infection that support the hypothesis that type I IFN had a beneficial effect for antifungal immunity. However, type I IFN had a deleterious effect during infection by the fungi *Histoplasma capsulatum* (Inglis et al., 2010) or *C. glabrata* (Bourgeois et al., 2011). In addition, *Ifnar1*$^{-/-}$ mice were recently reported to have an improved survival in response to *C. albicans*, although strikingly this increased survival was not paralleled by a lower fungal burden (Majer et al., 2012). Type I IFN has also been demonstrated to have opposing beneficial or detrimental effects on antiviral and antibacterial immunity depending on the infectious process (Trinchieri, 2010). During viral infections, type I IFNs contribute to host defense through their antiviral and immunomodulatory properties, but they can also mediate tissue damage and inflammatory or autoimmune reactions. Type I IFN can also contribute to protective antibacterial immunity essentially by blocking intracellular bacterial replication and through the induction of nitric oxide and proinflammatory cytokines. However, type I IFN production is often detrimental for defense against bacteria through several mechanisms. In this regard, type I IFN can increase the susceptibility of T cells and macrophages to apoptosis, interfere with microbicidal mechanisms, favor bacterial replication, limit T cell responses, and alter the recruitment and activation of myeloid cells to the site of infection (Stetson and Medzhitov, 2006).

Our results revealed that IFNAR1 deficiency led to lower survival after *C. albicans* infection that was paralleled by a defective renal neutrophil recruitment and a lower production of the neutrophil-chemoattractant chemokines CXCL1 and CXCL2. These findings support that type I IFN plays a crucial role in defense against *C. albicans* by promoting the mobilization of neutrophils to the kidney. Neutrophils are required for an efficient protection against systemic candidiasis due to their high capacity to kill *C. albicans* (Mansour and Levitz, 2002), as demonstrated by experiments of neutrophil depletion in *C. albicans*-infected mice, in which survival was severely compromised (Dejima et al., 2011). CXCL1 and CXCL2 have a critical function in the recruitment of neutrophils (Kobayashi, 2006), and interestingly they appear to be highly expressed in the kidney of *C. albicans*-infected mice, as revealed by gene expression microarray analysis (MacCallum, 2009). In this regard, our data suggest that type I IFN controls renal neutrophil infiltration by controlling the production of CXCL1 and CXCL2 by neutrophils, in contrast to previous evidence on the negative regulation of these chemokines by type I IFN (Trinchieri, 2010).

More importantly, the experiments revealing that the production of IFN-β by renal infiltrating leukocytes was severely

reduced in *C. albicans*-infected CD11c-Cre^{+/−} *Syk*^{fl/fl} mice, in which DCs are not responsive to Syk-dependent signaling, have been decisive to establish the link between the compromised survival of *Ifnar1*^{−/−} mice and the Dectin and Syk-dependent pathway of IFN-β production by DCs. These data support the hypothesis that most of type I IFN required for protection against *C. albicans* was produced by renal-infiltrating inflammatory DCs through Dectin-Syk signaling and that there was only a minor contribution from DCs through Syk-independent signaling, and/or from the rest of non-DC infiltrating leukocytes, to type I IFN production during *C. albicans* infection.

In conclusion, the data presented in this report demonstrate that the production of type I IFN by DCs induced by *C. albicans* is essentially controlled by a Dectin-1-mediated signaling pathway, dependent on Syk, Card9 and IRF5. The existence of this pathway extends the physiological relevance of Dectin-1-mediated signaling, particularly in the context of the induction of antifungal immunity because, in addition to driving the synthesis of cytokines that are essential for the induction of Th17 cell responses, it triggers the production of IFN-β that, as revealed by our data, is crucial for defense against *C. albicans*.

## EXPERIMENTAL PROCEDURES

### Mice
C57BL/6 (10–12 weeks old) female mice were purchased from Harlan (Bicester, UK). *Ifnar1*^{−/−} mice were kindly provided by Dr. U. Kalinke (Center for Experimental and Clinical Infection Research, Hannover, Germany). CD11c-Cre^{+/−} *Syk*^{fl/fl} mice and *Clec4e*^{−/−} mice were provided by Dr. D. Sancho (Centro Nacional de Investigaciones Cardiovasculares, Madrid, Spain). C57BL/6, *Ifnar1*^{−/−}, and CD11c-Cre^{+/−} *Syk*^{fl/fl} mice were housed at the animal facility of Centro Nacional de Biotecnología-CSIC, Madrid, Spain. *Card9*^{−/−} mice were generated by Dr. J. Ruland (Technische Universität München, München, Germany). Bone marrow from *Clec7a*^{−/−} mice was generously provided by Dr. G. Brown (University of Aberdeen, Aberdeen, UK), from *Tlr2*^{−/−} mice by Dr. M. Fresno (Centro de Biología Molecular Severo Ochoa-CSIC-UAM, Madrid, Spain), from *Tlr9*^{−/−} mice by Dr. J. Pardo (Universidad de Zaragoza, Spain), from *Irf3*^{−/−} and *Irf7*^{−/−} mice by Dr. T. Decker (Max F. Perutz Laboratories, Vienna, Austria) and from *Irf5*^{−/−} mice by Dr. T. Mak (University Health Network, Toronto, Ontario). All the experiments were approved by the Animal Care and Use Committee of the Centro Nacional de Biotecnología-CSIC, Madrid.

### C. albicans
*C. albicans* (strain SC5314; kindly provided by Prof. C. Gil, Complutense University, Madrid) was grown on YPD plates (Sigma, St Louis, MO) at 30°C. HKC were obtained by incubation of *C. albicans*, strain SC5314, for 2 hr at 65°C.

### Stimulation of BMDCs and BMMs
BMDCs or BMMs obtained as described in Supplemental Information, were rested for 6 hr in complete cell culture medium and subsequently stimulated at the indicated times with 100 ng.ml^{−1} LPS from *Escherichia coli* (Sigma), 10 μg.ml^{−1} Curdlan (Wako chemicals, Neuss, Germany), 10 μg.ml^{−1} Zymosan (Invivogen, San Diego, CA), or 5 × 10^5 HKC. To address the contribution of Dectin-2 to IFN-β production, we incubated BMDCs for 2 hr with 10 μg.ml^{−1} blocking anti-Dectin-2 antibodies (clone D2.11E4) kindly provided by Dr. P. Taylor (Cardiff Institute of Infection and Immunity, Cardiff, UK) or isotype-matched control antibodies, and subsequently stimulated as indicated above. The phenotypic analysis of BMDCs and BMMs was performed by flow cytometry. IFN-β mRNA expression by BMDCs and BMMs was analyzed by real-time PCR. RelA, c-Jun, and IRF3 activation on BMDCs was assessed by immunoblot. Flow cytometry, real-time PCR, and immunoblot methods are described in Supplemental Information.

### C. albicans In Vivo Infection
Mice were intravenously infected with 1 × 10^5 *C. albicans* and monitored daily for health and survival following the institutional guidance. Kidney fungal burden was determined at day 6 after infection by plating organ homogenates in serial dilutions on YPD plates; colony-forming units (cfu) were counted after growth for 48 hr at 30°C. Flow cytometry analysis of renal leukocyte infiltrates was performed on cell suspensions obtained from organ homogenates that were digested with 0.5 μg.ml^{−1} of collagenase A (Roche, Mannheim, Germany) for 10 min at 37°C and filtered through 40 μm cell strainers (BD PharMingen, San Diego, CA). The phenotypic analysis of renal leukocyte infiltration was performed by flow cytometry as described in Supplemental Information. For real-time PCR and Luminex analyses, performed as described in Supplemental Information, renal infiltrating leukocytes were purified from kidney cell suspensions by centrifugation on a gradient of Ficoll-Paque Plus (GE Healthcare, Uppsala, Sweden) and immunomagnetic positive selection after incubation with biotin-conjugated anti-CD45 and streptavidin-conjugated microbeads. Splenic DCs were purified by immunomagnetic positive selection after incubation with biotin-conjugated anti-CD11c and streptavidin-conjugated microbeads.

### Cytokine Detection
IFN-β production was quantified by using the *Verikine* mouse IFN beta ELISA kit (PBL, Piscataway, NJ). IFN-β production values for unstimulated controls were below the detection level of this ELISA kit (15.6 pg/ml) for all the experiments analyzing IFN-β production. CXCL1 and CXCL2 production was analyzed by Luminex technology as described in Supplemental Information.

## SUPPLEMENTAL INFORMATION

Supplemental Information includes seven figures, two tables, and Supplemental Experimental Procedures and can be found with this article online at http://dx.doi.org/10.1016/j.immuni.2013.05.010.

## REFERENCES

Barnes, B.J., Kellum, M.J., Field, A.E., and Pitha, P.M. (2002). Multiple regulatory domains of IRF-5 control activation, cellular localization, and induction of chemokines that mediate recruitment of T lymphocytes. Mol. Cell. Biol. *22*, 5721–5740.

Biondo, C., Midiri, A., Gambuzza, M., Gerace, E., Falduto, M., Galbo, R., Bellantoni, A., Beninati, C., Teti, G., Leanderson, T., and Mancuso, G. (2008). IFN-alpha/beta signaling is required for polarization of cytokine responses toward a protective type 1 pattern during experimental cryptococcosis. J. Immunol. *181*, 566–573.

Biondo, C., Signorino, G., Costa, A., Midiri, A., Gerace, E., Galbo, R., Bellantoni, A., Malara, A., Beninati, C., Teti, G., and Mancuso, G. (2011). Recognition of yeast nucleic acids triggers a host-protective type I interferon response. Eur. J. Immunol. *41*, 1969–1979.

Bourgeois, C., Majer, O., Frohner, I.E., Lesiak-Markowicz, I., Hildering, K.S., Glaser, W., Stockinger, S., Decker, T., Akira, S., Müller, M., and Kuchler, K. (2011). Conventional dendritic cells mount a type I IFN response against

Candida spp. requiring novel phagosomal TLR7-mediated IFN-β signaling. J. Immunol. *186*, 3104–3112.

Decker, T., Müller, M., and Stockinger, S. (2005). The yin and yang of type I interferon activity in bacterial infection. Nat. Rev. Immunol. *5*, 675–687.

Dejima, T., Shibata, K., Yamada, H., Hara, H., Iwakura, Y., Naito, S., and Yoshikai, Y. (2011). Protective role of naturally occurring interleukin-17A-producing γδ T cells in the lung at the early stage of systemic candidiasis in mice. Infect. Immun. *79*, 4503–4510.

González-Navajas, J.M., Lee, J., David, M., and Raz, E. (2012). Immunomodulatory functions of type I interferons. Nat. Rev. Immunol. *12*, 125–135.

Gratz, N., Hartweger, H., Matt, U., Kratochvill, F., Janos, M., Sigel, S., Drobits, B., Li, X.D., Knapp, S., and Kovarik, P. (2011). Type I interferon production induced by Streptococcus pyogenes-derived nucleic acids is required for host protection. PLoS Pathog. *7*, e1001345.

Gross, O., Gewies, A., Finger, K., Schäfer, M., Sparwasser, T., Peschel, C., Förster, I., and Ruland, J. (2006). Card9 controls a non-TLR signalling pathway for innate anti-fungal immunity. Nature *442*, 651–656.

Inglis, D.O., Berkes, C.A., Hocking Murray, D.R., and Sil, A. (2010). Conidia but not yeast cells of the fungal pathogen Histoplasma capsulatum trigger a type I interferon innate immune response in murine macrophages. Infect. Immun. *78*, 3871–3882.

Kobayashi, Y. (2006). Neutrophil infiltration and chemokines. Crit. Rev. Immunol. *26*, 307–316.

Kurtzman, C.P., and Robnett, C.J. (1997). Identification of clinically important ascomycetous yeasts based on nucleotide divergence in the 5′ end of the large-subunit (26S) ribosomal DNA gene. J. Clin. Microbiol. *35*, 1216–1223.

LeibundGut-Landmann, S., Gross, O., Robinson, M.J., Osorio, F., Slack, E.C., Tsoni, S.V., Schweighoffer, E., Tybulewicz, V., Brown, G.D., Ruland, J., and Reis e Sousa, C. (2007). Syk- and CARD9-dependent coupling of innate immunity to the induction of T helper cells that produce interleukin 17. Nat. Immunol. *8*, 630–638.

Lionakis, M.S., Lim, J.K., Lee, C.C., and Murphy, P.M. (2011). Organ-specific innate immune responses in a mouse model of invasive candidiasis. J. Innate Immun. *3*, 180–199.

MacCallum, D.M. (2009). Massive induction of innate immune response to Candida albicans in the kidney in a murine intravenous challenge model. FEMS Yeast Res. *9*, 1111–1122.

Majer, O., Bourgeois, C., Zwolanek, F., Lassnig, C., Kerjaschki, D., Mack, M., Müller, M., and Kuchler, K. (2012). Type I interferons promote fatal immunopathology by regulating inflammatory monocytes and neutrophils during Candida infections. PLoS Pathog. *8*, e1002811.

Mansour, M.K., and Levitz, S.M. (2002). Interactions of fungi with phagocytes. Curr. Opin. Microbiol. *5*, 359–365.

Pandey, A.K., Yang, Y., Jiang, Z., Fortune, S.M., Coulombe, F., Behr, M.A., Fitzgerald, K.A., Sassetti, C.M., and Kelliher, M.A. (2009). NOD2, RIP2 and IRF5 play a critical role in the type I interferon response to Mycobacterium tuberculosis. PLoS Pathog. *5*, e1000500.

Panne, D., Maniatis, T., and Harrison, S.C. (2007). An atomic model of the interferon-beta enhanceosome. Cell *129*, 1111–1123.

Pfaller, M.A., and Diekema, D.J. (2007). Epidemiology of invasive candidiasis: a persistent public health problem. Clin. Microbiol. Rev. *20*, 133–163.

Purtha, W.E., Swiecki, M., Colonna, M., Diamond, M.S., and Bhattacharya, D. (2012). Spontaneous mutation of the Dock2 gene in Irf5-/- mice complicates interpretation of type I interferon production and antibody responses. Proc. Natl. Acad. Sci. USA *109*, E898–E904.

Robinson, M.J., Osorio, F., Rosas, M., Freitas, R.P., Schweighoffer, E., Gross, O., Verbeek, J.S., Ruland, J., Tybulewicz, V., Brown, G.D., et al. (2009). Dectin-2 is a Syk-coupled pattern recognition receptor crucial for Th17 responses to fungal infection. J. Exp. Med. *206*, 2037–2051.

Romani, L. (2011). Immunity to fungal infections. Nat. Rev. Immunol. *11*, 275–288.

Saijo, S., Fujikado, N., Furuta, T., Chung, S.H., Kotaki, H., Seki, K., Sudo, K., Akira, S., Adachi, Y., Ohno, N., et al. (2007). Dectin-1 is required for host defense against Pneumocystis carinii but not against Candida albicans. Nat. Immunol. *8*, 39–46.

Sancho, D., and Reis e Sousa, C. (2012). Signaling by myeloid C-type lectin receptors in immunity and homeostasis. Annu. Rev. Immunol. *30*, 491–529.

Schoenemeyer, A., Barnes, B.J., Mancl, M.E., Latz, E., Goutagny, N., Pitha, P.M., Fitzgerald, K.A., and Golenbock, D.T. (2005). The interferon regulatory factor, IRF5, is a central mediator of toll-like receptor 7 signaling. J. Biol. Chem. *280*, 17005–17012.

Stetson, D.B., and Medzhitov, R. (2006). Type I interferons in host defense. Immunity *25*, 373–381.

Strasser, D., Neumann, K., Bergmann, H., Marakalala, M.J., Guler, R., Rojowska, A., Hopfner, K.P., Brombacher, F., Urlaub, H., Baier, G., et al. (2012). Syk kinase-coupled C-type lectin receptors engage protein kinase C-σ to elicit Card9 adaptor-mediated innate immunity. Immunity *36*, 32–42.

Taylor, P.R., Tsoni, S.V., Willment, J.A., Dennehy, K.M., Rosas, M., Findon, H., Haynes, K., Steele, C., Botto, M., Gordon, S., and Brown, G.D. (2007). Dectin-1 is required for beta-glucan recognition and control of fungal infection. Nat. Immunol. *8*, 31–38.

Trinchieri, G. (2010). Type I interferon: friend or foe? J. Exp. Med. *207*, 2053–2063.

Xu, S., Huo, J., Lee, K.G., Kurosaki, T., and Lam, K.P. (2009). Phospholipase Cgamma2 is critical for Dectin-1-mediated Ca2+ flux and cytokine production in dendritic cells. J. Biol. Chem. *284*, 7038–7046.

## Supplemental Information

## Interferon-β Production via Dectin 1-Syk-IRF5

## Signaling in Dendritic Cells

## Is Crucial for Immunity to *C. albicans*

Carlos del Fresno, Didier Soulat, Susanne Roth, Katrina Blazek, Irina Udalova, David Sancho, Jürgen Ruland, and Carlos Ardavín
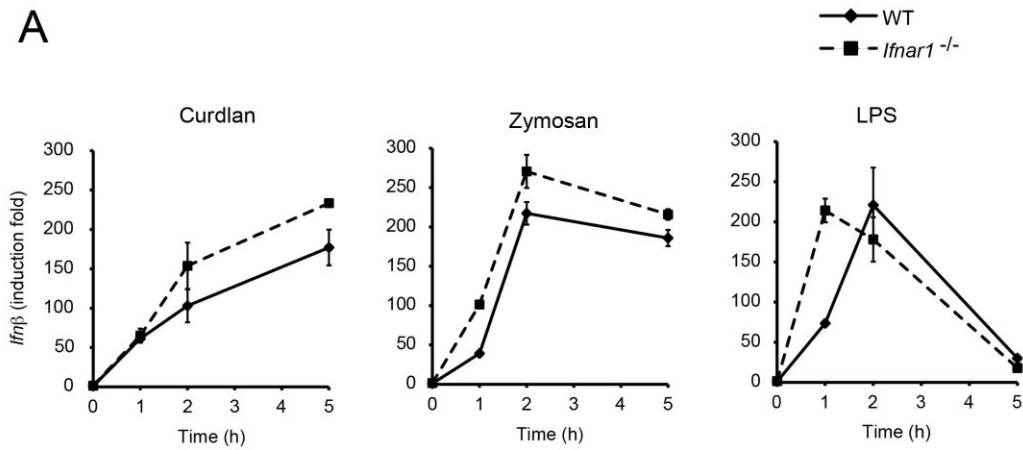
**Supplemental Inventory**

**1. Supplemental Figures and Tables**

**2. Supplemental Experimental Procedures**
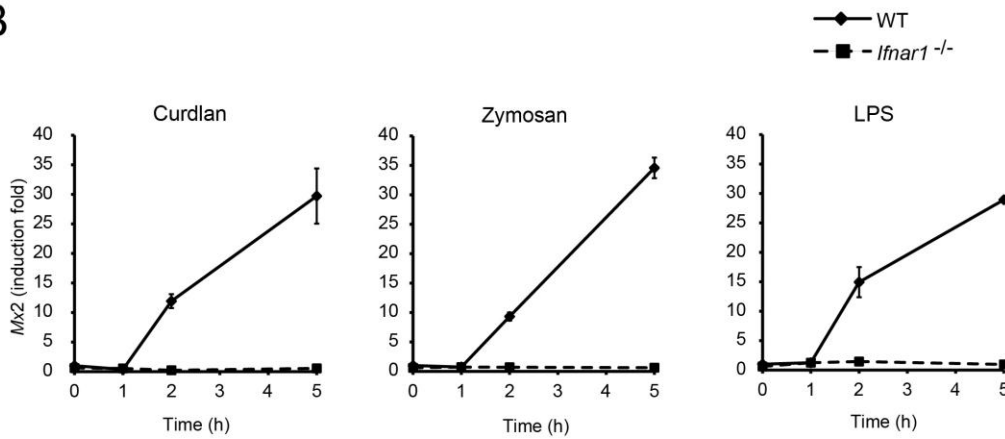
**Figure S1. Contribution of Autocrine IFNAR1 Signalling to IFNβ Production in BMDCs, Related to Figure 1**
BMDCs from wild type (WT) or *Ifnar1*^{-/-} mice, unstimulated or stimulated for the indicated times with Curdlan, Zymosan or LPS, were analyzed for the expression of mRNA for IFNβ (A) or IFN-inducible antiviral gene *Mx2* (B) by real-time PCR, normalized to β-actin. Data are expressed as induction fold relative to unstimulated controls (mean ± SD of triplicates).
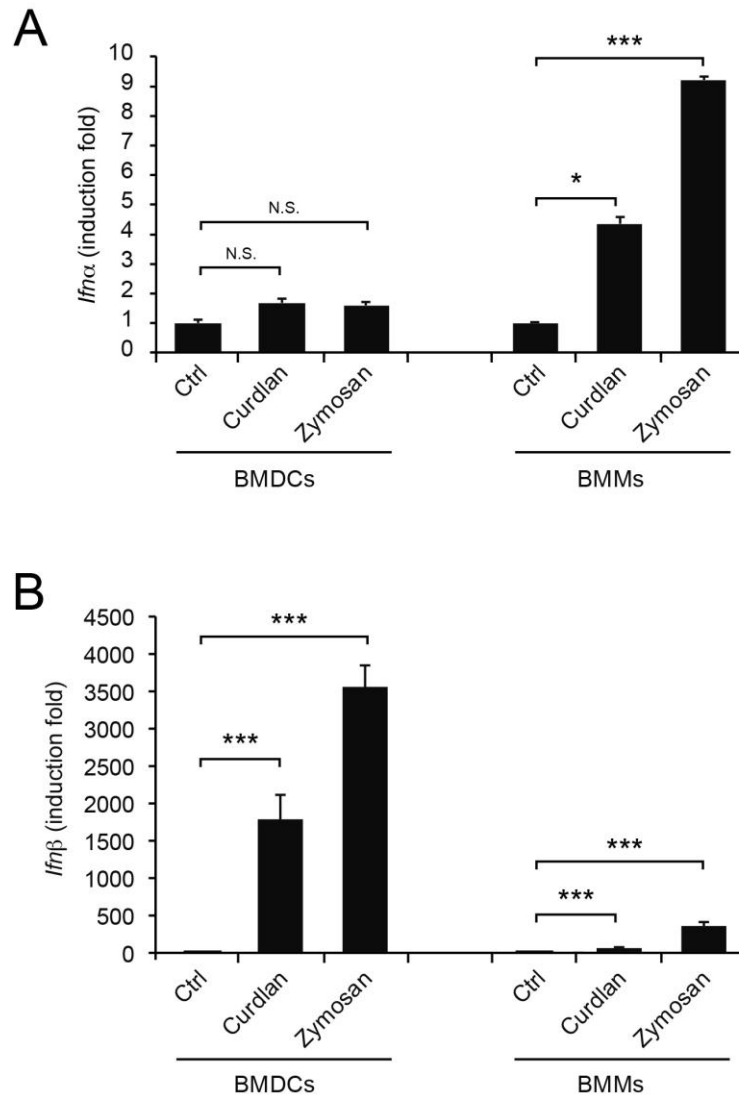
**Figure S2. Expression of mRNA for IFNα and IFNβ by Activated BMDCs and BMMs, Related to Figure 1**

BMDCs or BMMs unstimulated (Ctrl) or stimulated for 5 hr with Curdlan or Zymosan, were analyzed for the expression of mRNA for IFNα (A) or IFNβ (B) by real-time PCR, normalized to β-actin. Data are expressed as induction fold relative to unstimulated controls (mean ± SD of triplicates). Significant differences, as determined by the unpaired t-test, are indicated *p<0.05; ***p<0.001; N.S. not significant.
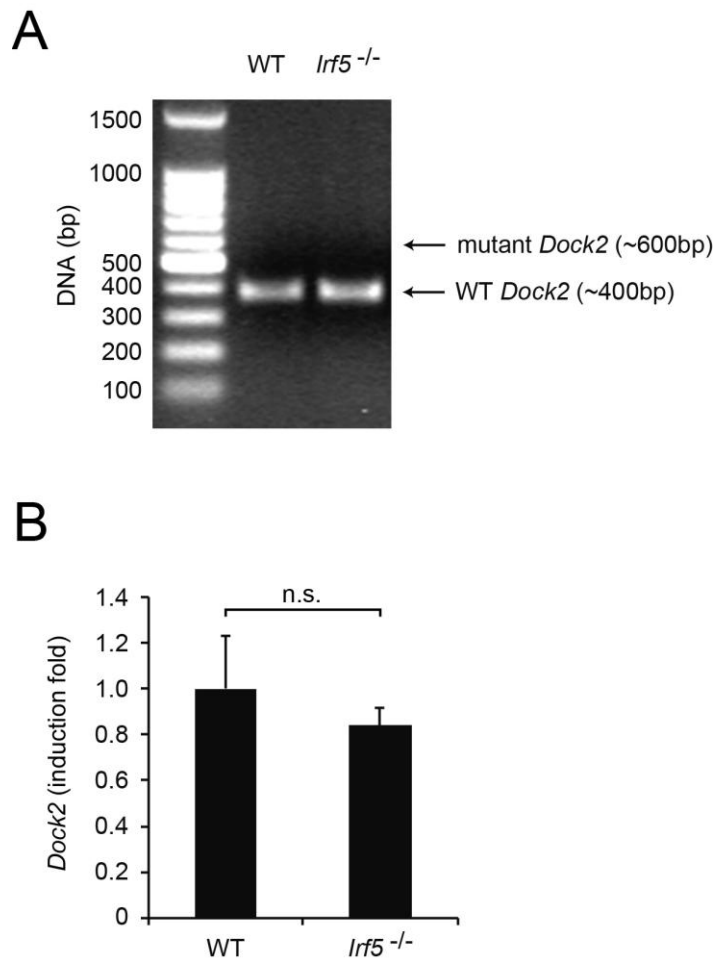
**Figure S3. Analysis of *Dock2* Gene in *Irf5*^{-/-} Mice, Related to Figure 4**

(A) Analysis of the *Dock2* genotype in wild type (WT) and *Irf5*^{-/-} mice was performed by PCR using primers allowing the detection of the normal and the mutant *Dock2* gene, as described (Purtha et al., 2012. Proc Natl Acad Sci U S A *109*, E898-904). Both WT and the *Irf5*^{-/-} mice used in this study yielded a band of around 400 bp corresponding to the normal *Dock2* gene.

(B) Analysis of the expression of Dock2 by BMDCs from WT and *Irf5*^{-/-} mice analyzed by real-time PCR normalized to β-actin, showing that WT and *Irf5*^{-/-} BMDCs expressed comparable levels of Dock2 mRNA, and confirming that the *Irf5*^{-/-} mice used in our study had a normal *Dock2* genotype. Data are expressed as relative expression of Dock2 in *Irf5*^{-/-} versus WT mice (mean ± SD of triplicates). n.s: not significant.
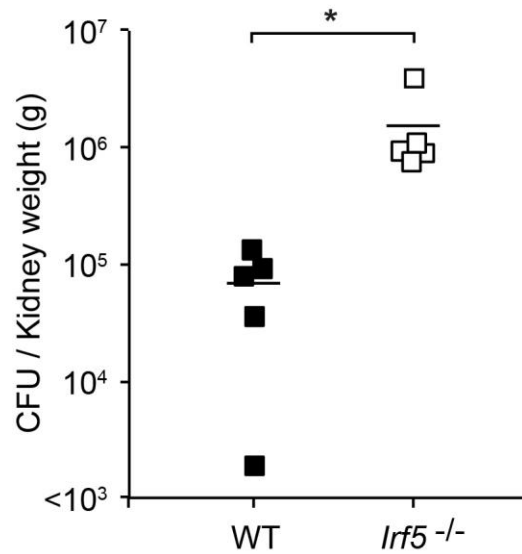
**Figure S4. Effect of *Irf5* Deficiency on Kidney Fungal Load after *C. albicans* Infection, Related to Figure 5**

Kidney fungal burden of wild type (WT; n = 5) and *Irf5*^{-/-} (n = 5) mice at day 6 post-infection with 1 x 10$^5$ *C. albicans*. Data are expressed as CFU/g kidney. Significant differences as determined by the unpaired t-test are indicated *p<0.05. The higher susceptibility of *Irf5*^{-/-} mice to *C. albicans* infection is probably due, at least in part, to a defective Dectin/Syk/IRF5-dependent type-I IFN production, although *Irf5* deficiency could also negatively affect the production of other mediators involved in anti-fungal immunity, since *Irf5* has been demonstrated to regulate the production of several cytokines in response to TLR signalling.
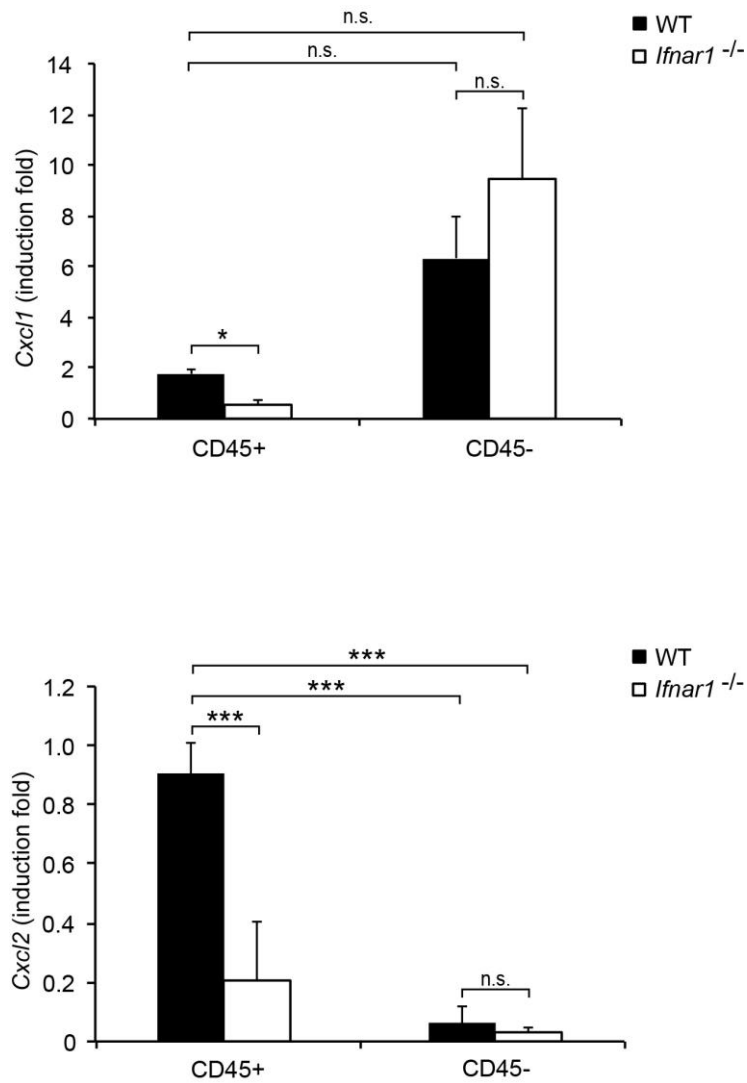
**Figure S5. Expression of mRNA for *Cxcl1* and *Cxcl2* by the CD45⁺ and the CD45⁻ Kidney Cell Fractions, Related to Figure 5**

Expression of mRNA for *Cxcl1* and *Cxcl2* by CD45⁺ renal infiltrating leukocytes and by CD45⁻ non-hematopoietic kidney cells obtained from wild type (WT) or *Ifnar1*⁻/⁻ mice at day 4 post-infection with 1 x 10⁵ *C. albicans*, was assessed by real-time PCR, normalized to β-actin. Data are expressed as induction fold relative to the expression by CD45⁺ cells from wild type mice (mean ± SD of 4 mice per condition). Significant differences as determined by the unpaired t-test are indicated *p<0.05; ***p<0.001. n.s: not significant.
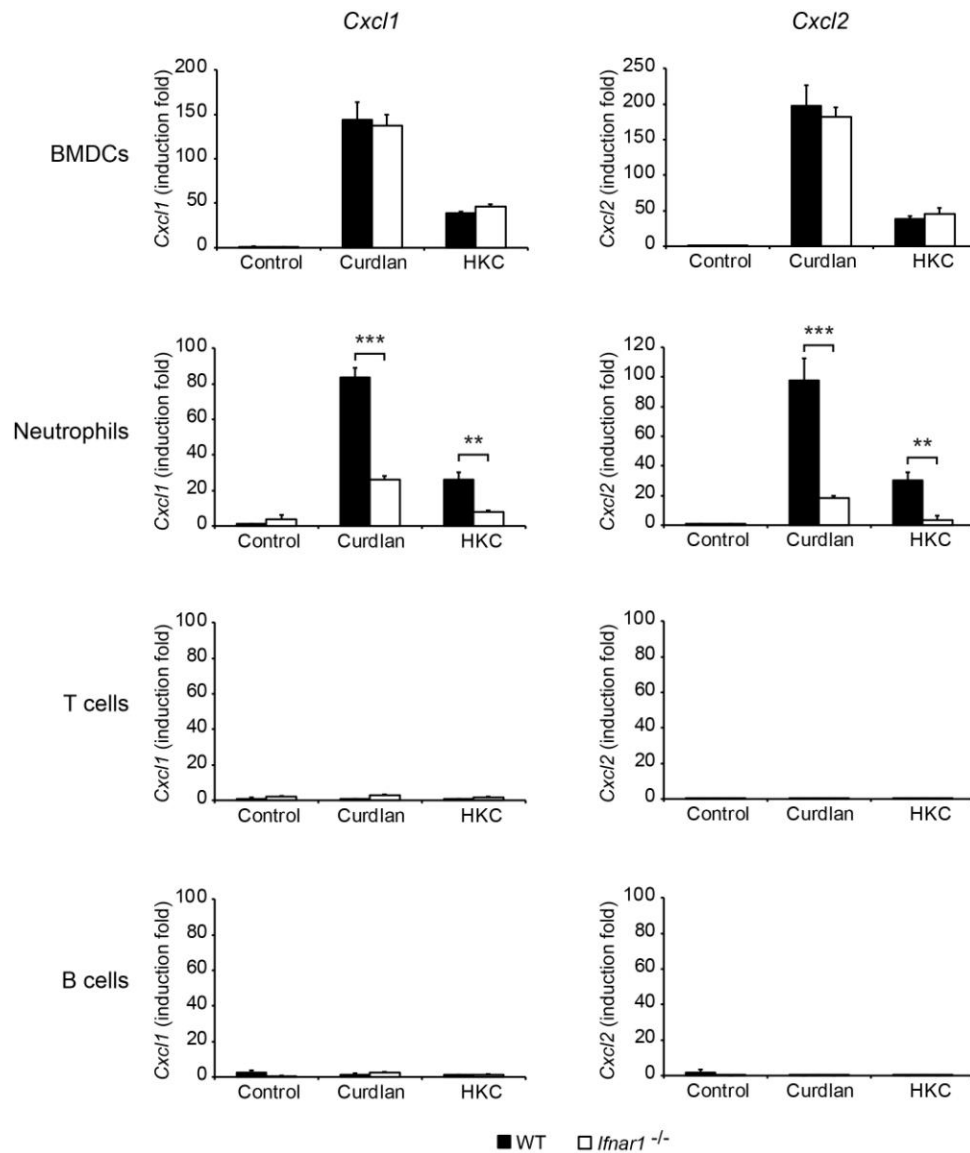
**Figure S6. Expression of mRNA for *Cxcl1* and *Cxcl2* by BMDCs, Neutrophils, T Cells and B Cells, Related to Figure 5**

Expression of mRNA for *Cxcl1* and *Cxcl2* by the indicated cell types, purified from wild type (WT) or $^{-/-}$ mice, unstimulated (Control) or stimulated for 5 hr with Curdlan or HKC, was assessed by real-time PCR, normalized to β-actin. Neutrophils were isolated from the bone marrow by immunomagnetic positive selection after incubation with anti-Ly-6G; T and B cells were isolated from the spleen by immunomagnetic negative selection. Data are expressed as induction fold relative to unstimulated controls (mean ± SD of triplicates). Significant differences as determined by the unpaired t-test are indicated **p<0.01; ***p<0.001.
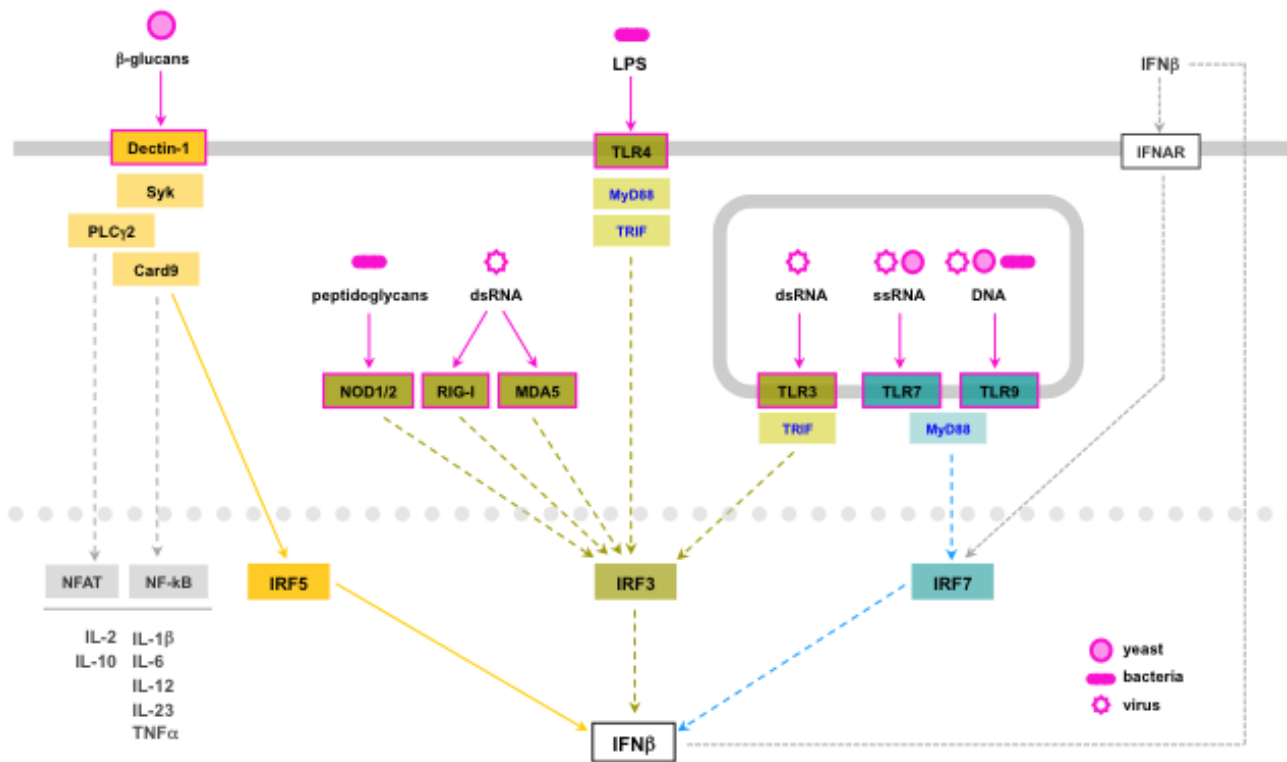
**Figure S7. Integrated View of the Signalling Pathways Leading to IFNβ Production Emerging from the Main Type I IFN-Inducing Receptors**

IFNβ production in response to viruses or intracellular bacteria mainly occurs after engagement of the cytosolic receptors RIG-I, MDA5 (both sensing viral dsRNA), and NOD1/2 (sensing bacterial peptidoglycans), or the TLR receptors TLR4 (sensing Gram-negative bacteria LPS at the cell surface), TLR3, 7 and 9 (sensing viral, fungal or bacterial nucleic acids at endosomal compartments). In addition, as demonstrated in this report IFNβ can be produced in response to *C. albicans* by the new Dectin-1-mediated pathway, dependent on Syk, Card9 and IRF5, described in this report (yellow arrows).

**Supplemental Experimental Procedures**
**Culture of BMDCs and BMMs**
BMDCs were obtained from bone marrow cell suspensions after culture on non-treated culture 150-mm Petri dishes in complete RPMI 1640 medium supplemented with 10% FCS, 2 mM L-glutamine, 100 U.ml$^{-1}$ penicillin, 100 µg.ml$^{-1}$ streptomycin, 50 µM 2-mercaptoethanol and 20 ng.ml$^{-1}$ recombinant GM-CSF (Peprotech, London, UK). Cells were collected at day 8, and BMDCs were purified by immunomagnetic positive selection after incubation with biotin-conjugated anti-CD11c and streptavidin-conjugated microbeads (Miltenyi Biotec, Bergisch Gladbach, Germany). After positive selection, preparations of BMDCs, characterized as CD11c$^{+}$ MHCII$^{+}$ Ly6G$^{-}$ cells, had a purity >95%. BMMs were obtained from bone marrow cell suspensions after culture on non-treated culture 60-mm Petri dishes in complete DMEM medium supplemented with 20% FCS, 2 mM L-glutamine, 100 U.ml$^{-1}$ penicillin, 100 µg.ml$^{-1}$ streptomycin, 50 µM 2-mercaptoethanol and 30% supernatant of the M-CSF-producing cell line L929. At day 7, preparations of BMMs, characterized as CD11b$^{+}$ F4/80$^{+}$ cells, had a purity >95%.

**RNA Extraction and Real-Time PCR**
RNA from BMDCs or BMMs was extracted using the High Pure RNA Isolation kit (Roche, Mannheim, Germany). RNA from renal leukocyte infiltrates was extracted using the RNAqueous-Micro kit (Ambion, Austin, TX). RNA was retro-transcribed using the High Capacity cDNA Reverse Transcription kit (Applied Biosystems, Carlsbad, CA). Real-time PCR was performed using a FluoCycle SYBR Green mix (EuroClone, Milano, Italy) on an ABI PRISM 7700 Sequence Detection System (Applied Biosystems). Primer sequences are listed in Table S1.

**Luminex**

CXCL1 and CXCL2 production was analyzed by Luminex technology using a MILLIPLEX MAP Mouse Cytokine/Chemokine assay (Merck Millipore, Billerica, MA) on cell lysates from MACS-sorted renal infiltrating leukocytes that were prepared after treatment with Cell Extraction Buffer containing 20 mM Tris-HCL, 150 mM NaCl, 0,05% Tween-20, 1 mM PMSF, and a protease inhibitor cocktail (Sigma, St Louis, MO).

**Flow Cytometry Methods**
Phenotypic analysis of BMDCs was performed after triple staining with fluorescein isothiocyanate (FITC)-conjugated anti-MHC II (BD Pharmingen, San Diego, CA), phycoerythrin *(*PE)-conjugated anti-Ly6G (BD Pharmingen), and allophycocyanin (APC)-conjugated anti-CD11c (eBioscience, San Diego, CA). Phenotypic analysis of BMMs was performed after double staining with PE-conjugated anti-CD11b (BD Pharmingen) and APC-conjugated anti-F4/80 (BD Pharmingen). Phenotypic analysis of renal leukocyte infiltration was performed after five-color staining with FITC-conjugated anti-CD45 (BD Pharmingen), PECy7-conjugated anti-CD11b (BD Pharmingen), APC-conjugated anti-CD11c, PE-conjugated anti-CD49b, anti-CD90.2 and anti-CD19 (BD Pharmingen), and biotin-conjugated anti-Ly6C, anti-Ly6G or anti-MHCII, followed by streptavidin-PerCP (BD Pharmingen). Antibodies anti-CD49b, CD90.2 and CD19 were used together as PE-conjugates with the purpose of gating out NK, T and B cells, respectively. Analysis of NK, T and B cells was performed after four-color staining with FITC-conjugated anti-CD45, PECy7-conjugated anti-CD11b, APC-conjugated anti-CD11c and PE-conjugated anti-CD49b or anti-CD90.2 or anti-CD19, respectively. Data were acquired on a LSRII cytometer and analyzed using the Cell Quest Pro software (BD Pharmingen).

**Immunoblot**
Nuclear and cytosolic protein extracts were prepared from BMDCs stimulated for 2 hr with LPS, Zymosan or Curdlan as described (Solan et al., 2002. J Biol Chem *277*, 1405-1418), and quantified by Bradford measurement using the Bio-Rad protein assay (Bio-Rad Laboratories, Hercules, CA). 10µg of nuclear or cytosolic protein extracts were subjected to SDS–PAGE and transferred onto a nitrocellulose membrane (Bio-Rad Laboratories). After blocking with 5% bovine serum albumin, fraction V (Sigma), membranes were incubated overnight with the antibodies listed in Table S2. Signals were detected with HRP-conjugated secondary antibodies (Cell Signaling Technology, Danvers, MA) using the ECL system (Amersham Biosciences, Freiburg, Germany).

**Table S1. Primers for Real-Time PCR Used in This Study**

| Gene | Primer | Sequence 5'-3' |
|------|--------|----------------|
| *Ifn*β | *Ifn*β-for | TCAGAATGAGTGGTGGTTGC |
| | *Ifn*β-rev | GACCTTTCAAATGCAGTAGATTCA |
| *Mx2* | *Mx2*-for | CCAGTTCCTCTCAGTCCCAAGATT |
| | *Mx2*-rev | TACTGGATGATCAAGGGAACGTGG |
| all *Ifn*α | pan-*Ifn*α-for | CCTGAGA(A/G)AGAAGAAACACAGCC |
| | pan-*Ifn*α-rev | GGCTCTCCAGA(C/T)TTCTGCTCTG |
| *Cxcl1* | *Cxcl1*-for | CCGCTCGCTTCTCTGTGC |
| | *Cxcl1*-rev | CTCTGGATGTTCTTGAGGTGAATC |
| *Cxcl2* | *Cxcl2*-for | CGCCCAGACAGAAGTCATAG |
| | *Cxcl2*-rev | TCCTCCTTTCCAGGTCAGTTA |
| β-*actin* | β-*actin*-for | GGCTGTATTCCCCTCCATCG |
| | β-*actin*-rev | CCAGTTGGTAACAATGCCATGT |

**Table S2. Antibodies for Immunoblot Used in This Study**

| | Specificity | Source | Reference |
|------|-------------|--------|-----------|
| p-RelA | phospho-Nf-kb p65 (Ser536) | Cell Signaling Technology [1] | 3033S |
| RelA | Nfkb p65 | Santa Cruz Biotechnology [2] | sc-372 |
| p-c-Jun | phospho-c-Jun (Ser63) | Cell Signaling Technology | 9261 |
| c-Jun | c-Jun | Cell Signaling Technology | 2315 |
| p-IRF3 | phospho-IRF3 (Ser396) | Cell Signaling Technology | 4947 |
| IRF3 | IRF3 | Cell Signaling Technology | 4962 |
| β-tubulin | β-tubulin | Cell Signaling Technology | 2146 |
| Histones | H1 and core proteins | Merck Millipore [3] | MAB052 |

[1] Cell Signaling Technology, Danvers, MA
[2] Santa Cruz Biotechnology, Santa Cruz, CA
[3] Merck Millipore, Billerica, MA